HYDRAULICS OF PADDLE WHEELS IN HIGH-RATE ALGAE PONDS

by

SACHA SETHAPUTRA

D.Eng., Asian Institute of Technology
(1975)

SUBMITTED IN PARTIAL FULFILLMENT
OF THE REQUIREMENTS FOR THE
DEGREE OF

MASTER OF SCIENCE

at the

MASSACHUSETTS INSTITUTE OF TECHNOLOGY

January, 1981

Signature of Author Signature redacted
Department of Civil Engineering
January 20, 1981

Certified by Signature redacted
Gedaliah Shelef
Thesis Supervisor

Accepted by Signature redacted
C. Allin Cornell
Chairman, Department Committee

HYDRAULICS OF PADDLE WHEELS IN HIGH-RATE ALGAE PONDS

by

SACHA SETHAPUTRA

Submitted to the Department of Civil Engineering
in January 1981, in partial fulfillment of the requirements
for the Degree of Master of Science

ABSTRACT

Analytical and experimental analysis of paddle wheels as used in wastewater treatment high-rate algae ponds were conducted. It was found experimentally that the efficiency of paddle wheels in transfer of mechanical energy to water flow energy depends primarily on the paddle wheels' geometry such as the radius, the width, the number of paddles and the submergence.

An analytical approach based on the concept of the drag coefficient was developed. The drag coefficient was determined by calibrating the analytical model with the experimental data. The calibrated model can be used to estimate the speed of rotation and the power input required from the specified wheel dimensions and flow conditions in the pond.

With this analytical design approach, it is possible to improve the efficiency of the paddle wheels from the level of 20-25 percent currently attainable to 40-70 percent. Thus, the foreseeable improvement in efficiency is in the order of two to three fold. Since the paddle wheels constitute the major energy demand in the operation of the ponds, the improvement can have a significant effect on the overall economics of the high-rated algae pond systems.

Thesis Supervisor: Gedaliah Shelef
Title: Professor of Civil Engineering

ACKNOWLEDGEMENT

I wish to give special acknowledgement to the support, advice and personal interest of my advisor, Professor Gedaliah Shelef.

Appreciation is extended to Margaret Ann Underdown for her expert typing and Patricia Dixon for general assistance in the research project without which this work would not be accomplished. Ed McCaffrey and Arthur Rudolp's help in apparatus fabrication is very much appreciated. I am also grateful to Professor Keith Stolzenbach for his invaluable suggestions.

The faculty, staff and fellow students of the Ralph M. Parsons Laboratory have provided a congenial and stimulating working environment.

TABLE OF CONTENTS

TABLE OF CONTENTS (Contd.)

LIST OF SYMBOLS

A, $\bar{A}$ = sections of flow in the channel

b = width of the paddle wheel

b_m = minimum width of the paddle wheel

B = width of the channel

B, $\bar{B}$ = sections of flow in the channel

C = a section of flow in the channel

C_D = drag coefficient

C_{FR} = frictional coefficient of the bearings ($= \mu R_B$)

C_L = leak coefficient

d = depth of submergence

e = efficiency of the paddle wheel

f = force due to fluid friction

$F_{\bar{A}}$ = force acting on the water control volume of section $\bar{A}$

$F_{\bar{B}}$ = force acting on the water control volume at section $\bar{B}$

F_H = force acting on the water control volume by the wheel

F_h = horizontal force on an individual paddle

F_{hT} = horizontal force on all paddles in contact with water

$\bar{F}_{hT}$ = representative steady-state value of F_{hT}

F_{SA} = force acting on the water control volume by the downstream side of the sill

F_{SB} = force acting on the water control volume by the upstream side of the sill

F_v = vertical force on an individual paddle

F_{vT} = vertical force on all paddles in contact with water

$\bar{F}_{vT}$ = a representative steady-state value of F_{vT}

g = gravitational constant

h = liquid level difference

k_1 = number of 90° bends in the channel (pond)

k_2 = number of 180° bends in the channel (pond)

L = length of the channel in the pond

m = a dimensionless number used to prescribe the shape of the water surface profile in the wheel

n = the Manning's roughness coefficient of the channel

N = number of paddles in the wheel

P_A = power loss due to air turbulence created by the rotating wheel

P_{FR} = power loss due to bearing frictions

P_{in} = power input at the wheel shaft

P_w = water power including the losses at the contraction and expansion

P'_w = water power excluding the losses at the contraction and expansion

P_{wh} = power delivered to the paddles

Q = flow rate in the channel

Q_a = flow rate through the wheel

R = radius of the wheel

R_B = effective radius of the wheel bearings

$\bar{R}$ = hydraulic radius of the channel

S = sill height

S_c = critical sill height

T = torque on an individual paddle (except in Chapter 3 where it is the total torque applied to the wheel)

T_{FR} = torque due to bearing friction

T_T = torque on all paddles in contact with water

$\bar{T}_1$ = representative steady-state value of T_T

U = total force acting on the bearings

V_A = velocity of flow at section A

$V_{\bar{A}}$ = velocity of flow at section $\bar{A}$

V_B = velocity of flow at section B

$V_{\bar{B}}$ = velocity of flow at section $\bar{B}$

V_w = velocity of flow under the wheel

w = rotating speed of the wheel

W = weight of the wheel

x = distance from the wheel rotating center to the point where the paddle meets the water

x_h = dimensionless horizontal force on individual paddle

x_H = dimensionless horizontal force on the multiple-paddle wheel

x_v = dimensionless vertical force on individual paddle

x_V = dimensionless vertical force on the multiple-paddle wheel

x_t = dimensionless torque on individual paddle

x_T = dimensionless torque on the multiple-paddle wheel

y = depth of flow

y_A = depth of flow at section A

$y_{\bar{A}}$ = depth of flow at section $\bar{A}$

y_B = depth of flow at section B

$y_{\bar{B}}$ = depth of flow at section $\bar{B}$

y_o = static water depth

$\bar{y}_o$ = average water depth at the wheel

α = an angle associated with the wheel geometry

$\bar{\alpha}$ = an angle associated with the wheel geometry

β = angle formed between paddle and the radial line from the wheel center

γ = specific weight of the water in the pond

δ = an angle associated with the wheel geometry

θ = a variable angle specifying the location of paddles

θ_o = initial value of θ

μ = coefficient of friction of the bearings

ρ = density of the water in the pond

ψ = angle formed between two adjacent paddles

LIST OF FIGURES

LIST OF TABLES

CHAPTER I: INTRODUCTION

1.1 Overview

1.2 Statement of Problem and Purposes

1.3 Scope and Approach

1.4 Outline of the Report

1.5 Literature Review

a. History of paddle wheel uses

b. Present uses of paddle wheels

Use of paddle wheels in high-rate algae ponds

c. Analytical work on paddle wheels

Existing rule of thumb

d. High-rate algae ponds

Economic aspects

e. Depth and velocity in high-rate ponds

f. Roughness coefficient in high-rate ponds

CHAPTER I

INTRODUCTION

1.1 Overview

Future population demands on world resources will necessitate resource conservation of the highest order. Treatment of waste by conventional techniques such as activated sludge plants and aerated lagoons without reclamation of nutrients and reuse of the treated water is both expensive and wasteful. Algae can be used to treat and recycle wastewater and itself can be used as food for animals [1]*. Algae play an important role in the photosynthetic process of a facultative stabilization but even more so in the more intensive "High-Rate Algae Pond" (HRAP). A schematic diagram for wastewater treatment and algae harvesting utilizing a high-rate algae pond is shown in Fig. 1.1.

The process begins with influent wastewater which may be domestic or agricultural. Some pretreatment, such as bar screening and comminution can be provided. The influent is added continuously to the pond which is mixed continuously so that the algae is kept in suspension and no thermocline is being formed. The pond effluent is the mixture of algae and water. Algae are harvested and dried by some means and can be used as animal feed. The clarified pond effluent can be reused for agricultural purposes or disposed.

The purpose of the high-rate pond is to utilize sunlight for algae photosynthesis. During photosynthesis, the algae produce oxygen which is used by bacteria for biodegradation of waste organics fed into the pond as wastewater. Conversion of waste nutrients into algae is enhanced if the

*Number in [ ] indicates the reference number.

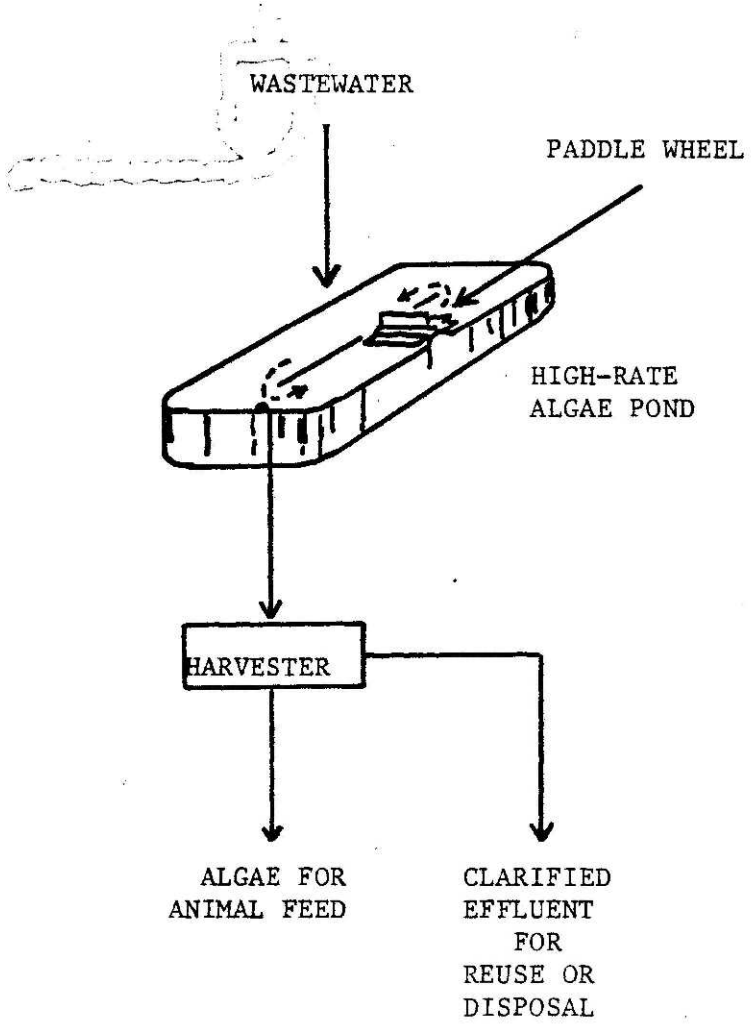

Fig. 1.1 Scheme for Wastewater Treatment by High-Rate Algae Pond

algae are dispersed throughout the pond depth. This is accomplished by circulating the water in the pond continuously. The circulation also prevents stratification that will occur as a result of solar light absorption at the upper part of the pond cross section.

In order to achieve this, a slowly rotating paddle wheel is normally used (Fig. 1.1). The rotating wheel gives rise to a small water level difference or head, in the order of 2 $\sim$ 10 cm, between its downstream and upstream sides. This head causes the water to circulate in the pond. Paddle wheels are employed (instead of other pumping devices such as centrifugal pumps) because they provide gentle agitation that does not disturb the growth of algae and they are relatively simple and inexpensive. A rotating paddle wheel requires energy which is usually supplied by a motor or an engine through some sort of speed reduction devices. Since the paddle wheel constitutes the major energy demand in the operation of the algae pond, a properly designed paddle wheel can have an important impact in the energy requirement and the overall economics of the HRAP system.

1.2 Statement of Problem and Purposes

Up to now, there are no analytical procedures for paddle wheel design that enable the wheel performance to be estimated. The practical question that has to be answered is - given a high-rate pond with specified flow requirements, what should be the wheel geometry, dimensions and speed of rotation, such that the power requirement is minimum. The present study intends to answer the above question. To be specific, the purposes of the present study are:

(i) to analyze the hydraulics of paddle wheels using theoretical and experimental approaches

(ii) to determine the major factors affecting the efficiency of paddle wheels

(iii) to develop an analytical procedure for paddle wheel design.

1.3 Scope and Approach

Paddle wheels such as those used in algal ponds are a kind of hydraulic pump. Their main function is to provide enough head (difference in water levels between the downstream and upstream sides of the wheel) required to push the water to flow at an average velocity at the given depths. A paddle wheel converts mechanical energy into water flow energy by receiving energy through a rotating shaft connected to a prime mover such as an electric motor and releasing that energy through the interaction of its paddles and the water. In the process of energy transfer, there are inevitably some energy losses. These losses affect directly the efficiency and performance of the paddle wheel.

The energy (or power) flow diagram for a paddle wheel is shown in Fig. 1.2 where the energy flows from left to right. Starting with the energy available at the output shaft of a prime mover, some energy is lost in the mechanical power transmission devices such as gear boxes, belts or couplings.

During operation, the top half of the wheel is exposed to ambient air and may be subject to the effect of wind velocity. The wheel rotation causes air turbulence which extracts some part of the energy. Some energy is lost in the bearings due to the inherent bearing friction. From this point on, the energy reaches the paddles. Part of it is lost due to leakage, eddies, waves, bubbles and noise. The rest of the energy is converted to the useful water energy which maintains the circulatory flow in the pond.

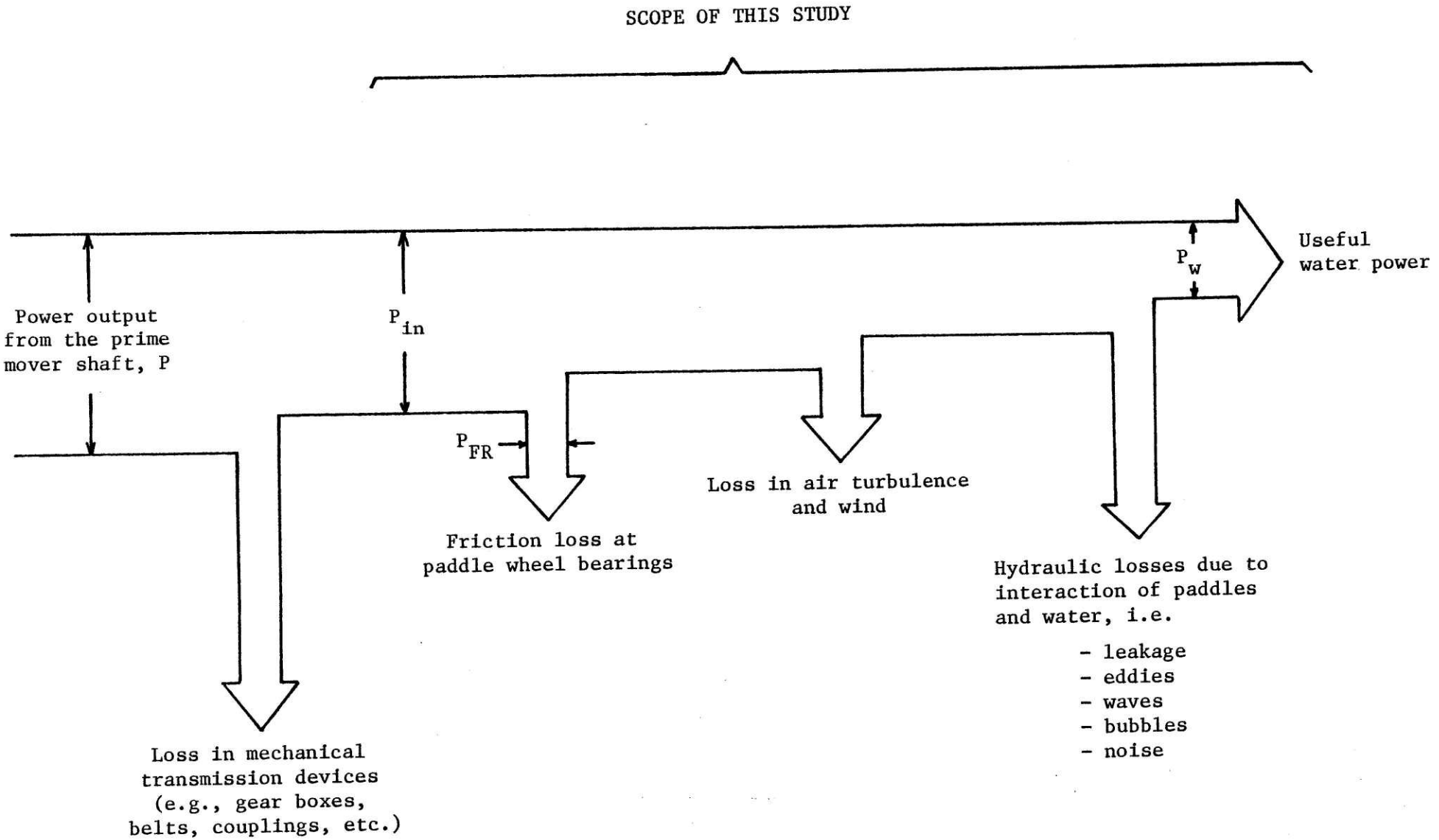

Fig. 1.2 Energy Flow Diagram for Paddle Wheels

The scope of this study covers only the indicated portion of the energy flow diagram in Fig. 1.2, i.e., the study does not include the energy losses in mechanical transmission devices. In addition, it ignores the bio-chemical reaction occurring during the pond operation. It assumes that the mixture (water + bacteria + algae + nutrients + etc.) behaves hydraulically similar to fresh water at all times irrespective of the biomass and nutrient concentrations.

In this study, both laboratory work and development of an analytical description of a paddle wheel are pursued. The laboratory results are used to calibrate and verify the analytical model. After being calibrated and verified, the steps in the analytical model are translated into the design procedure. Flow observation from laboratory study also reveals significant limitations of paddle wheels capability in delivering the head required for the circulatory flow.

1.4 Outline of the Report

In this report, Chapter 1 provides the background information on paddle wheels and high-rate algae ponds. Chapter 2 presents the analysis aiming at assessment of paddle wheel performance. The analysis has to use experimental data to determine the drag coefficient (C_D) required in the process. Chapter 3 describes the apparatus used for experimentation. Chapter 4 combines the analysis of Chapter 2 and experimental data of Chapter 3 to determine the value of C_D. Chapter 4 also describes observation of events occurring in paddle wheel operation. The previously determined value of C_D together with the analysis of Chapter 2 are combined to produce a design flow chart applicable to the design of energy efficient high-rate algae ponds and paddle wheels in Chapter 5. Chapter 6 concludes

the findings and presents an assessment on foreseable improvements in paddle wheel efficiency when the design procedure of Chapter 5 is used.

1.5 Literature Review

(a) History of Paddle Wheel Uses

Historically, paddle wheels had been used as three types of devices: (i) pumping devices, (ii) propulsion devices and (iii) turbine devices. As pumping devices, paddle wheels were probably used by the ancient Egyptians for irrigation. No documents were available except for some rare archaeological evidence that can be inferred to the use of paddle wheels during that era. In South East Asia, paddle wheels made of wood have been used in rice paddy irrigation for many hundreds of years and still can be found today. These primitive machines were usually driven by animals, man or wind.

In the 19th century, paddle wheels were used extensively as a propulsion device in steam ships in North America and Britain. All of the literature available concerns the historical aspect of the ships [2 to 9]. Very scant engineering information can be extracted from this literature. It was probably due to the invention of the steam engine by James Watt and Matthew Boulton (1774) that initiated the use of paddle wheels in steam ships. During that time, the engineering attention was mainly focused on the development of reliable steam engines. According to BODY [5] one of the main problems was the explosion of boilers.

During the period of paddle steamer development the paddle wheel was given some attention. At first floats were fixed and were notable for the mighty thump with which they hit the water and the amount of useless energy expended in lifting water as they emerged. Schemes for improvement

were mainly directed towards feathering paddles. Analysis of feathering paddle wheels can be found in SAUNDERS [10].

Paddle wheels were also used as water turbines during the ninteenth century. Historical account of the development of water wheels is discussed in SMITH [11]. Analytical work on turbine aspect of paddle wheels is better documented than both the pumping and propulsion aspects. The earliest documented work on turbine aspect of the paddle wheel is that by BACH, 1886 [12].

(b) Present Uses of Paddle Wheels

At present paddle wheels are mostly used in water and wastewater treatment work as mixing or aerating devices. As mixing devices, they are used mainly for flocculation processes and they are usually fully submerged during operation. Their power consumptions can be estimated from the drag produced by the liquid resistance at the paddles. Analysis of these devices is treated in most standard textbooks in wastewater engineering such as METCALF & EDDY [13] and FAIR, GEYER and OKUN [14].

Another present use of paddle wheels is in military amphibious vehicles [10]. Paddle wheels are used because they can work as propulsion devices in water and as treading devices on land. This enables only one propelling mechanism to be used on such vehicles.

A special form of paddle wheel is used as an aerator in an oxidation ditch. These wheels consist of many small paddles arranged such that, when rotating, they provide an opportunity for oxygen in the ambient air to be dissolved readily into the wastewater in the ditch. Here, the "splashing" of water droplets is encouraged to enhance oxygen transfer. These devices are usually known as 'brush aerators', 'Pasveer wheels', 'cage rotors' or 'bladed rotors'. The wheel also provides circulation of

water in the ditch which is an advantage for the intended biological process occurring in the ditch.

Experimental data relating to power consumption, speed of rotation and oxygenation capacity for various sizes and shapes of brush aerators were conducted by BAARS and MUSKAT [15]. The graphs summarizing these data can be used for design purposes. One example of such use is discussed in AGRAMAN and SPIVAK [16].

Uses of paddle wheel in high-rate algae pond:

Recent development in algae cultivation in a high-rate pond utilizing nutrients abundantly available in domestic and agricultural wastewater leads to the use of paddle wheels as a pumping device. Theoretically, any other pumping devices such as centrifugal pumps can be used. However, it is evident that most researchers rely on paddle wheels. The apparent reasons for this are:

(i) Paddle wheels are simple and inexpensive to construct due to their slow rotation speed. There are no components that require high precision fabrication.

(ii) Operation of paddle wheels do not disturb the growth of algae in contrast to other pumping devices such as centrifugal pumps.

The experimental data for brush aerators (BAAR and MUSKAT [15]) is not applicable to paddle wheels in high-rate ponds. The purpose of the paddle wheels in high-rate ponds is to circulate water in the pond and not for aeration purposes as in the case of a brush aerator. The aeration or oxygenation in the pond is to be accomplished by algal photosynthesis.

The efficiency of a brush aerator with respect to creating the

circulatory flow alone is in the order of five percent (ARGAMAN and SPIVAK [16]). This is because part of the energy is used for aeration, i.e., creating water droplets, bubbles and turbulence. A paddle wheel in a high-rate pond designed to circulate the water without aeration can attain a higher efficiency than that of the brush aerator.

(c) Analytical Work on Paddle Wheels

At present there is no literature available on design of paddle wheels. This is probably because most of the users of paddle wheels - those concerned with high-rate algae ponds - focus their attention on the biomass production and algae harvesting which are of primary importance. An attempt to estimate the efficiency of the wheel by measuring the power input (in the form of power transmitted through a shaft) and the power output (water power) was made by BENEMANN et al. [17]. The document reported the average efficiency of the paddle wheel used in the study to be approximately 64%. Another attempt by ARGAMAN and SPIVAK [16] using a brush aerator to create the circulatory flow reported their wheel efficiency to be in the order of 2 to 10%. The difference can probably be attributed not only to the inaccuracy in measurement but also to the fact that ARGAMAN and SPIVAK's brush aerator was primarily designed for oxygenation (aeration) rather than purely creating the circulatory flow as in the case of BENEMANN et al. [17]. ARGAMAN and SPIVAK's wheel resembled that of BARRS and MUSKAT [15], the data of which were used to estimate the required power input.

Existing Rules of Thumb

The only known analytical procedure for the design of a paddle wheel can be summarized as follows:

First, the head loss corresponding to the design velocity of flow in the channel is estimated. One way to estimate this is to use the Manning's equation with assumed value of the Manning's roughness coefficient. From the head loss, the water power (= specific wt of water x flow rate x head loss) can be determined. It is then assumed that the wheel efficiency is about 25% which enables the required power input to be estimated. The 25% efficiency is purely guess work. This computed power input does not include the power loss in the power transmission devices such as a gear box, belt, etc. In order to determine the size of the wheel, it is assumed that the velocity of the paddle at the wheel perimeter is about 2 times the average velocity of flow in the channel. Assuming a reasonable wheel radius, the required wheel speed can be determined. The width of the wheel (i.e., the length of the wheel measured in the direction of its axis of rotation) is taken to be the same as the width of the channel. This procedure enables the wheel to be designed. However, there are some important parameters of the wheel that have to be specified - for example; the depth of submergence and the number of paddles. These parameters significantly affect the wheel's efficiency.

Without any detail analysis, it can be inferred that the above design procedure usually results in overall overdesign of the paddle wheel - otherwise the constructed wheel could not operate and the procedure could have been changed. However, overdesign means higher than necessary initial and operating costs.

If an improved design procedure exists, that will lead to a more efficient paddle wheel, the result will be the significant saving in energy input, operating costs and capital investment.

(d) High-Rate Algae Ponds

The concepts of waste oxygenation and stabilization occurring in a high-rate pond are embodied in Fig. 1.3. In the figure, organic wastes enter a cycle containing two groups of micro-organisms, aerobic bacteria and micro-algae. The bacteria oxidize the biodegradable organics in the entering wastes and produce mainly bacterial biomass, carbon dioxide and ammonia. The bacterial biomass is decomposed within the system when the bacteria die or is harvested together with the algae while carbon dioxide, ammonia and other decomposition products are taken up by the algae which in the presence of sunlight produce, through photosynthesis, both oxygen and algae biomass. Oxygen is used immediately for bacterial oxidation while nutrients such as nitrogen and phosphorus are removed by incorporation into the harvestable biomass. Design aspects of high-rate ponds can be found in OSWALD [18] and OSWALD et al. [19].

The beneficial uses of high-rate algae ponds include wastewater treatment, protein production, water reclamation, biomass production for fuel and fertilizer. In terms of wastewater treatment, high-rate ponds can be a more simple, reliable and economical method of attaining a high degree of secondary and tertiary waste treatment than are the systems currently applied when climatic conditions of abundant solar insolation and moderate to high temperature prevail.

The bioregenerative farm concept discussed by SHELEF [1] offers another promising solution to the developing countries in an effort to increase food for human consumption. It is based on a model-farm in rural regions of developing countries when domestic and farm wastes are recycled and recovered to a maximum level through a chain of biological processes and farming practices. McGARRY and TONGKASAME [22] studied an Asian urban

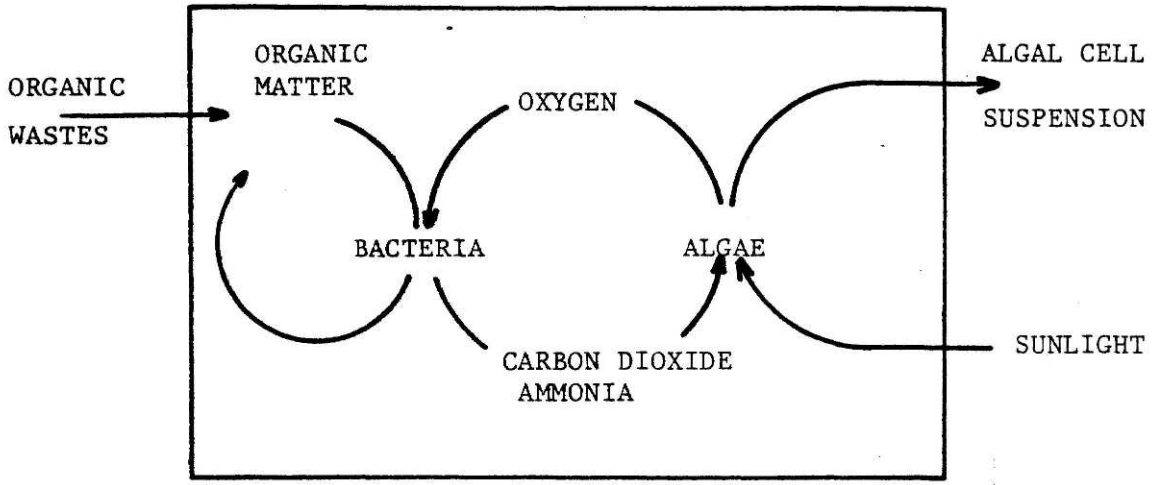

Fig. 1.3 Cycle of Photosynthetic Oxygenation in High-Rate Algae Ponds [19]

model that incorporates recycling of the reclaimed clarified effluent for household cleaning purposes while potable drinking water would be supplied through a separate distribution system. They also claim that use of such a dual distribution system with reclamation would effect a two-thirds reduction of conventional water supply requirements.

The cultivation technology of microalgae for solar energy conversion was investigated by BENEMANN et al. [18]. The key aspects studied were maintenance of a stable high productivity culture and the development of low-cost harvesting technologies. An engineering-economic feasibility analysis indicates that the production of microalgal biomass for chemicals and fuels may be feasible at favorable locations if a simple bioflocculation-settling harvesting process can be developed.

Economic Aspects

Economic aspects of algae production on sewage in high-rate algae ponds was considered by SHELEF et al. [21]. These economic considerations are based on two premises: (i) the cost-benefit analysis of combined treatment and resource recovery, and (ii) the comparison of costs between algal sewage treatment plants and conventional activated sludge plants. Figure 1.4 indicates schematically and conceptually the basic cost-benefit approach of wastewater treatment combined with resource recovery of by-products. The by-products for algal wastewater treatment systems are the reclaimed water and algal protein which can be used for irrigation and animal feed, respectively.

In Fig. 1.4, the horizontal axis indicates the cost of the system in relative terms while the vertical axis indicates values (in the same relative terms as above) of direct benefit and damage prevented, respectively. Both horizontal and vertical axes have the same arbitrary

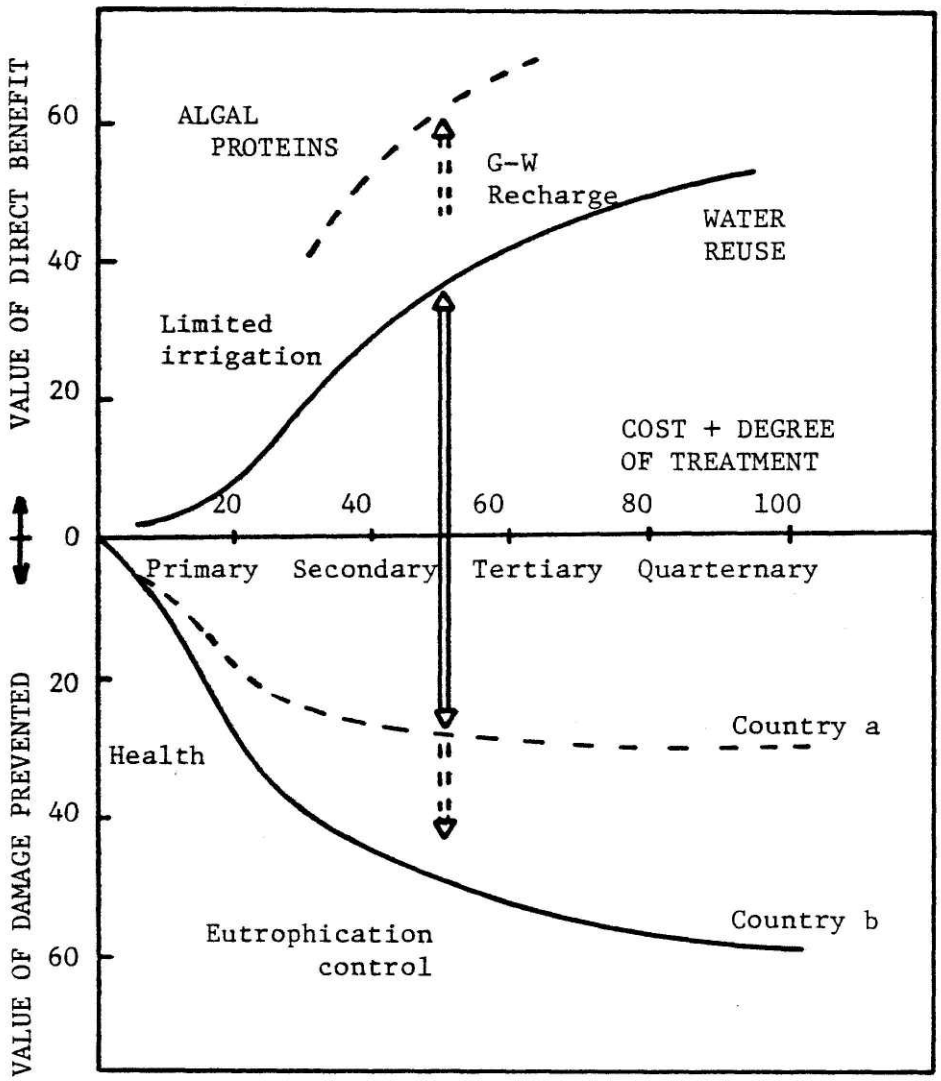

Fig. 1.4 Schematic Cost-Benefit Analysis of Wastewater Treatment by High-Rate Algae Ponds [21].

scale. For example, the benefits of wastewater treatment by high-rate algae ponds are (i) the value of reusable water, (ii) the value of algal proteins and (ii) the prevention of health hazards as well as eutrophication that would have occurred if wastewater is untreated. The length of the arrow in the figure indicates the combined benefits. The curves for countries a and b in the figure indicate the difference in priority assigned to health and environment among countries.

(e) Depth and Velocity in High-Rate Ponds

The major factor that determines the feasible depth of an algae production pond is the extent of light penetration. The desired depth as a function of algal concentration and incident light intensity is given by BOGAN et al. [23] as shown in Table 1.1.

The data are based on the absorption of light energy as determined according to the Beer-Lambert Law, an extinction coefficient of 2×10^{-3} cm^2/mg and a lower light limiting range of 1000 foot-candles. In practice, the depth usually ranges from 20 to 40 cm. depending on incident light intensity and climatic conditions. In countries where annual temperature fluctuation is significant, it may be necessary to operate the pond at different depths during different seasons. An example taken from SHELEF et al. [24] is shown in Table 1.2.

Mixing in high-rate ponds is necessary in order to: (1) disperse nutrients, dissolved gases and microbial cells such that all are in contact with each other; (2) keep algae and bacterial cells in suspension, and (3) breaking up thermal stratification. Mixing can be accomplished by circulating the flow of wastewater in the pond at a certain velocity and it is usually done with paddle wheels. A rotating paddle wheel creates

Table 1.1 Relationship Between Incident Light Intensity and Depth [23]

Algal Concentration (mg/liter)	Depth in cm for Corresponding Incident Light Intensity			
	1,000 foot-candles	2,000 foot-candles	5,000 foot-candles	10,000 foot-candles
50	23	30	39	46
100	11.5	15	19.5	23
200	5.8	7.5	9.8	11.5
400	2.9	3.8	4.9	5.8

NOTE: Algae concentration such that light intensity at any depth is 100 foot-candles.

Table 1.2 Operational Data from Four Seasons of Operation of Ponds with Variable Depths and Detention Times in Haifa, Israel [24]

	Fall 1978	Winter 1978/79	Spring 1979	Summer 1979	Average
Pond depth (cm)	40	50	35	25	37.5
Retention (days)	3.4	4.25	2.9	2.0	3.14
Pond effluent biomass (mg/l)	385	240	400	440	366
Biomass production (g/m^2-day)	45.3	27.7	48.4	55.0	44.2
Algal biomass production (g/m^2-day)	24.7	11.0	29.0	35.6	25.2
Solar radiation (cal/cm^2-day)	418	335	540	653	488
Algal solar conversion efficiency (based on total irradiance)	3.25	1.81	2.95	3.00	2.84
Total seasonal (yearly) dry biomass production (t/ha)	41.2	24.9	44.5	50.6	(161)

difference in water levels between its downstream and upstream sides. The water level difference in turn causes the wastewater to flow. The average flow velocity, i.e., the flow rate divided by the cross-sectional area of flow, can be used as an indicator to the degree of mixing. If this velocity is too low, an excessive settling of algal and bacterial biomass will occur, nutrients and gas supply to algal and bacterial biomasses will be impaired, severe thermal stratification will occur resulting in failure of the pond. On the other hand, too high velocity may shock the algal culture, may bring to suspension undesirable bottom sludges, could cause scouring and erosion of the bed and constitute an unnecessary waste of energy. In practice, the velocity usually ranges from 3 to 20 cm/sec. in wastewater treatment ponds and from 20 to 40 cm/sec. in algae grown on inorganic media.

(f) Roughness Coefficient in High-Rate Ponds

In designing a high-rate pond, the power required to cause the wastewater to flow at the desired velocity depends on the magnitude of the velocity, the channel roughness, channel geometry and the number of channel bends. The channel roughness is characterized by the roughness coefficient, n, which depends on the type of materials used to construct channel walls and bed. The values of n for various materials are shown in Table 1.3 which is taken from CHOW [25].

Table 1.3 Values of the Roughness Coefficient [25]

Type of channel and description	Minimum	Normal	Maximum
LINED OR BUILT-UP CHANNELS			
Metal			
a. Smooth steel surface			
1. Unpainted	0.011	0.012	0.014
2. Painted	0.012	0.013	0.017
b. Corrugated	0.021	0.025	0.030
Nonmetal			
a. Cement			
1. Neat, surface	0.010	0.011	0.013
2. Mortar	0.011	0.013	0.015
b. Concrete			
1. Trowel	0.011	0.013	0.015
2. Float finish	0.013	0.015	0.016
3. Finished, with gravel on bottom	0.015	0.017	0.020
4. Unfinished	0.014	0.017	0.020
5. Gunite, good section	0.016	0.019	0.023
6. Gunite, wavy section	0.018	0.022	0.025
7. On good excavated rock	0.017	0.020	
8. On irregular excavated rock	0.022	0.027	
c. Brick			
1. Glazed	0.011	0.013	0.015
2. In cement mortar	0.012	0.015	0.018
d. Masonry			
1. Cemented rubble	0.017	0.025	0.030
2. Dry rubble	0.023	0.032	0.035
e. Asphalt			
1. Smooth	0.013	0.013	
2. Rough	0.016	0.016	
f. Earth	0.016	0.018	0.02

CHAPTER II: ANALYTICAL APPROACH

2.1 Assumptions

Steady flow assumption

2.2 Hydraulic of Flow in the Pond

a. Flow in channel from A to C to B
   Head loss

b. Flow through contraction from B to $\bar{B}$
   Limitation to the width of the wheel - choked flow

c. Flow through the wheel from $\bar{B}$ to $\bar{A}$
   Momentum equation
   Limitation to the sill height - choked flow
   Leakage

d. Flow through expansion from $\bar{A}$ to A

e. Power required for the flow

f. Notes on computation

2.3 Analysis of Wheel

a. Wheel with single paddle
   Horizontal component of force
   Vertical component of force
   Torque
   Force and torque diagrams

b. Wheel with multiple paddles

c. Power consumption

d. Notes on computation

e. Variation of the drag coefficient, C_D

2.4 Summary of the Analytical Model

2.5 Characteristic Curves

2.6 Optimum Pond Dimensions

CHAPTER II

ANALYTICAL APPROACH

The purpose of this chapter is to describe the analytical method used to assess the performance of a paddle wheel in a high-rate algae pond. Section 2.1 points out the major assumptions made in the analysis. In Section 2.2, the classical theory of hydraulics in open channel flow is applied to describe the flow in the pond. Section 2.3 attempts to quantify the conversion of mechanical energy to water flow energy which occurs through the interaction between rotating paddles and the water surrounding them. The analysis of Sections 2.2 and 2.3 are then combined to form an analytical model described in Section 2.4. The analytical model is then used to produce a set of characteristic curves which can be used to describe the performance of paddle wheels in high-rate algae ponds. These characteristic curves are hypothetical in a sense that they have not been verified with an actual system - which is done in Chapter 4. Finally, in Section 2.6 the design of a suitable pond configuration is discussed.

Diagrammatic layout of the paddle wheel in a high-rate algae pond system is shown in Fig. 2.1(a). In the figure, the paddle wheel width is b while the channel width is B which is assumed to be constant for the entire channel. The channel is assumed to be rectangular. Sections $\bar{A}$ and $\bar{B}$ represent the flow sections immediately downstream and upstream of the wheel respectively. Water flowing from section $\bar{A}$ to section A undergoes expansion in channel width from b to B. From section A, the water flows along the channel to section C and section B. The water then flows from section B to section $\bar{B}$ where the channel width contracts from B to b. This completes the cycle of flow in the pond. In an actual pond, the path of the channel may be more meandering than the one shown in Fig. 2.1(a) in order to accommodate a longer channel in the same area.

2.1 Assumptions

As usual with most fluid flow phenomena, flow of water created by paddle wheels is very complicated. Analytical description of the phenomenon can not be made without making some assumptions. Part of the assumptions made in the following discussion are those assumptions normally employed in the traditional hydraulic analysis of open channel flow, such as hydrostatic pressure distribution and uniform velocity in a channel. These assumptions are somewhat well tested and perhaps need no further verification. On the other hand, there are some assumptions, made in the following discussion, that are needed for the sake of analysis.

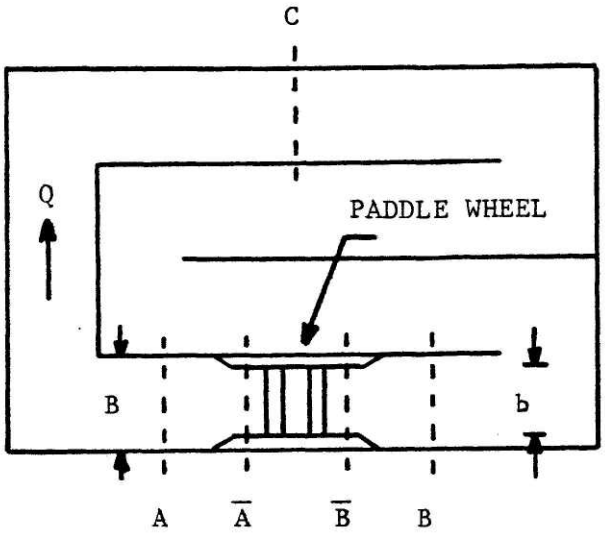

(a) Diagram of High-Rate Algae Pond

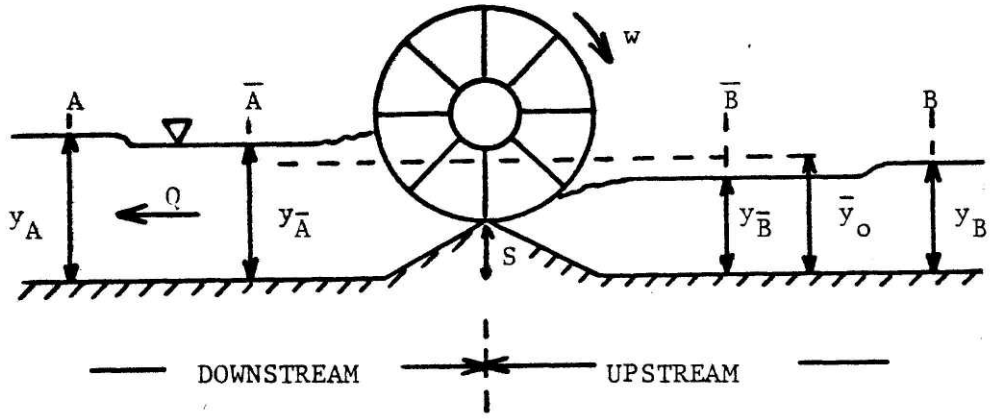

(b) Flow Condition at the Wheel

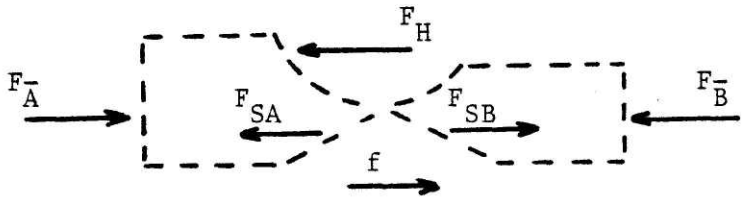

(c) Control Volume of the Water

Fig. 2.1 Schematic Paddle Wheel Layout

These assumptions may or may not be acceptable with respect to what actually happens, depending on the ability of the analytical model in predicting the performance of the paddle wheel which can be verified by experiment. This is the reason why laboratory tests of paddle wheels must be conducted.

Steady-flow assumption

If we consider the motion of the rotating paddles, a quantity of water is captured in the chamber formed between two adjacent paddles while the chamber is in the upstream side (see Fig. 2.1(b)). As the wheel rotates, the chamber moves from upstream side to downstream side while releasing the water to the downstream side. The water is transported in the form of "lumps". The number of lumps transported per second and the volume of water in a lump depend on the wheel rotation speed, geometry and the hydraulic conditions in the vicinity of the wheel. As a result, the flow of water through the wheel is not a steady flow even if the wheel speed is constant. It depends on time in a periodic fashion determined by the wheel speed. It is, however, necessary to assume that the flow can be considered steady in the following analysis for the simple reason that unsteady flow as described above is too complicated to be analyzed.

There are other specific assumptions that will be raised in the following analysis when it is appropriate to do so.

With reference to Fig. 2.1(a), we will separate our analysis into two major sections, i.e., (i) the water and (ii) the wheel. By (i) we intend to understand the physical factors that are required to cause the

water to flow in the channel from A to C to B at the average velocity V_o and average depth y_o required in the pond. By (ii) we intend to understand the process in which energy (or power) is transferred from the wheel to the water. These two conditions must be compatible and simultaneously satisfied. The following two sections discusses these aspects.

2.2 Hydraulics of Flow in the Pond

The analysis in this section follows the traditional analysis in open channel flow such as in HENDERSON [27] and CHOW [26]. It is repeated here to facilitate future reference to be made in this report. The analysis is made assuming that the channel is rectangular with constant width B. The above two references also cover analysis for shapes of channel cross sections other than rectangular. The following headings are made with reference to Fig. 2.1(a).

(a) Flow in channel from A to C to B

Assuming steady flow and horizontal bed, the flow profile in the channel from A to C to B is of the H_1 type as shown diagrammatically in Fig. 2.2.

The energy equation can be written

$$y_A + \frac{V_A^2}{2g} = y_B + \frac{V_B^2}{2g} + h$$

where y and V are the depth and velocity of flow at the sections indicated by subscript, g is the gravitional constant and h is the

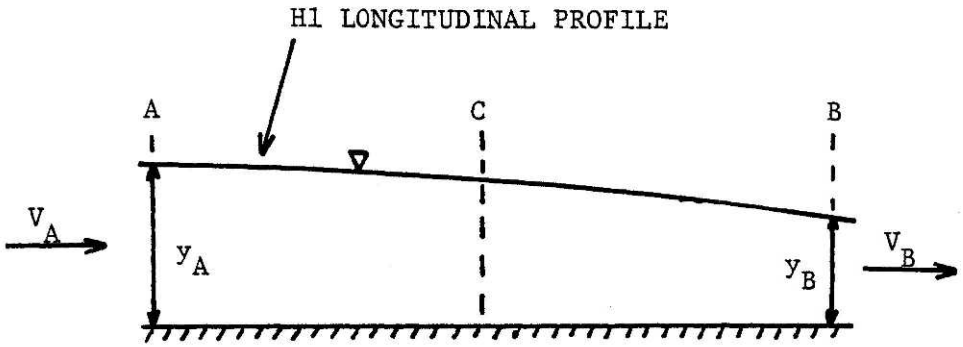

Fig. 2.2 Flow Profile in Channel

head loss in flow from A to B. In most cases, the velocity head terms, $\frac{V^2}{2g}$, are much smaller than the other terms and can be neglected. Thus, the above equation can be written as

$$y_A \cong y_B + h$$

If the channel length (measured from sections A via C to B) is not too long, the longitudinal profile of the water level in the channel can be approximated by a straight line (instead of the indicated H_1 curve). In such a case

$$y_A = y_o + \frac{h}{2} \qquad (2.1)$$

and

$$y_B = y_o - \frac{h}{2} \qquad (2.2)$$

where y_o is the static water depth in the channel.

Head loss

The head loss h is caused by the flow resistance in the channel which can be attributed to the channel roughness and bends. The loss due to roughness can be estimated using the Manning equation to be

$$\frac{V_o^2 n^2 L}{\bar{R}^{4/3}}$$

where V_o = average flow velocity

n = Manning's roughness coefficient

L = length of the channel

$\bar{R}$ = hydraulic radius = $B y_o/(B + 2 y_o)$

B = width of the channel

It should be noted that the loss due to roughness, $\frac{V_o^2 n^2 L}{\bar{R}^{4/3}}$ is to be computed based on the Metric System of units, i.e., V_o in m/sec, L and R in m and n can be obtained from the Table in most hydraulic texts (see Table 1.3).

The loss due to a bend can be expressed as $c \frac{V_o^2}{2g}$ where c is a coefficient depending mainly on the bend radius, the width of the channel and the bend angle. The detail discussion of the determination of c can be found in HENDERSON's section 7.3 and VEN TE CHOW's section 16.3. In this study it is assumed that the values of c for 90° and 180° bends are 8 and 16, respectively. Using these values, it follows that the head loss due to bends in a pond can be written as

$8 (k_1 + 2 k_2) \frac{V_o^2}{2g}$

where k_1 = number of 90° bends

k_2 = number of 180° bends

Future experiments may provide a better estimate of the bend loss coefficient. However, it is not the scope of this present study.

Combining the head loss due to channel roughness and bends we obtain the total head loss

$$h = \left[\frac{2g\, n^2 L}{\left(\frac{B\, y_o}{B + 2y_o} \right)^{4/3}} + 8(k_1 + 2\, k_2) \right] \frac{V_o^2}{2g} \qquad (2.3)$$

Actually, h can be determined more accurately by considering that the average velocity of flow (discharge/cross-sectional area) is not constant along the length of the channel due to the nature of non-uniform flow. This is equivalent to plotting of the flow profile or "Back Water Curve".

By continuity, the flow rate Q in the channel is $V_o\, y_o\, B$. Using Eq. (2.3) the relationship between Q and h can be written

$$Q = C_A\, h^{C_B} \qquad (2.4)$$

where

$$C_A = \frac{B\, y_o \sqrt{2g}}{\left[\frac{2g\, n^2 L}{\left(\frac{B\, y_o}{B + 2y_o} \right)^{4/3}} + 8(k_1 + 2\, k_2) \right]^{1/2}}$$

and $C_B = 0.5$

Eq. (2.4) indicates that Q is proportional to $\sqrt{h}$.

The power required can be computed from

$$p'_w = \gamma Q h \tag{2.5}$$

(b) Flow through contraction from B to $\bar{B}$

The energy equation applicable to this situation can be written as

$$y_B + \frac{V_B^2}{2g} = y_{\bar{B}} + \frac{V_{\bar{B}}^2}{2g} + 0.23 \frac{V_{\bar{B}}^2}{2g} \tag{2.6}$$

where $V_B = Q/(B\, y_B)$

$V_{\bar{B}} = Q/(b\, y_{\bar{B}})$

and the last term on the right hand side represents the energy loss term. The coefficient 0.23 is taken from HENDERSON's section 7.2. It depends on the design of the transition structure. Smooth design reduces it. The value we use (0.23) is somewhat conservative. Knowing Q, B, y_B and b, we can determine $y_{\bar{B}}$ from Eq. (2.6).

Limitation to the width of the wheel - choked flow

It should be noted that for any given pond, b must not be smaller than a value b_m. If $b < b_m$, the flow is choked (see HENDERSON's section 2.6) and the required flow condition can not be met. When the flow is choked, critical flow occurs at section $\bar{B}$ and the value of b_m can be determined from solving

$$y_B + \frac{1}{2g} [Q/(B\, y_B)]^2 = y_{\bar{B}} + 1.23 \frac{V_{\bar{B}}^2}{2g} \tag{2.7}$$

where $V_{\bar{B}}^2 = g\, y_{\bar{B}}$

and $b_m = Q/(y_{\bar{B}}\, V_{\bar{B}})$

assuming that Q, B and y_B are known.

(c) Flow through the wheel from $\bar{B}$ to $\bar{A}$

Momentum equation

Consider a control volume for water as shown in Fig. 2.1(c) where F_H, $F_{\bar{A}}$, $F_{\bar{B}}$, F_{SA}, F_{SB} and f are the forces acting on the control volume by the wheel, by the pressure distribution at sections $\bar{A}$ and $\bar{B}$, by the downstream and upstream sides of the sill and by the boundary friction respectively. The momentum conservation equation can be written as

$$F_H + F_{\bar{B}} - F_{\bar{A}} + F_{SA} - F_{SB} - f = \frac{\gamma}{g} Q (V_{\bar{A}} - V_{\bar{B}}) \qquad (2.8)$$

If the pressure distributions at $\bar{A}$ and $\bar{B}$ are assumed to be hydrostatic,

$$F_{\bar{A}} = \frac{1}{2} \gamma b y_{\bar{A}}^2$$

and

$$F_{\bar{B}} = \frac{1}{2} \gamma b y_{\bar{B}}^2$$

The forces F_{SA} and F_{SB} can be approximated by

$$F_{SA} = \frac{1}{2} \gamma b y_{\bar{A}}^2 - \frac{1}{2} \gamma b (y_{\bar{A}} - S)^2$$

and

$$F_{SB} = \frac{1}{2} \gamma b y_{\bar{B}}^2 - \frac{1}{2} \gamma b (y_{\bar{B}} - S)^2$$

The right hand side of Eq. (2.8) is usually small compared to other terms and can be neglected. Also f is negligible since the flow distance under consideration is relatively short. With the above approximation, Eq. (2.8) reduced to

$$F_H - \frac{1}{2} \gamma b (y_{\bar{A}} - S)^2 + \frac{1}{2} \gamma b (y_{\bar{B}} - S)^2 = 0 \qquad (2.9)$$

Equation (2.8) is the coupling equation between the water and the wheel. The force F_H in Eq. (2.8) can be determined from the water depths $y_{\bar{A}}$ and $y_{\bar{B}}$ at the wheels. This is the force acting on the water by the wheel. It follows that the force acting on the wheel by the water must be equal but opposite to the force F_H determined from Eq. (2.8). We will consider the force acting on the wheel by the water in Section 2.3.

Limitation to the sill height-choked flow

The sill height, S, can not be more than a certain value S_c. If $S > S_c$, the flow is choked and the required flow condition can not be met. The value of S_c can be determined from solving

$$S_c = E_{\bar{B}} - E_c \tag{2.10}$$

where $$E_{\bar{B}} = y_{\bar{B}} + \frac{1}{2g} [Q/b\ y_{\bar{B}}]^2$$

and $$E_c = \frac{3}{2} [Q^2/gb^2]^{1/3}$$

assuming that Q, b and $y_{\bar{B}}$ are known.

Leakage

Even though the overall water motion is from $\bar{B}$ to $\bar{A}$ it is possible that some amount of water moves in the reverse direction through inevitable clearances between the rotating wheel and its surroundings. This is defined as leakage in this study. Leakage is caused by the difference in water levels between the upstream (lower) and the downstream (higher) sides of the wheel. If the flow rate in the channel is Q, the flow rate that the wheel must carry will be Q + leakage. If we assume that the leakage is directly proportional to Q, we can write

$$Q_a = (1 + C_L)Q \tag{2.11}$$

where Q_a = Actual flow passing through the wheel

C_L = Leak coefficient

Actually it is more realistic to say that the leakage depends on the water level difference between the downstream and upstream side of the wheel and the clearance, but this makes it more difficult to handle the computation. In this study, no attempt is made to measure C_L experimentally. $C_L = 0.1$ is used throughout.

(d) Flow through expansion from $\bar{A}$ to A

The energy relation written for flow from $\bar{A}$ to A is

$$y_{\bar{A}} + \frac{V_{\bar{A}}^2}{2g} = y_A + \frac{V_A^2}{2g} + \frac{(V_{\bar{A}} - V_A)^2}{2g} \tag{2.12}$$

where $V_A = Q/(B\ y_A)$

and $V_{\bar{A}} = Q/(b\ y_{\bar{A}})$

and the last term on the right-hand side represents the energy loss term (see HENDERSON's section 7.2). Regarding the value of the energy loss coefficient, the same comment as in 2.2(b) applies. Knowing Q, B, y_A and b, we can determine $y_{\bar{A}}$ from Eq. (2.12).

(e) Power required for the flow

The power required for the flow as given by Eq. (2.5) does not consider the energy loss in the contraction and expansion. Once the wheel whose width b < B is installed in the channel, contraction and expansion of flow are created. In order to account for the energy losses due to contraction and expansion, the power must be computed from

$$P_w = \gamma Q(y_{\bar{A}} - y_{\bar{B}}) \qquad (2.13)$$

(f) Notes on computation

Up to this point we should summarize the computational steps involved in order to simplify further discussion. We note that, given the values of the average flow velocity (V_o), the static water depth (y_o) and the channel dimensions we can determine the head required to drive the flow and the water depths at the wheel. However, we are not yet capable of estimating the power input required at the wheel which is the content of the next section. The computation steps are shown in Fig. 2.3.

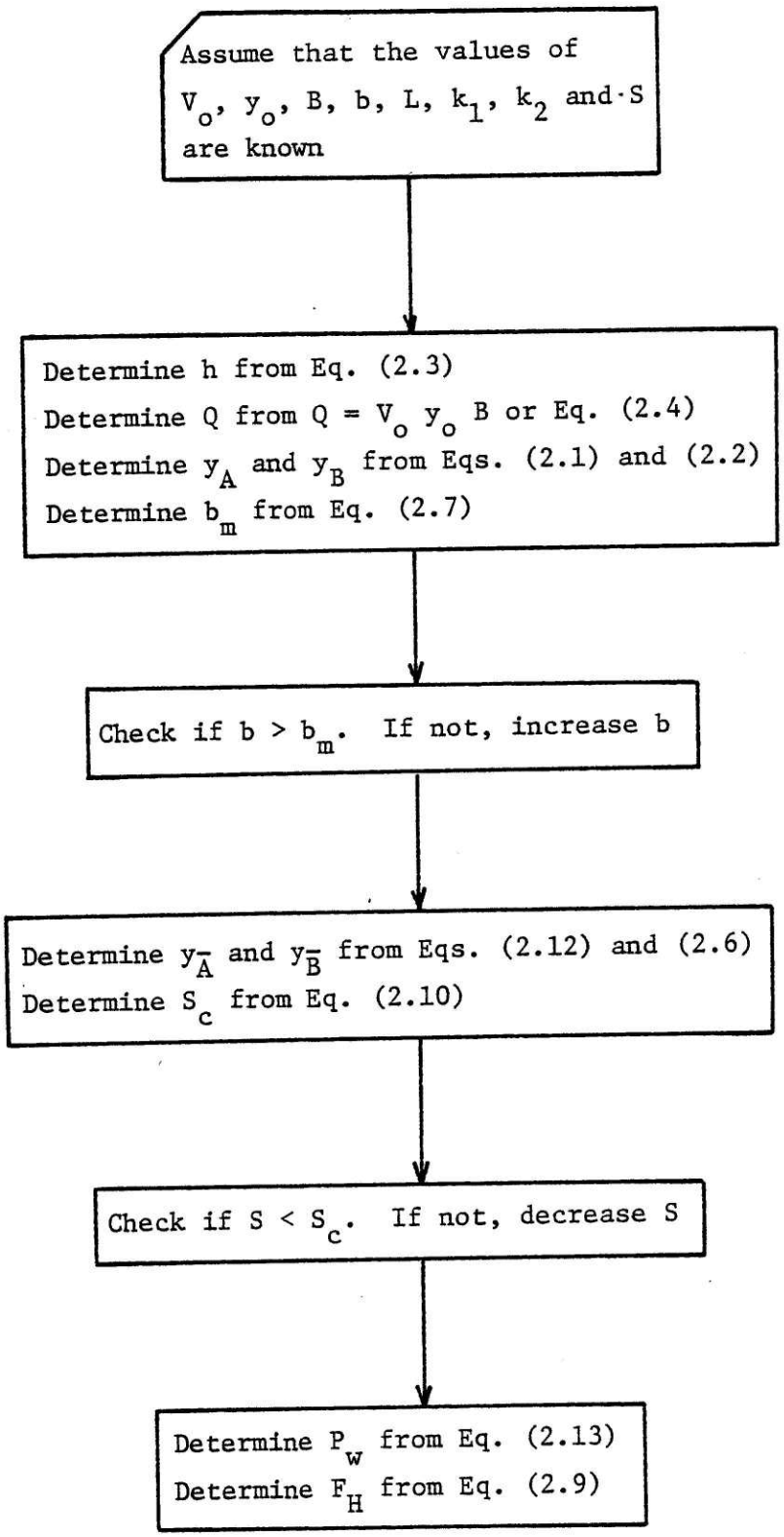

Fig. 2.3 Computation Steps in Section 2.2

2.3 Analysis of the Wheel

In this section we turn our attention to the wheel in order to find the relationship among the resisting force and torque, the wheel speed and its geometry. We will first consider a simple case where the wheel has only one paddle. Later we will extrapolate the result to the case of a multi-paddle wheel. We will focus our attention on the horizontal component of the force acting on paddles because it is required in satisfying the momentum conservation expressed in Eq. (2.8).

(a) Wheel with single paddle

Consider a wheel with a single paddle rotating clockwise with constant angular speed, w, as shown in Fig. 2.4(a). The wheel has radius R and width b. The water depths at the upstream and downstream side of the wheel are $y_{\bar{B}}$ and $y_{\bar{A}}$, respectively. S is the height of the sill which has an assumed shape as shown. We will assume that the water level varies smoothly in a prescribed manner within the wheel and that the water levels are smooth in the vicinity of the wheel. (This is not really true since a lot of disturbances are created at both ends and inside the wheel.) Neglecting the clearance between the wheel and the sill, the depth of submergence d is defined as $d = \bar{y}_o - S$ where $\bar{y}_o = \frac{1}{2}(y_{\bar{A}} + y_{\bar{B}})$. Let the depth and velocity of flow inside the wheel be y and V_w, respectively. Assume that V_w is horizontal and uniform in the vertical direction. As shown, the part of the paddle in contact with the water is from r = x to r = R. If we measure the position of the paddle by the angle θ relative to a reference line parallel to the line connecting the water levels on both sides of the wheel and passing through the wheel center as shown in Fig. 2.4(b), the following angles can be written from trigonometric consideration:

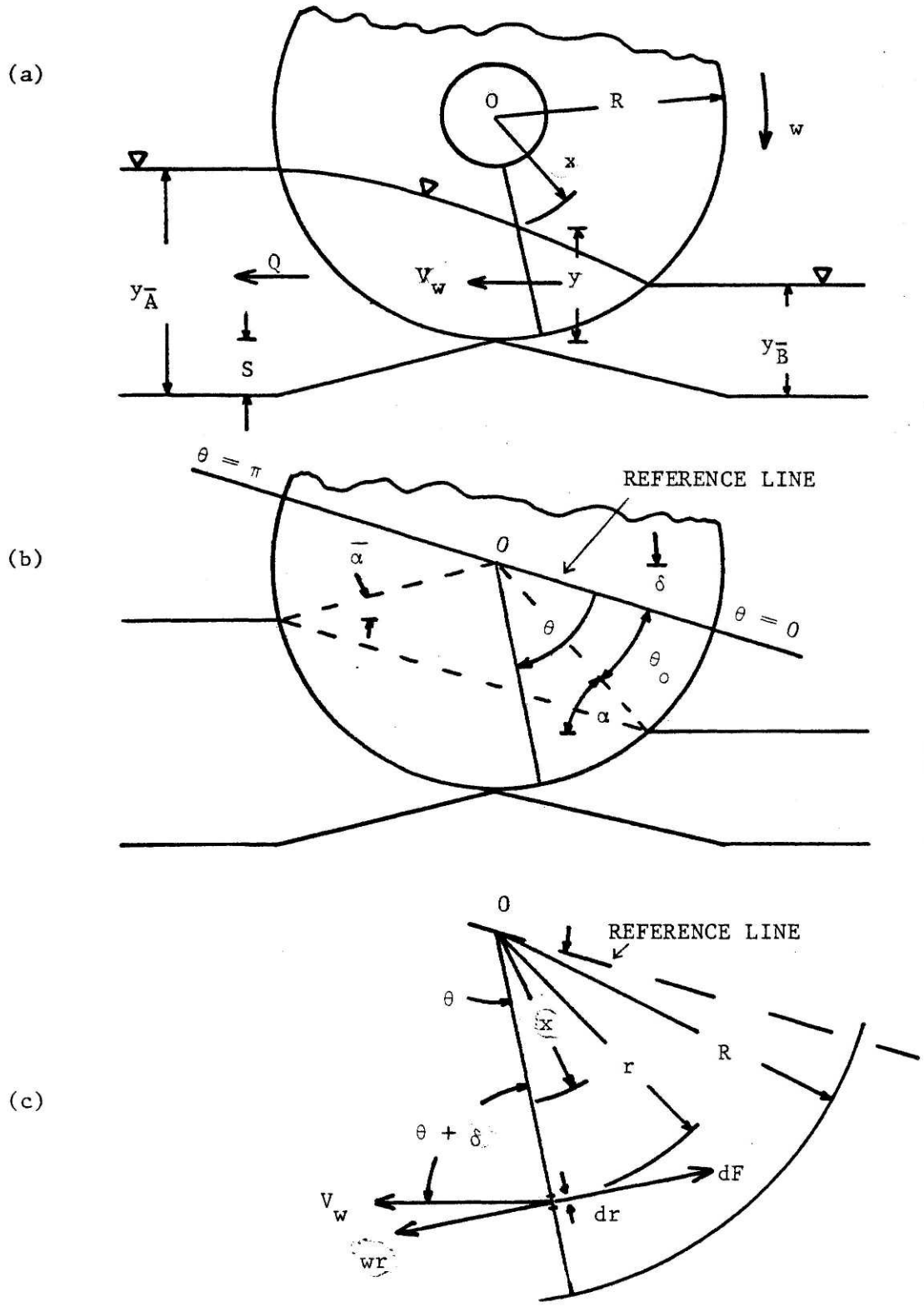

Fig. 2.4 Geometry of a Wheel with One Paddle

$$\alpha = \sin^{-1}\left(1 - \frac{y_{\bar{B}} - S}{R}\right)$$

$$\bar{\alpha} = \sin^{-1}\left(1 - \frac{y_{\bar{A}} - S}{R}\right) \qquad (2.14)$$

$$\delta = \frac{1}{2}(\alpha - \bar{\alpha})$$

$$\theta_o = \alpha - \delta$$

The distance x is the distance from the wheel center in the radial direction along the paddle to the point where the water level meets the paddle. The expression used to describe x as a function of θ is

$$x = R\left(\frac{\sin\theta_o}{\sin\theta}\right)^m \qquad (2.15)$$

where m is a positive number. This form is selected because it enables a variety of water surface profiles to be selected. For example, if m = 1, the water surface profile is a straight line joining the two sides. If m = 2 the water surface profile concaves upward a little bit as shown in Fig. 2.4(a). The idea behind this arises from experimental observation of water surface inside the wheel (see Section 4.1). The value of m (to be specified) provides another flexibility in the calibration process. The value of m = 2 is selected and used throughout this report.

The depth y measured from the point where the paddle clears the water down to the sill (see Fig. 2.4a) and can be computed from

$$y = \ell + q \qquad (2.16)$$

where $\ell = (R - x + s)\sin(\theta + \delta)$

$$s = R\left(\frac{1}{\sin(\theta + \delta)} - 1\right)$$

$$q = pS/R$$

and $$p = x|\cos(\theta + \delta)|$$

Equation (2.16) can be derived from trigonometric consideration of the wheel shown in Fig. 2.4.

The force on the paddle can be estimated by considering an element of length dr on the paddle (Fig. 2.4c). The force dF on the element dr can be written as

$$dF = \frac{C_D}{2} \rho V|V| dA \tag{2.17}$$

where C_D = drag coefficient

ρ = density of water

$dA = bdr$

$V = wr - V_w \sin(\theta + \delta)$

$V_w = Q_a/by$

and $Q_a = (1 + C_L)Q$

In Eq. (2.17), the term $V|V|$ has to be used instead of V^2 in order to take into account the possible negative value of V.

Horizontal component of force: From Eq. (2.17), the horizontal component of dF is

$$dF_h = \frac{C_D}{2} \rho V|V| \sin(\theta + \delta)\, bdr$$

Integrate this equation from r = x to r = R, and rearrange yields

$$\frac{F_h}{\frac{C_D}{2} \rho b w^2 R^3} = \sin(\theta + \delta) \int_c^1 (z - a)|z - a| dz \tag{2.18}$$

where $$c = x/R = \left(\frac{\sin \theta_o}{\sin \theta}\right)^m$$

$$a = \frac{V_w}{wR} \sin (\theta + \delta)$$

It is convenient to define

$$x_h = \sin (\theta + \delta) \int_c^1 (z - a)|z - a| \, dz \tag{2.19}$$

which represents the right hand side of Eq. (2.18) and can be obtained by numerical integration. Note that x_h is dimensionless.

Vertical component of force: Let F_v denote the positively upward component of F. By the method similar to the previous manipulation

$$\frac{F_v}{\frac{C_D}{2} \rho b w^3 R^3} = x_v \tag{2.20}$$

where $$x_v = \cos (\theta + \delta) \int_c^1 (z - a)|z - a| \, dz \tag{2.21}$$

Torque: Let T denote the resisting torque. From Eq. (2.17),

$$dT = \frac{C_D}{2} \rho V|V| \, r dA$$

Integrating this equation from r = x to r = R and rearranging yields

$$\frac{T}{\frac{C_D}{2}\rho b\, w^2 R^4} = x_t \tag{2.22}$$

where $$x_t = \int_c^1 z(z-a)|z-a|\, dz \tag{2.23}$$

The dimensionless parameters x_h, x_v and x_t can be thought of as dimensionless representation of horizontal force, vertical force and torque.

Force and torque diagrams: Since the coordinate θ varies with time, i.e.,

$$\theta = wt$$

it follows that F_h, F_v and T also vary with time. We can study the variations of F_h, F_v and T by studying the variations of x_h, x_v, and x_t. Typical variations of x_h, x_v and x_t are shown in Fig. 2.5. Physically these diagrams represent the estimation of horizontal force, vertical force and torque exerted on the paddle by the water. It is observed that they all are periodic functions of θ with period 2π which corresponds to one revolution of the paddle. The variation of x_h, x_v and x_t against θ as shown in Fig. 2.5 will be referred to as 'Force Diagram' or 'Torque Diagram', respectively in the following discussion.

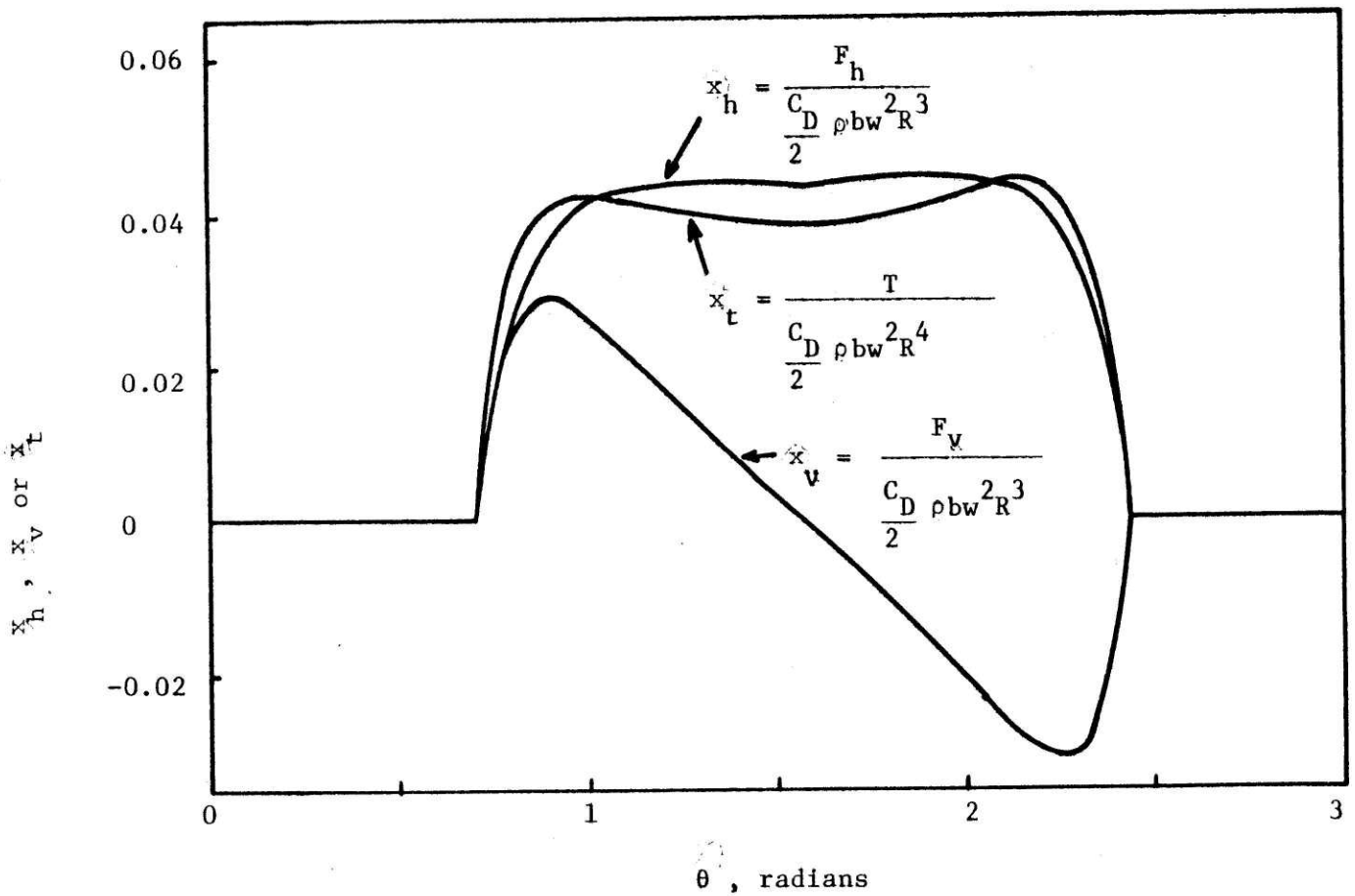

DATA: $y_o = 0.4m$; $y_{\bar{A}} = 0.4045m$; $y_{\bar{B}} = 0.3934m$; $R = 1m$; $b = 20m$; $N = 8$;
$S = 0.05m$; $Q_a = 1.68\ m^3/sec$

Fig. 2.5 Force and Torque Diagrams

(b) Wheel with multiple paddles

Let N be the number of paddles in a wheel. Assuming that all paddles are equally spaced and are similar. The angle of spacing between two adjacent paddles is

$$\psi = 2\pi/N \tag{2.24}$$

In terms of the coordinate θ, each successive paddle lags the one before it by ψ radian. The total forces or torque will be the summation of forces or torques exerted on every paddle. In what follows we will discuss the process of summation only for F_h. The same procedure is also applicable to F_v and T.

Our purpose is to estimate a representative value of F_h for the complete wheel, i.e., the wheel with N paddles. One way to do this is to plot the force diagram of every paddle in a single graph as shown in Fig. 2.6. Since each paddle is separated by ψ from its neighbor, the force diagrams for every paddle will also be separated by ψ. The total force diagram can then be obtained by summing up forces acting on every paddle (at the same value of θ). The total force diagram represents the variation of the total force acting on the wheel. Let F_{hT} represent this total force. Since F_{hT} is obtained from a linear combination of F_h which are periodic of period length 2π, it follows that F_{hT} will be periodic of period length ψ.

The total force diagram reveals that the wheel is subject to fluctuating force of period ψ. The magnitude of fluctuation becomes smaller as N increases. In order to couple this force to the one

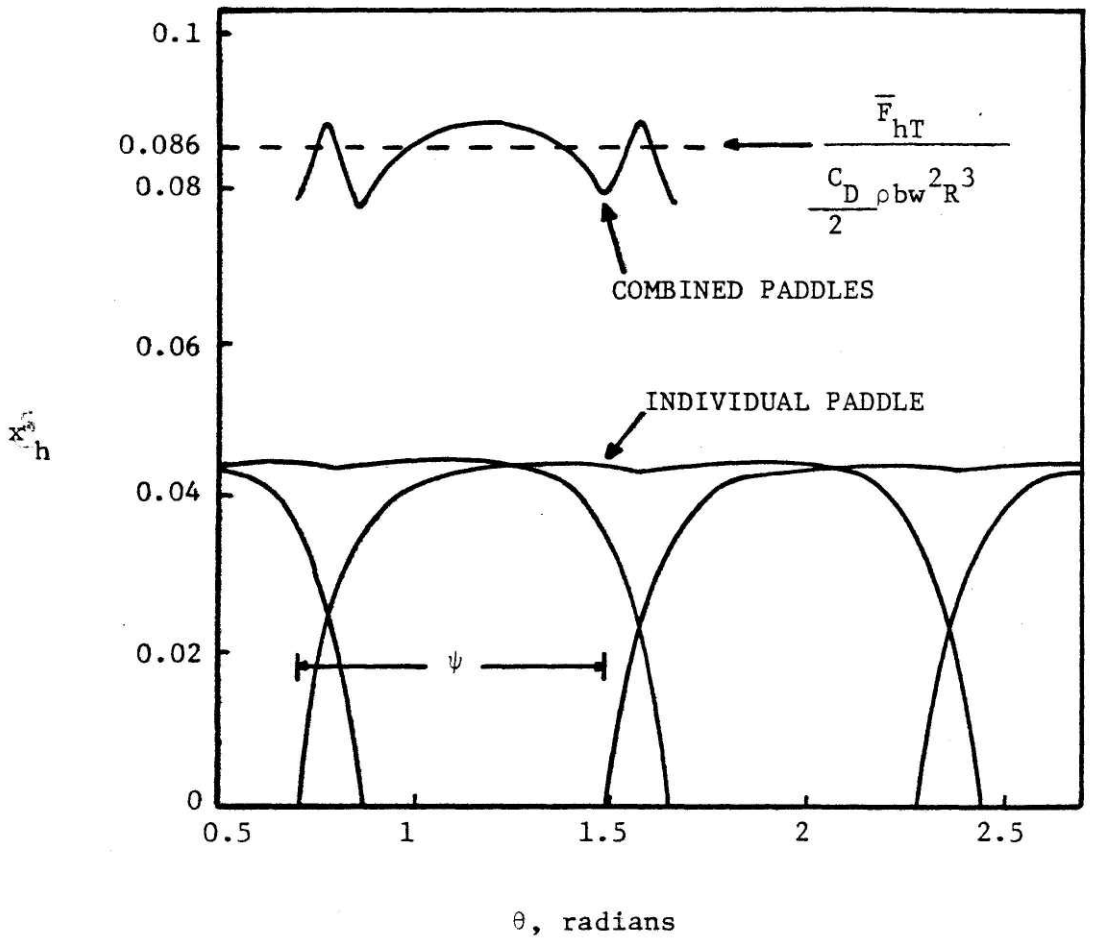

DATA: Same as that of Fig. 2.5 and N = 8

Fig. 2.6 Summation of x_h from Individual Paddles

required in Eq. (2.8), we need to find a representative steady-state value ($\bar{F}_{hT}$) from the total force diagram. One way to obtain this average value is to find

$$\bar{F}_{hT} = \frac{1}{\psi} \int_{\theta}^{\theta + \psi} F_{hT} \, d\theta \tag{2.25}$$

Performing the above summation and averaging processes for F_h, F_v and T, the final results can be written as follows:

$$\frac{\bar{F}_{hT}}{\frac{C_D}{2} \rho b w^2 R^3} = x_H \tag{2.26A}$$

$$\frac{\bar{F}_{vT}}{\frac{C_D}{2} \rho b w^2 R^3} = x_V \tag{2.26B}$$

$$\frac{\bar{T}_T}{\frac{C_D}{2} \rho b w^2 R^4} = x_T \tag{2.26C}$$

In Eqs. (2.26), $\bar{F}_{hT}$, $\bar{F}_{vT}$ and $\bar{T}_T$ are the representative steady-state values for horizontal force, vertical force and torque, respectively for wheel with N paddles. The dimensionless parameters x_H, x_V and x_T can be determined if the values of R, b, N, S, w, $y_{\bar{A}}$, $y_{\bar{B}}$ and Q_a are known.

Knowing x_H, x_V and x_T, the values of $\bar{F}_{hT}$, $\bar{F}_{vT}$ and $\bar{T}_T$ can be determined from Eqs. (2.26). The value of $\bar{F}_{hT}$ determined as such must be equal to the value of F_H determined from the momentum conservation of Eq. (2.8). Since we do not know the wheel speed w in advance, an iterative computational procedure has to be employed.

(c) Power Consumption

The power delivered to the paddles P_{wh} is

$$P_{wh} = w \bar{T}_T \tag{2.27}$$

which can be determined once w and $\bar{T}_T$ are known.

In practice, the power input to the wheel (P_{in}) can be measured at the wheel shaft. This measurable power input includes the power loss due to friction at the wheel bearings (P_{FR}) and the power loss due to the creation of air turbulence (P_A), i.e.,

$$P_{in} = P_{wh} + P_{FR} + P_A \tag{2.28}$$

In this study, P_A is assumed to be negligible and P_{FR} is estimated from the following consideration. The torque due to bearing friction can be expressed as

$$T_{FR} = \mu \, U \, R_B$$

where μ = coefficient of friction of the bearings

R_B = effective radius of the bearings

and U = total force supported by the bearings.

The force U is the vectorial combination of $\bar{F}_{hT}$, $\bar{F}_{vT}$ and the weight of the wheel W, i.e.,

$$U = \left[(F_{hT})^2 + (W - F_{vT})^2 \right]^{1/2} \tag{2.29}$$

The power loss in the bearings is

$$P_{FR} = T_{FR}\, w = C_{FR}\, U\, w \tag{2.30}$$

where $C_{FR} = \mu R_B$. If the value of C_{FR} is known, P_{FR} can be estimated. The experimentally determined value of C_{FR} is discussed in Section 4.4 b. The wheel efficiency e is then

$$e = P_w/P_{in} \tag{2.31}$$

where P_w is determined from Eq. (2.13).

(d) Notes on computation

The computation involved in this section is summarized and shown in Fig. 2.7.

(e) Variation of the drag coefficient, C_D

The drag coefficient C_D is an important coefficient determining the transfer of force from the paddles to the water. If $C_D = 0$, there will be no force transfer at all no matter how fast the wheel rotates. On the other hand, the wheel will have to rotate slowly in order to transfer the required force if C_D is large. In a hypothetical situation where the paddle moves (in relation to the water) at a constant speed and perpendicular to the free stream, C_D is known to be about 1.2 if the paddle is circular in shape and the Reynold number exceeds a certain value ensuring fully turbulent flow. The value of C_D for this hypothetical situation was determined experimentally by many investigators and is discussed in most fluid mechanics text books (e.g., DAILY and HARLEMAN [27]). Unfortunately,

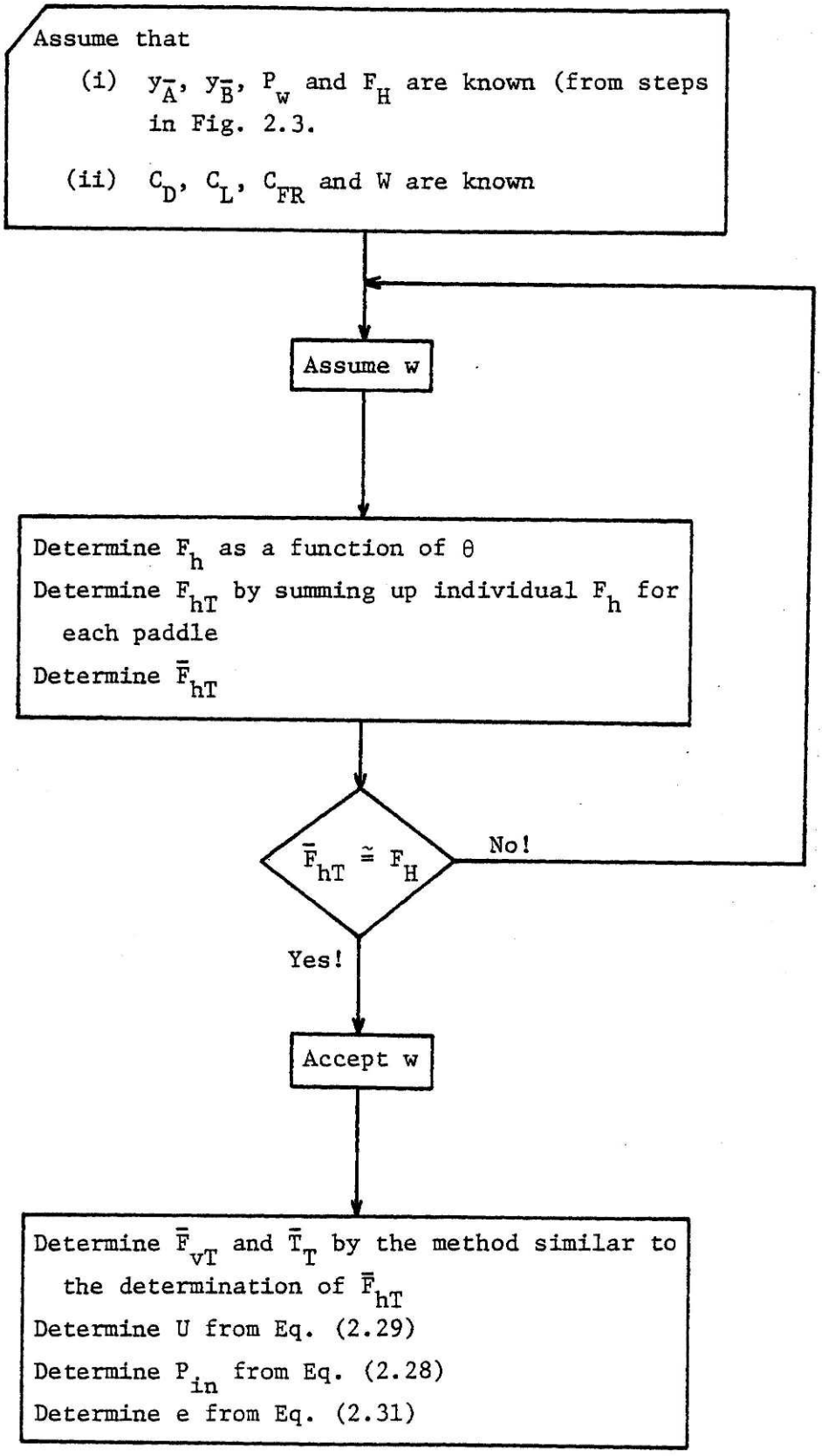

Fig. 2.7 Computation Steps in Section 2.3

for the case of a paddle wheel, the following departures from the hypothetical situations exist.

(i) The paddles are not circular in shape.

(ii) The free stream velocity is neither steady nor normal to the paddles.

(iii) There is more than one paddle in contact with the water at the same time. The flow disturbance created by one paddle may affect the hydraulic performance of the other paddles.

These departures from the ideal situation imply that C_D may not be constant. Analysis of experimental results discussed in Section 4.4 reveals that C_D depends both on N and d/R. Their relationship is shown in Fig. 4.13.

One problem arises when the value of C_D determined from a scaled down model is used to assess the performance of a full size machine. The value of C_D obtained from the model will be higher than that appropriate to the prototype. This effect is known as "scale effect" in the theory of hydraulic machines. For paddle wheels, this will result in underestimated power input and overestimated efficiency of the prototype.

The scale effect in paddle wheels results from the variation in C_D with the Reynolds number (Re). For a disk oriented perpendicular to the free stream, the variation of C_D with respect to Re is as shown in DAILY and HARLEMAN's [27] Fig. 15-13 which indicates that C_D starts to increase as Re decreases for $Re < 10^3$. A similar trend is expected in the case of paddle wheels. Since a scaled down model of a paddle wheel generally has smaller Re than that of the prototype, C_D of the model will be higher.

It is difficult to quantify the magnitude of the scale effect. The safe way to avoid it is to make sure that the model in which the value of

C_D is obtained is not too small relative to the prototype.

2.4 Summary of the Analytical Model

Having analyzed both the wheel and the hydraulics of flow in the pond, we can now couple them together. It is simply a matter of connecting the computation steps in Fig. 2.3 to those of Fig. 2.7 forming some sort of analytical model of the system.

However, the computation steps discussed earlier lack the ability to present an encapsulated view of the problem structure. It is the purpose of this section to provide the readers with such a view.

Referring back to Fig. 2.1, we can write the functional relationships among different components of the system as follows:

(i) Force provided by the rotating wheel (F_H)

$$F_H = f_1(R,b,N,S,w,Q,y_{\bar{A}},y_{\bar{B}},C_D,C_L)$$

where f_1 indicates functional relationship. This equation states that the force provided by the rotating wheel is a function of the wheel radius, width, number of paddles, sill height, wheel speed, flow rate, water levels at both sides, drag and leak coefficients. The form of the function can not be written out explicitly and is the content of Section 2.3.

(ii) Head-flow relationship of the channel

This can be described functionally as

$$Q = f_2(y_A,\ y_B,\ \text{channel roughness and geometry})$$

which has the form shown in Eq. (2.4).

(iii) Relationships between depths of flow at the contraction and expansion

$$y_{\bar{A}} = f_3(y_A,\ Q,\ b,\ B,\ \text{shape of the expansion})$$

and

$$y_{\bar{B}} = f_4(y_B,\ Q,\ b,\ B,\ \text{shape of the contraction})$$

The equivalent forms of these two functional relationships are Eqs. (2.6) and (2.12).

(iv) Momentum conservation

Since the force provided by the rotating wheel must satisfy the conservation of momentum of the flowing water, neglecting friction we have

$$F_H + F_{\bar{B}} - F_{\bar{A}} + F_{SA} - F_{SB} = \frac{\gamma}{g} Q\ (V_{\bar{A}} - V_{\bar{B}})$$

The above equation is equivalent to Eq. (2.8).

In an actual paddle wheel set up, it is usual that R, b, N, S, y_A, y_B, B, channel roughness and geometry, shapes of the expansion and contraction are known. Assuming that C_D and C_L are also known, this leaves us with the unknown: w, F_H, Q, $y_{\bar{A}}$ and $y_{\bar{B}}$ with 5 available relationships discussed above. It is therefore possible to determine all the 5 unknowns and the problem is solved.

2.5 Characteristic Curves

Assuming that the values of C_D and C_L are known, we can use the computation procedures of Figs. 2.3 and 2.7 to predict the system

performance. The performance of the system is best described by a set of curves relating important parameters to the wheel speed. The most important are the curves of h and P_{in} versus w because they are the key parameters in the design.

Characteristic curves determined analytically as described above are shown in Fig. 2.8. Actual characteristic curves (i.e., those obtained from measurement) will be different from the ones shown in Fig. 2.8 due to many phenomena that can not be taken into consideration in the analytical model. For example, when w is sufficiently high, waves and bubbles are formed reducing the wheel efficiency. These phenomena are observed in experiment and reported in Chapter 4. However, the analytical model can be used to estimate the system performance when the above phenomena are relatively mild or do not occur. Experimentally obtained characteristic curves are shown in Fig. 4.1.

2.6 Optimum Pond Dimensions

In the past sections of this chapter, it was assumed that we are given the channel dimensions, i.e., the channel length L, the channel width B, the number of 90° bends k_1 and the number of 180° bends k_2. In this section, we will discuss how these parameters can be determined such that the power requirement, for the water to flow at specified values of V_o and y_o, is minimum.

We will start by assuming that the values of V_o and y_o are specified and that the shape and area of the land where the pond is to be located are given. V_o is specified by the requirement of mixing or prevention of stratification. y_o is specified by the requirement that sunlight should be able to reach the bottom of the pond (see Section 1.5). The

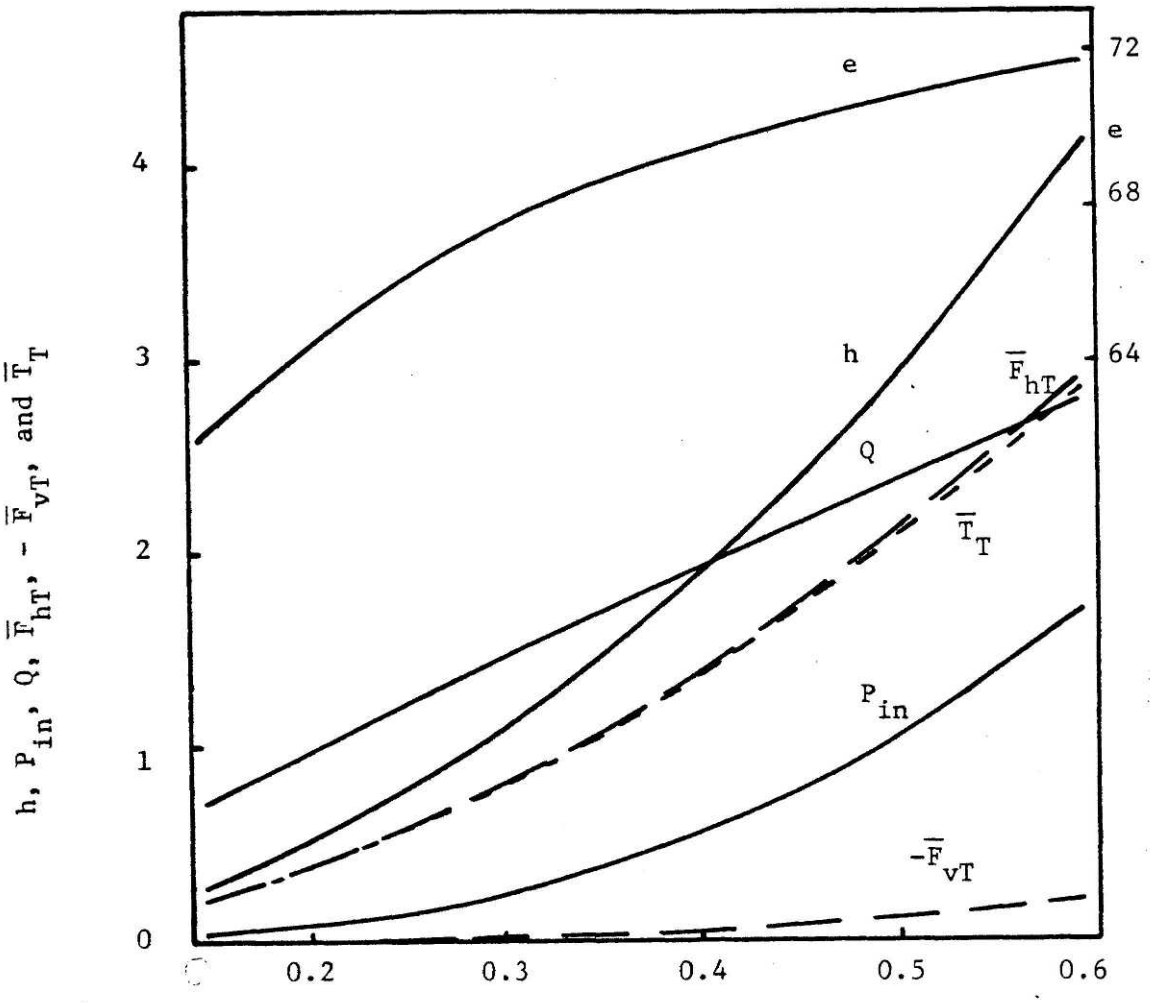

UNITS: e ~ %; h ~ cm; P_{in} ~ kW; Q ~ m^3/sec;
$\overline{F}_{hT}$ and $\overline{F}_{vT}$ ~ kN; $\overline{T}_T$ ~ kN.m

DATA: y_o = 0.4m; R = 1m; b = 20m; N = 8; S = 0.05m; L = 286m;
k_1 = 0; k_2 = 2; n = 0.015; B = 35m; W = 250kg;
m = 2; C_{FR} = 0.0082; C_L = 0.2; C_D = 10.

Fig. 2.8 Characteristic Curves

area required is dictated by the amount of waste load. The location and the shape of the available land are somewhat dictated by other considerations beyond the scope of this work. It is also assumed that the available land is leveled.

The criterion for the optimum pond dimensions in this work is that the power required to drive the flow should be minimum for the given conditions. For a given plot of land, there are many possible layouts for the pond. Each of the layouts has a unique set of values of L, B, k_1 and k_2. For the specified V_o and y_o, each layout requires different quantities of power to drive the flow. The optimum layout is the one that requires minimum power. The steps required to achieve this are discussed next.

Procedure:

(i) For the given plot of land, prepare various layouts graphically. Examples are shown below

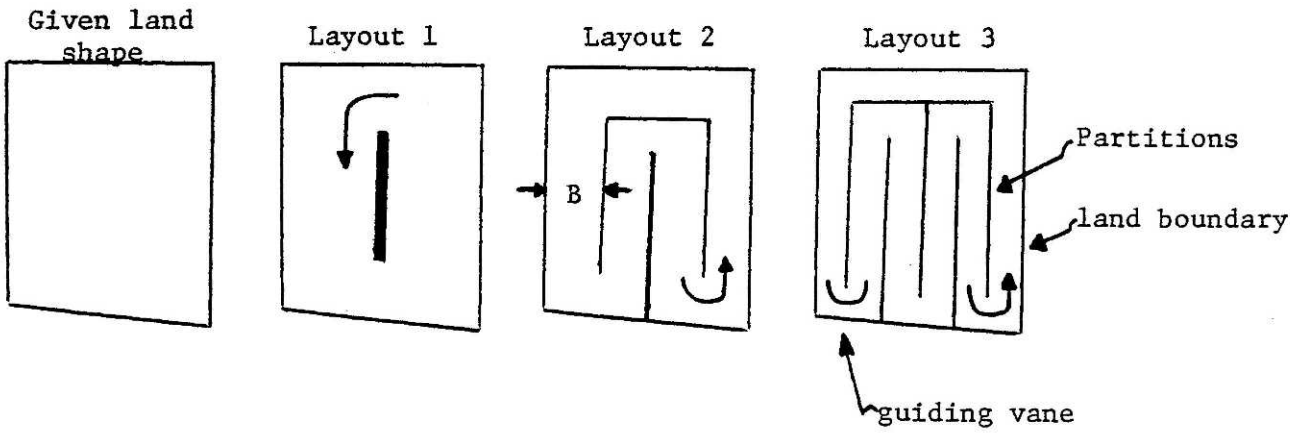

(ii) Fill in the values of B, L, k_1 and k_2 for each layout in the table below.

Note: B = channel width

L = total channel length

k_1 = number of 90° bends

k_2 = number of 180° bends

h = head required for the flow

Q = flow rate

P'_w = power required

Layout No.	B (m)	L (m)	k_1	k_2	h (m)	Q (m^3/sec)	P'_w (Watts)
1	x	x	x	x	c	c	c
2	x	x	x	x	c	c	c
3	x	x	x	x	c	c	c

x to be filled in from graph of layouts

c to be calculated

(iii) Compute h, Q and P'_w using Eq. (2.3), $Q = v_o y_o B$ and Eq. (2.5), respectively for each layout.

(iv) Select the layout that requires minimum P'_w.

A numerical example is discussed in Section 5.3.

CHAPTER III: DESIGN OF EXPERIMENT

3.1 Apparatus

a. Purposes and features

b. Apparatus components

3.2 Method of Measurement

a. Measurement of speed and torque

b. Measurement of water level difference and flow rate

3.3 Experimental Program

3.4 Procedure for Conduction of Experiment

3.5 Discussion

a. P.V.C. shaft for torque measurement

b. Flow resistance in the channel

c. Power loss due to bearing friction

CHAPTER III

DESIGN OF EXPERIMENT

This chapter describes the apparatus, the methods of measurement, the experimental program, the experimental procedure and general comments on the apparatus. Photographs of the apparatus are shown in Fig. 3.1.

3.1 Apparatus

a. Purposes and features

Initially, the apparatus was designed so as to provide sufficient data for calibrating the analytical model described in Chapter 2. However, as experiment was progressing, some complicated and initially unexpected phenomena became evident. For example, when the wheel speed was high enough, bubbles were generated, affecting the wheel performance to a certain extent. These phenomena are described in Section 4.2. Furthermore, some ideas came up during the study on how to improve the wheel efficiency. For example, it was thought that curvature on the paddle outer edge might improve the wheel efficiency by reducing the energy loss during impact between paddle and water. In the final stage of the paddle wheel design and fabrication, the apparatus contains the following features:

(i) the wheel radius (R) can be set at either 10.16 cm. or 13.97 cm.

(ii) the wheel width (b) can be set at either 24.05 cm. or 48.1 cm.

(iii) the number of paddles (N) can be set at either 4, 8 or 16.

(a) General Set Up

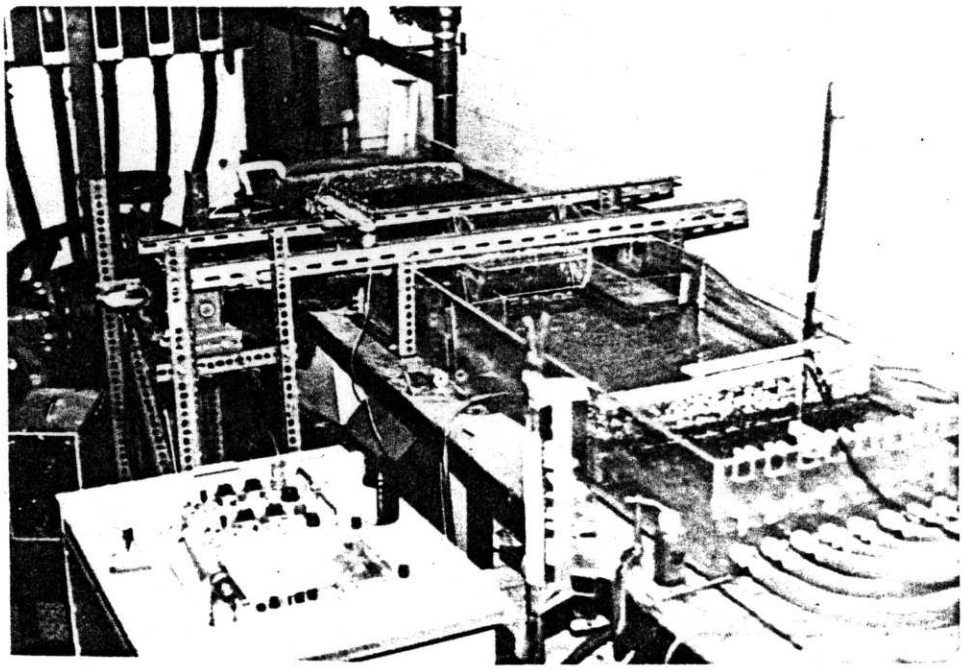

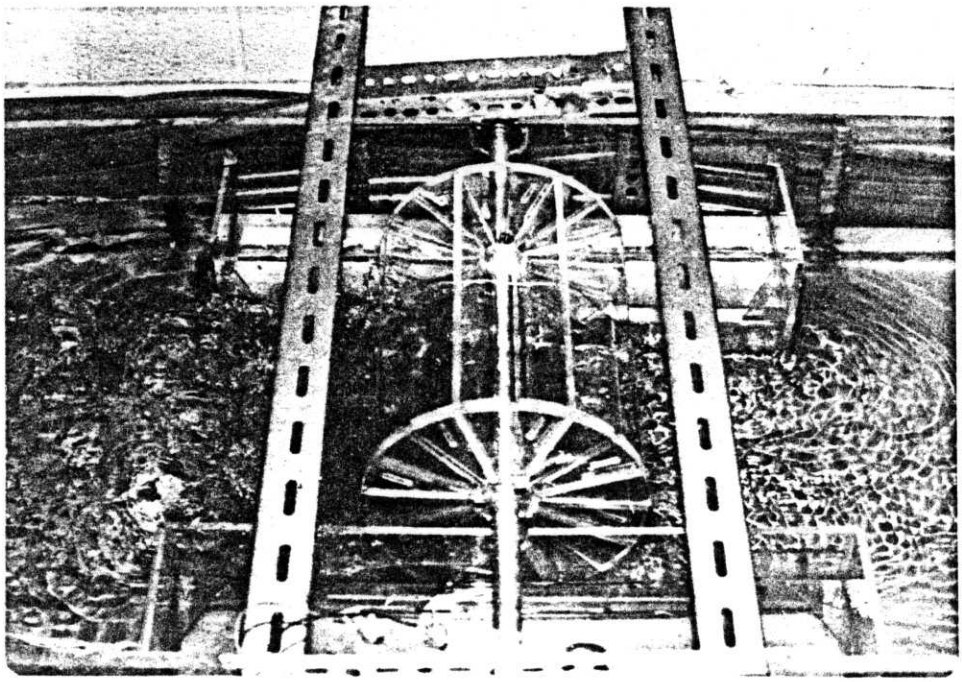

(b) Rotating Wheel (downstream on the left hand side)

Fig. 3-1: Photographs of the Apparatus

(c) Looking along the Flow Direction

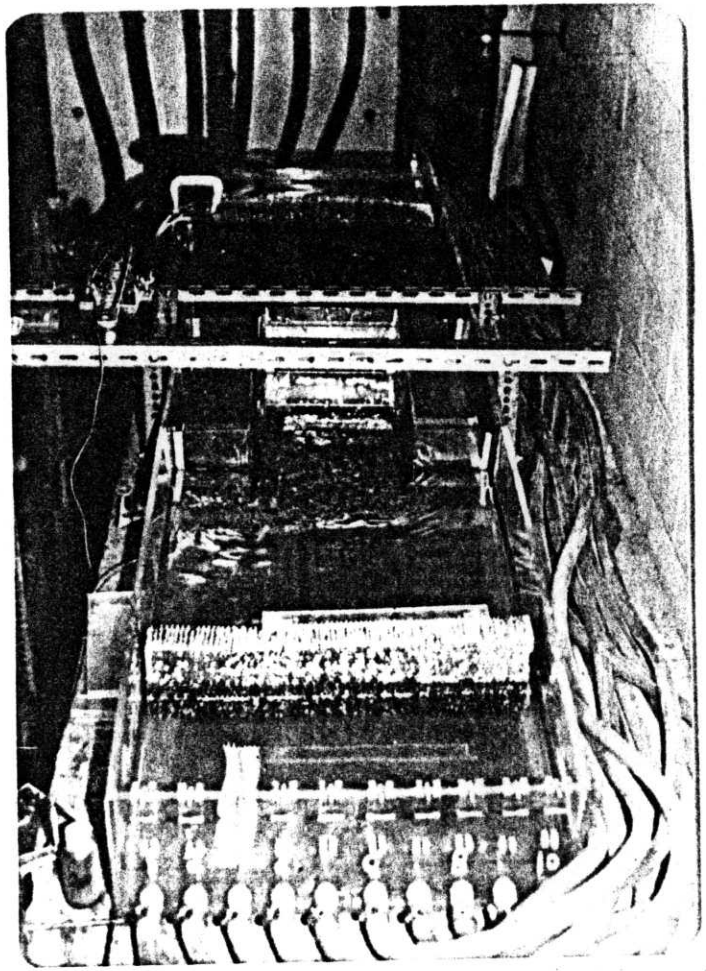

(d) The wheel, the P.V.C. Shaft and the Gear Box

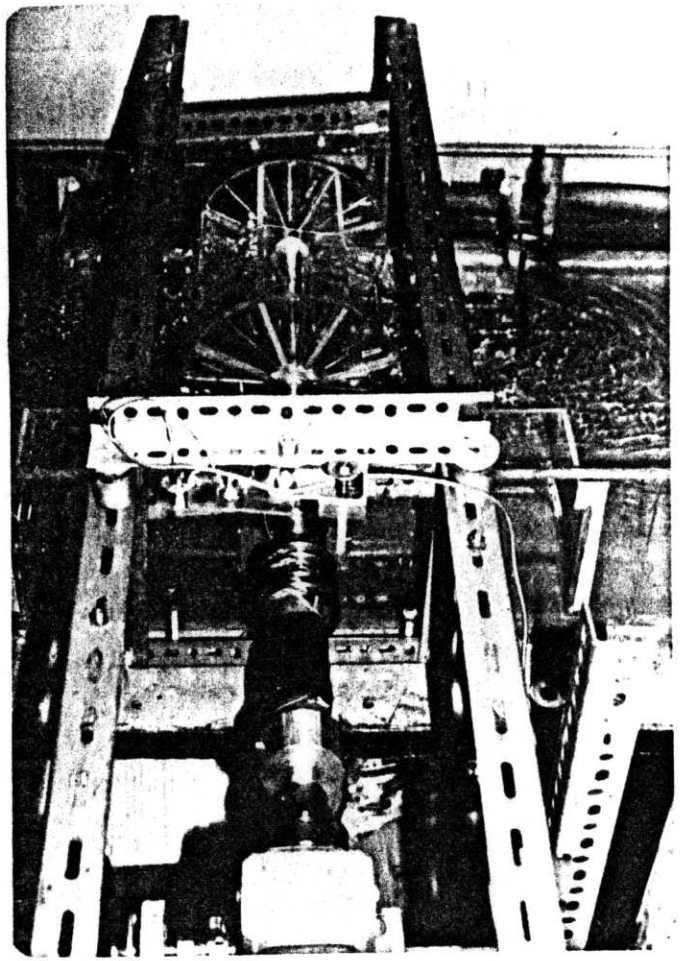

Fig. 3-1; Photographs of the Apparatus (Cont'd)

(iv) the depth of submergence (d) can be adjusted by adjusting the static water depth (y_o).

(v) the paddle angle (β) can be set at 0, +6, -6, +12.3 or -12.3 degrees.

(vi) paddles with curvatures on the outer edges can be tested.

(vii) contoured sill (a sill that follows the wheel curvature) can be tested.

All these features are discussed with respect to their design aspects in the following sections of this chapter. Their experimental results are discussed in Chapter 4. The apparatus described in this study is a scaled down model of full size paddle wheel. The advantages of using a scaled down model are (i) it offers the flexibility needed in laboratory measurements and modifications and (ii) it is inexpensive to build. The disadvantages are discussed in Section 3.5.

b. Apparatus components

Schematic assembly of the apparatus is shown in Fig. 3.2. The apparatus consists of three main components:-

(i) the channel

(ii) the paddle wheel

(iii) the motor and gear box

The channel: The channel is made from $\frac{1}{2}$" plexiglass sheet. The width of the channel is 50 cm. and the length is 2.67 m. A sketch of the channel is shown in Fig. 3.3. Slots are made on both walls of the channel to accept the wheel shaft. Ten 1" flexible plastic hoses are used to connect both ends of the channel. The plastic hoses enable water to flow from one end to the other - thus simulating flow in a long channel.

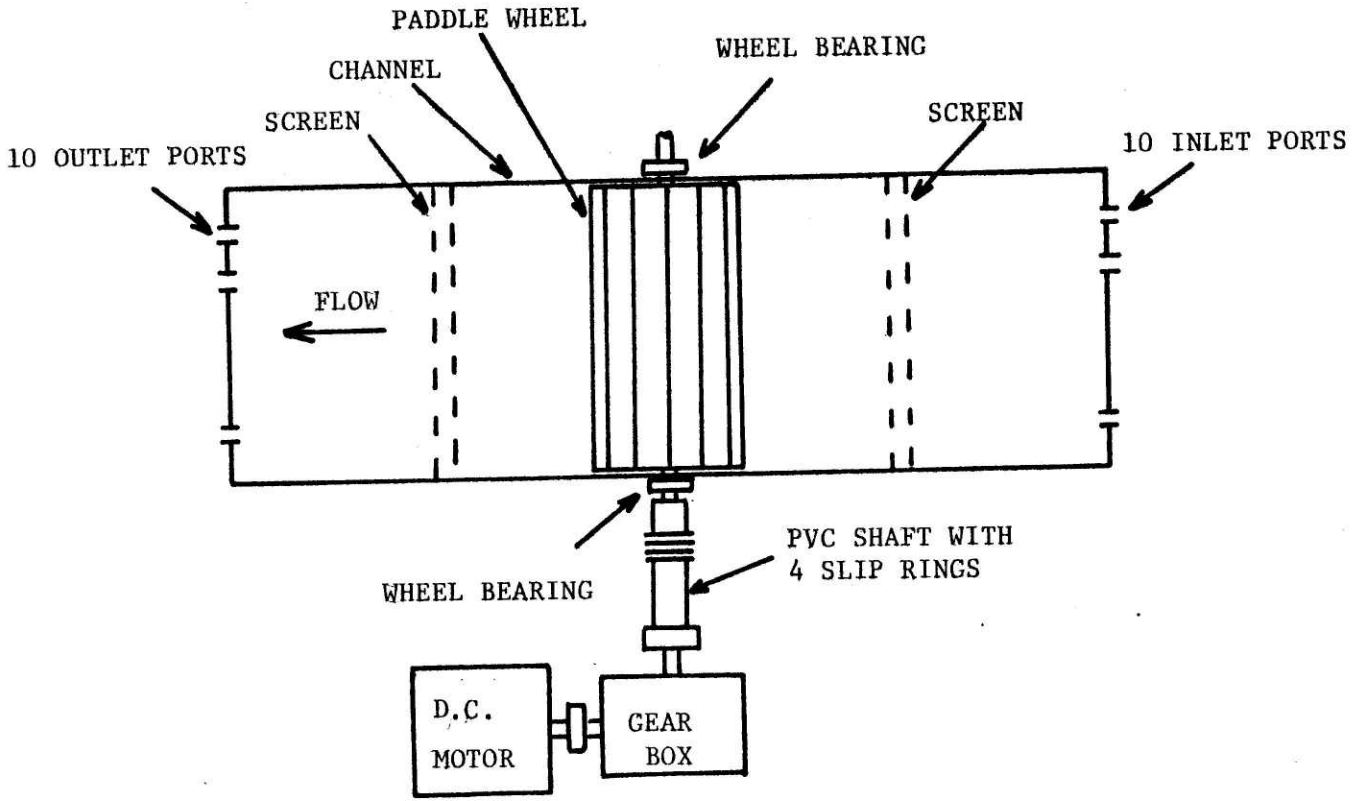

Fig. 3.2 Schematic Plan View of the Apparatus

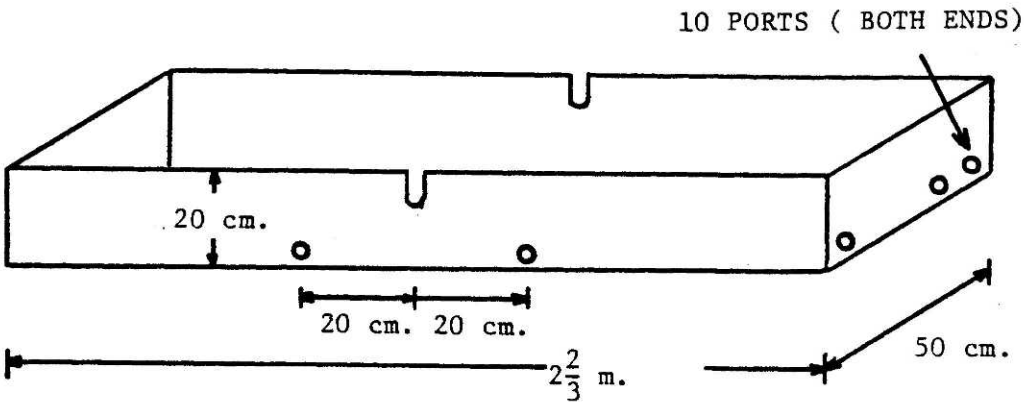

Fig. 3.3 Channel Dimensions

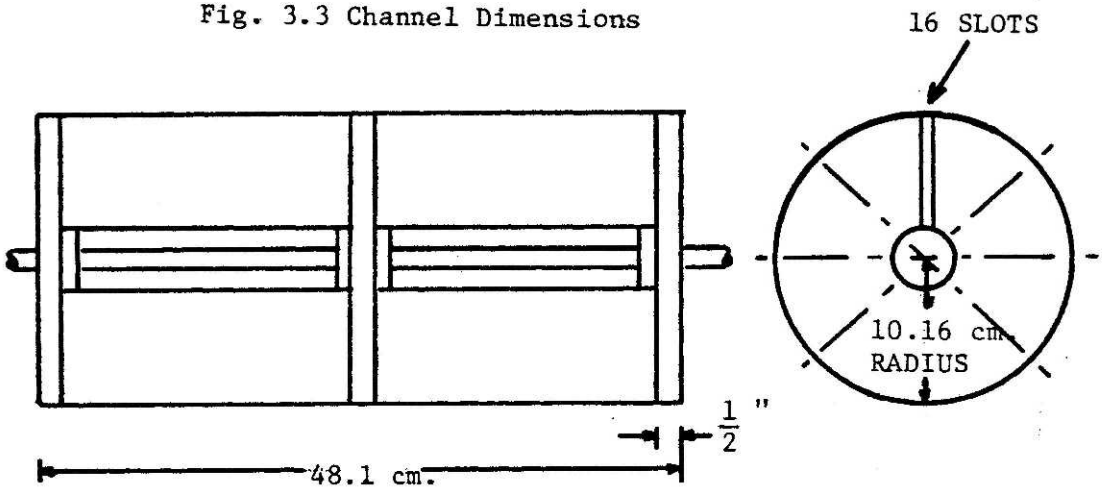

(a) Wheel

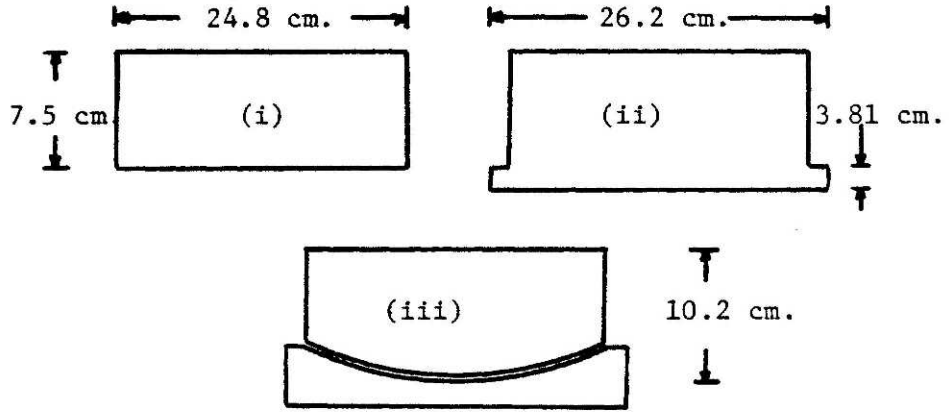

(b) Paddles

Fig. 3.4 Wheel and Paddle Dimensions

Two $\frac{3"}{8}$ holes are drilled on the lower part of a wall at 20 cm. apart from the middle section. These 2 holes are fitted with $\frac{3"}{8}$ flexible plastic tubes connected to manometers for measuring the water levels on both sides of the wheel.

The wheel: Fig. 3.4(a) shows the wheel dimensions. The wheel consists of three flanges of radius 10.16 cm., a $\frac{3"}{4}$ aluminum shaft and a number of paddles. All three flanges are machined from $\frac{1"}{2}$ plexiglass sheet. On the surfaces of these flanges, 16 slots are made. These slots are radially located and have depths of 0.3 mm. The middle flange has 16 slots on both surfaces while the two end-flanges have slots only on one surface. The flanges are attached to the shaft by means of set screws. Once these flanges are screwed on to the shaft, paddles can be inserted into the slots. Paddles are made of $\frac{1"}{4}$ plexiglass sheet. Three shapes of paddle are made as shown in Fig. 3.4(b). Once the paddles are inserted into the slots a steel wire is wrapped around the wheel to prevent the radial movement of the paddles.

In this study, it is necessary that the wheel is designed such that its important geometrical parameters such as its radius can be varied. The following paragraphs describe how these geometrical parameters are varied.

(i) The wheel radius (R): Two values of wheel radius can be set on the apparatus: R = 10.16 cm. and 13.97 cm. To vary the wheel radius, different paddle sizes are used. The paddles shown in Figs. 3.4(b)(i) and 3.4(b)(ii) are used for R = 10.16 cm. and R = 13.97 cm., respectively.

(ii) The wheel width (b): Two values of b can be set: b = 48.1 cm. and 24.05 cm. For b = 48.1 cm., all three flanges are used as shown in Fig. 3.4(a). For b = 24.05 cm., only the two end-flanges are used (i.e., the middle flange is removed).

(iii) The number of paddles (N): The number of paddles can be set at either 4, 8 or 16 by inserting the required number of paddles into places. Note that with this apparatus, N can not be set at 5, 6, 7, 9, 10, 11, 12, 13, 14 and 15 due to symmetry requirements.

(iv) The depth of submergence (d): The depth of submergence is varied by varying the static water depth (y_o). Another way to achieve this is to raise or lower the wheel, which can be done in the present set-up. If the wheel is raised or lowered, the sill height will also have to be varied accordingly. In this study, the sill height is kept constant at 2.28 cm. and y_o is adjusted to achieve the desired depth of submergence.

(v) The paddle angles (β): Five settings of β are possible in this study: $\beta = \pm 12.3^\circ, \pm 6^\circ$ and 0°. Three sets of flanges with slot angles of 12.3°, 6° and 0° are made. The angles β are defined as shown in Fig. 3.5(a). The set of flanges with $\beta = 0^\circ$ are shown in Fig. 3.4(a).

(vi) The curved paddles: To test the effect of the curvature of the paddles, paddles cut to shape as shown in Fig. 3.4(b)(iii) are used. The sill has to be modified to

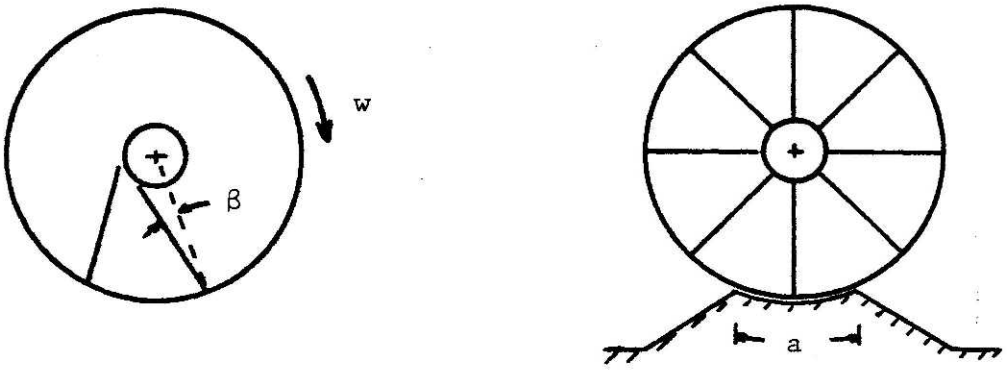

(a) Paddle Angles

(b) Contoured Sill

Fig. 3.5 Paddle Angles and Contoured Sill

accept these paddles. The sill is made of a piece of plexiglass cut with the curvature matching those of the paddles.

(vii) The contoured sill: A contoured sill is defined as a sill that has a radius matching that of the flanges. With a contoured sill set-up, the wheel assembly looks like the one shown in Fig. 3.5(b) if viewed along the axis of the wheel shaft. The arc length of the sill (a) is made equal to $\frac{2\pi}{N}$ R which is also the spacing between two adjacent paddles. The idea behind this is that such a sill may help reduce the leakage occurring during the passage of the wheel.

When assembled, clearances are provided between the wheel and the sill, and between the end flanges of the wheel and the channel walls (or its extension in cases where b = 24.05 cm.). These clearances inevitably cause leakage, i.e., the flow of water from the downstream to the upstream sides of the wheel due to the water level difference. However, without these clearances, the friction will be excessive and cause sluggish rotation of the wheel. In all experimental series indicated in Table 3.1, these clearances are approximately 0.15 cm. to 0.3 cm.

The prime mover: A 1/4 horsepower d.c. motor is used to drive the wheel. The motor speed can be controlled by regulating its field current. A reduction gear unit of 1:5 is used to reduce the motor speed to that of the required wheel speed.

3.2 Methods of Measurement

In order to compute the wheel efficiency, the following quantities must be known: the wheel speed (w), the input torque (T), the flow rate (Q) and the water level difference (h) between the downstream and upstream sections of the wheel. The water power (P_w) and the power input (P_{in}) can then be computed from γQh and wT, respectively. The wheel efficiency (e) is then $e = P_w/P_{in}$. In the following paragrahps, the methods employed to measure w, T, Q and h are discussed.

a. Measurement of speed and torque

Refer to Fig. 3.2, the power transfer from the gear box to the wheel shaft is made through a solid piece of P.V.C. shaft which is shown in more detail in Fig. 3.6. The P.V.C. shaft is used to measure the deflection caused by the twisting of the shaft during power transfer. The deflection is measured by a strain gage bonded on to the outer skin of the shaft according to the description given in DOEBELIN [28]. The deflection induces changes in the electrical resistance of the strain gage and is detected by a bridge circuit of the recorder. Since the shaft has to rotate during the measurement, slip rings have to be used to transfer the electrical signal. The slip rings are made of copper. The recorder is "Hewlett Pakcard, Model 350-1100 C' [29].

The wheel speed can be determined from the recorded deflection described above. Due to some small and inevitable misalignment of the wheel shaft and the P.V.C. shaft, small but detectable fluctuation of deflection is produced during shaft rotation. The recorder detects this small fluctuation and reproduces them on the chart. The period of fluctuation is exactly equal to the time required for one revolution of

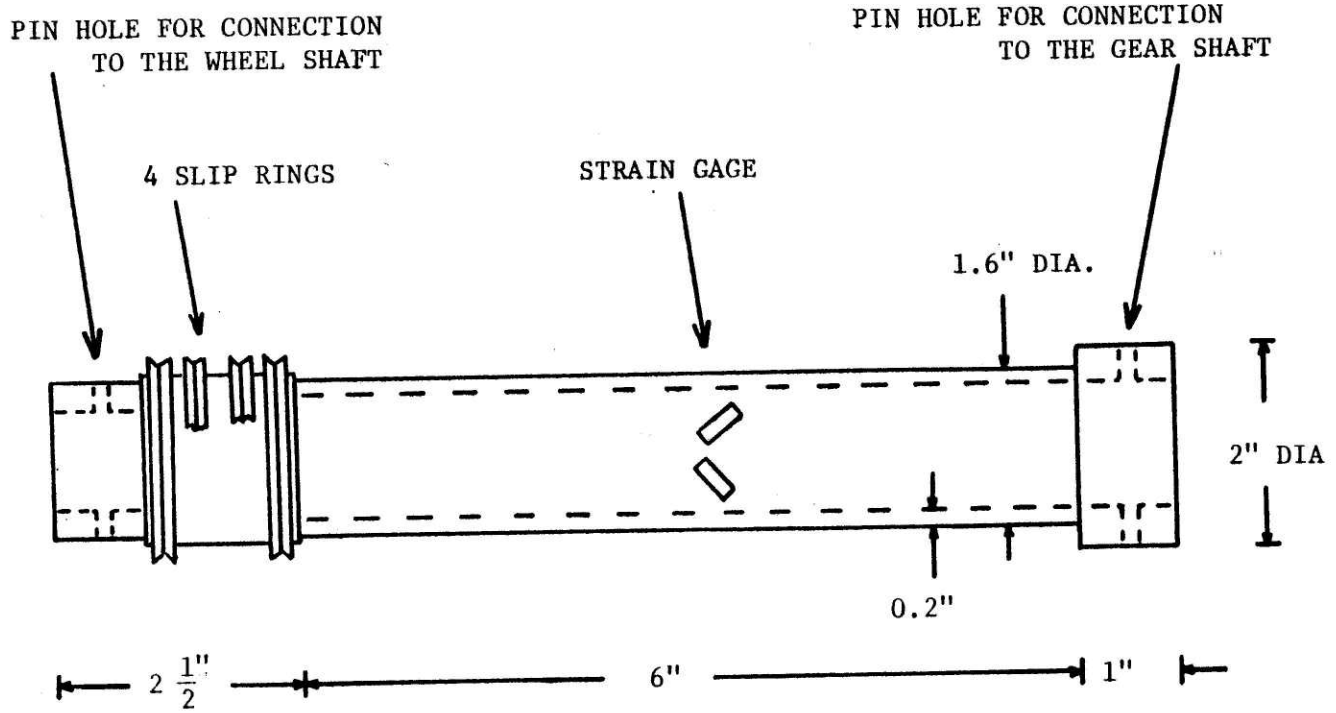

NOTE: Electrical wiring from strain gage to slip rings are not shown

Fig. 3.6 Dimensions of the P.V.C. Shaft

the shaft. Since the advancing speed of the chart on the recorder can be set accurately, the wheel speed can then be determined. Figure 3.7 shows a typtical record of deflection and its fluctuation.

The torque transmitted through the shaft can be determined from the amount of deflection. After each experimental run, the deflection is calibrated to a known static torque. The derived relationship between the deflection and the static torque can then be used to determine the torques from the deflections recorded during wheel rotation. The calibration is performed by stopping the machine and applying a known quantity of static torque to the shaft. This produces a certain amount of deflection which is recorded. The static torque is applied by hanging a known weight at a predetermined moment arm from the shaft axis. Several values of applied torque and deflection are obtained - enabling the curve relating torque and deflection to be drawn.

b. Measurement of water level difference and flow rate

The difference in water level (h) between the downstream and upstream sides of the wheel is measured by means of a simple manometer. The flow rate Q is related to h for each particular value of y_o (y_o is the static water level). The relationship between Q and h for various values of y_o used in the experiment are shown in Fig. 3.8.

The value of Q for any particular h is measured at the outlet ports (see Fig. 3.2) by means of a propeller meter which was developed by the Delft Hydraulic Laboratory [30]. In order to simplify future calculations, a relationship of the form $Q = a\ h^b$ is used to fit the data points. Least square criterion is used to determine a and b. The values of a and b are shown in Fig. 3.8.

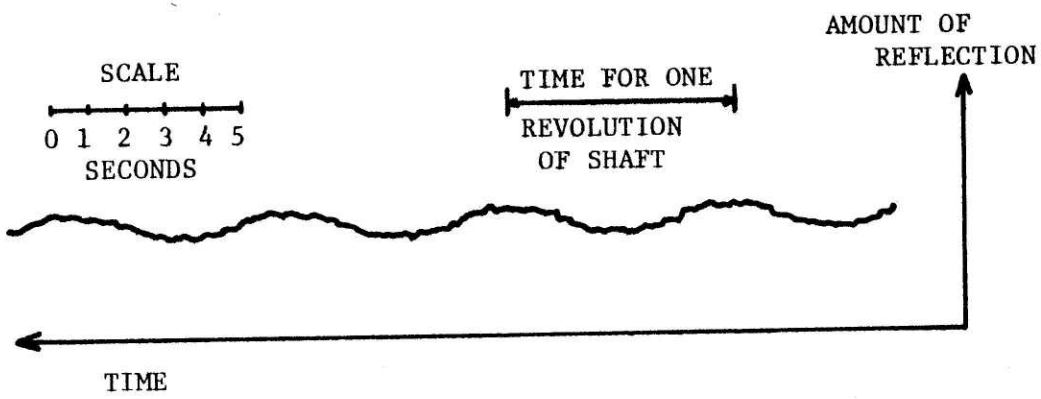

Fig. 3.7 Typical Record of Deflection of Rotating Shaft

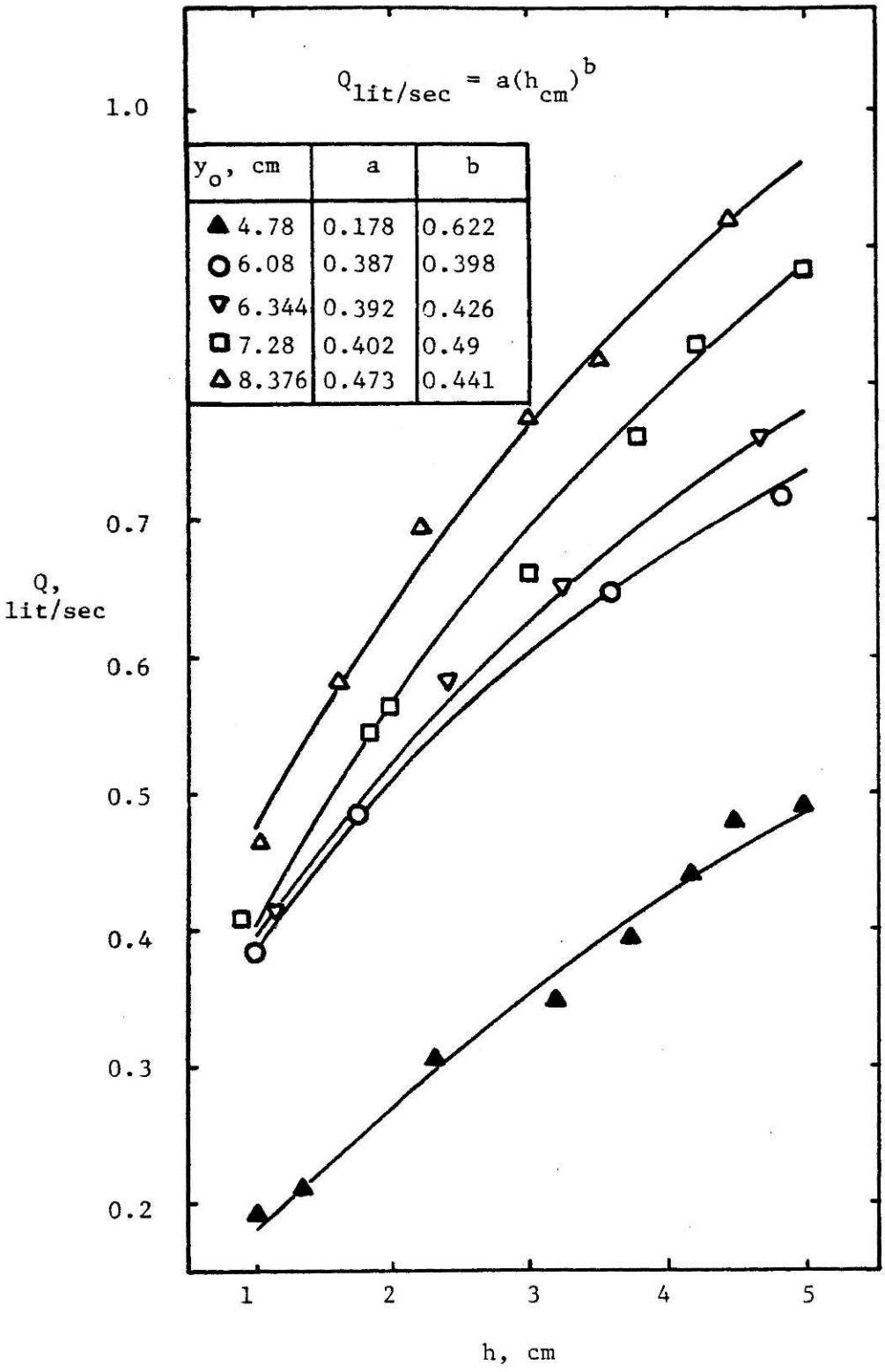

Fig. 3.8 Head-Flow Relationships of the Channel

3.3 Experimental Program

The experiments are arranged and labeled as shown in Table 3.1. An experimental series stands for experiments conducted for a wheel with specific values of radius (R), width (b), number of paddles (N), static water depth (y_o) and sill height (S), while the wheel speed is varied. The experimental results according to the purposes stated in Table 3.1 are discussed in Chapter 4.

3.4 Procedure for Conduction of Experiment

This section attempts to describe the procedure employed in experiment conduction. All experimental series indicated in Table 3.1 were conducted according to this procedure. The following paragraphs describe the procedure.

After the wheel is assembled so that its dimensions are according to the required specifications (i.e., the values of R, b, y_o and N indicated in Table 3.1), its shaft is connected to the P.V.C. shaft. The other end of the P.V.C. shaft is connected to the output shaft of the gear box. The alignment of shafts is made by adjusting the position of the gear box unit (which is rigidly attached to the motor unit) until it is visually observed that the shafts are aligned. No special equipment for alignment is used. Meanwhile, the recorder is switched on. It is recommended in the recorder handbook that it should be turned on at least half an hour before its use. However, it is found that the warm up time required for the recorder is more than the recommended value of 1/2 hour. Actually the warm up time should be around 2 hours. If the warm up time is shorter than approximately 2 hours, the recorder may behave erratically during operation.

Table 3.1 Experimental Program

(See Appendix A for more details)

SERIES	PURPOSES	WEIGHT OF WHEEL (kg)
B1 N8 6.08	Calibration and effects of variations in radius, width, number of paddles and depth of submergence	4.997
B1 N16 6.08		7.151
B1 N16 7.28		7.151
B1 N16 4.78		7.151
B1 N4 6.08		3.919
B2 N8 6.08		3.437
B2 N16 6.08		4.515
B2 N4 6.08		2.899
B2 N8 7.28		3.437
B2 N8 4.78		3.437
B2 N4 4.78		2.899
B2 N4 7.28		2.899
B2 N8 8.376		3.437
B2 N16 7.28		4.515
B2 N16 8.376		4.515
B2 N8 6.344		3.437
RN8 4.78	Verification	4.004
RN8 7.28		4.004
RN8 6.08		4.004
AN8 7.28 + 6	Effect of paddle angles	3.437
AN8 7.28 + 12		3.437
AN8 7.28 - 6		3.437
AN8 7.28 - 12		3.437
CP N8 6.08	Effect of curved paddle	3.782
CS N8 6.08	Effect of curved sill	3.437
SN8 6.08	Effect of sill	3.437

When it is ready to start the experiment, the motor is turned on and the wheel is adjusted to rotate at very slow speed (about 0.5 rad/sec). The minimum wheel speed is restricted by the sluggishness of the wheel which is probably caused by the inherent static friction at the bearings. The wheel is allowed to rotate at that constant speed for 3-5 minutes before readings are taken. This is to make sure that the system is operating at steady-state. Then the water level difference is observed and the recording chart is made to advance at the speed of 5 mm/sec. This records the shaft deflection onto the recorder. The chart is allowed to advance until approximately 10 revolutions are recorded. This completes the set of readings required for a fixed value of shaft speed.

Next, the wheel speed is increased and the same routine applies. This is done until it is visually observed that the water level difference remains virtually constant no matter how fast the wheel rotates. It is evident that this event occurs as a result of the drowned wheel condition discussed in Section 4.2(d). Once the drowned wheel condition is reached, the wheel is stopped and static torque calibration is performed. The technique used for static torque calibration is discussed in Section 3.2(a). The static torque calibration is necessary for the calibration of the reading recorded during the test. This completes the experimental procedure required for an experimental series.

After this, the chart (containing recorded deflection) is analyzed to obtain the shaft speed (w) and torque (T) (see Section 3.2a). The flow rate Q is then determined from the relationship shown in Fig. 3.8 and the recorded value of h. The water horsepower (P_w), the power input (P_{in}) and the wheel efficiency (e) can be computed from $P_w = \gamma Q h$,

$P_{in} = wT$ and $e = P_w/P_{in}$. The variation of these computed quantities can be plotted against w. Such a graph is shown in Fig. 4.1.

3.5 Discussion

This section attempts to bring out some improvable features of the apparatus in order to assist future researchers in apparatus design. There seem to be three major areas of drawback in the apparatus used in this study. They are (a) the creeping property of the P.V.C. shaft, (b) the range of velocity of flow in the channel is too narrow, and (c) more data on power losses due to friction is required.

a. P.V.C. shaft for torque measurement: In this study, the amount of torque transmitted is small (in the order of 1 Newton meter). To enable the deformation to be detectable, a shaft made of low torsional elasticity material must be used. Ordinary metals such as steel or aluminum have too high elasticity. If these metals are used to make the shaft, the wall thickness will be too thin to be practical. With this constraint, a P.V.C. shaft is used. However, P.V.C. is a kind of plastic which creeps when subject to continuous loading. This implies that if the wheel rotates continuously for a substantial amount of time, the shaft will creep thereby creating a somewhat permanent deformation which will show up in the recorder and may damage the transducer. Fortunately, it was found that the time required to cause detectable creeping is in the order of 3-4 hours of continuous loading. This time duration is larger than that required to complete an experiment conducted according to Section 3.4 which usually takes about 30-40 minutes.

With regard to the above problem, the following suggestions are offered.

(i) The wheel should be large enough to absorb sufficient torque such that metal shafts can be used to detect the deformation.

(ii) Some other means of measuring torque should be considered. Although a strain gage transducer (such as the one used in this study) offers good accuracy, the electronic gear sometimes behaves erratically probably due to outside (electrical) interference.

b. Flow resistance in the channel: In the apparatus, the flow resistance in a closed-loop high-rate pond is simulated by using 10 plastic hoses connecting both ends of the test section of the channel (see Fig. 3.2). It is found that the plastic hoses offer too much resistance (i.e., they simulate a channel that is too long) that the velocity of flow in the test section is generally lower than that encountered in practice.

A somewhat minor but nuisance problem associated with the previous problem is that standing waves do occur at some particular wheel speed. Apparently this is caused by wave reflection at the two end walls used to connect the hoses. In field situations, the waves produced at the wheel will propagate and dissipate along its path of travel in the channel and standing waves will unlikely occur. In conduction of the experiment, the wheel speed that allows standing waves to occur is avoided.

c. Power loss due to bearing friction: In Chapter 2, in order to estimate the bearing friction, it is postulated that the power loss

varies with the load applied to the bearing. In the study, the range of variation of the bearing load is too narrow, yet the results have to be extrapolated so that power loss in full size wheels can be estimated. By extrapolation, it is found that the ratio of the power loss at the bearing to the total power input is smaller for larger wheels. For example, in the apparatus, the ratio may be about 0.1 while in the full size wheel this ratio can be as low as 0.01. More experimental data has to be collected to confirm this.

CHAPTER IV: EXPERIMENTAL RESULTS AND THEIR ANALYSIS

4.1 Characteristic Curves

4.2 Observation of Flow

- a. Water levels and flow pattern
- b. Bubble formation
- c. Wave generation
- d. Drowned-wheel condition
- e. Noise

4.3 Effects of Wheel Geometry on its Performance

- a. Sill
- b. Wheel radius
- c. Wheel width
- d. Number of paddles
- e. Depth of submergence
- f. Paddle angles
- g. Curved paddles
- h. Contoured sill

4.4 Calibration

- a. Procedure
- b. Results

    Drag coefficient

    Mechanical friction loss

4.5 Verification

4.6 Discussion

- a. Scale effect
- b. Limitation of wheel size

CHAPTER IV

EXPERIMENTAL RESULTS AND THEIR ANALYSIS

The purposes of conducting the experiments are:

(i) To obtain the system characteristic curves experimentally.

(ii) To observe the flow in the vicinity of a paddle wheel.

(iii) To study how the wheel performance is affected by variations in its radius, width, number of paddles, depth of submergence, paddle angles and some modifications in geometry.

(iv) To use the data for calibrating the analytical model described in Chapter 2.

(v) To use part of the data for checking or verification of the calibrated model.

This chapter discusses all the above items. Experimental data employed are those obtained from the experimental series outlined in Table 3.1. In Section 4.1, the characteristic curves obtained experimentally are discussed to bring about some important features which are further discussed in Section 4.2. In Section 4.2, criteria for bubble formation and drowned-wheel condition are deduced from experimental data. These criteria are used in Chapter 5 in connection with the design procedure. Bubble formation and drowned-wheel condition are detrimental to the wheel efficiency. In Section 4.3, the effect of wheel geometry such as its radius, width and number of paddles on its efficiency are discussed with reference to the experimental data. Section 4.4 couples the analysis of Chapter 2 and experimental results together to determine the value of the drag coefficient C_D. The obtained value of C_D is used in the design procedure of Chapter 5. Verification of the obtained value of C_D is made in

Section 4.5.

Section 4.6 provides comment on significant aspects of this chapter.

4.1 Characteristic Curves

Using the apparatus discussed in Section 3.1, some important parameters such as the head difference, torque and wheel speed can be measured. From these measurements, the system characteristic curves can be determined (Section 3.4). Typical characteristic curves are shown in Fig. 4.1. From the figure, it is seen that as w increases the head difference h, the torque T, the flow rate Q and the power input P_{in} increase. However, h and Q increase up to a certain value of w and then remain relatively unchanged. This is due to the drowned-wheel condition discussed in Section 4.2(d). The efficiency, e, increases and then decreases, exhibiting a maximum value occurring at a particular w. It is interesting to note that e drops off shortly after the appearance of bubbles. The significance of bubble formation is discussed in the next section.

4.2 Observation of Flow

This section attempts to describe the flow in the vicinity of the wheel as observed visually. The description is made with reference to a paddle wheel set up whose characteristic curves are shown in Fig. 4.1. As the speed w of the wheel increases, many interesting flow phenomena occur. They are: (i) wave generation at the upstream and downstream side of the wheel, (ii) bubble formation as w reaches a certain value, (iii) noise and (iv) the drowned-wheel condition. Intuitively all of them consume energy when occurring. Hence they are believed to decrease the wheel

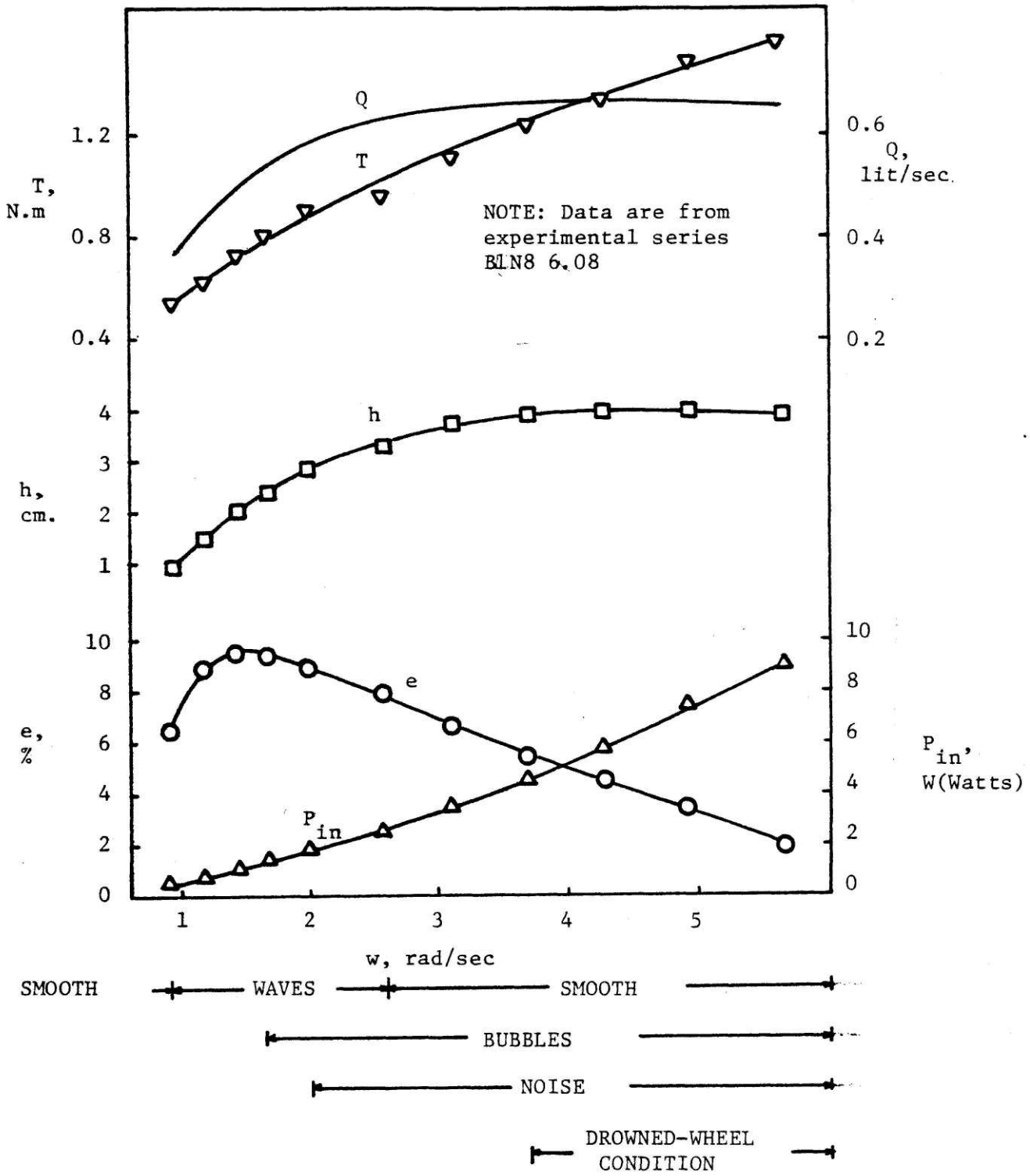

Fig. 4.1 Experimentally Obtained Characteristic Curves

efficiency.

a. Water levels and flow pattern

At very slow wheel speed, the water level inside the wheel appears to approximate a straight line connecting the upstream and downstream water levels (Fig. 4.2a). At moderate speed, the water level inside the wheel is higher on the side where a paddle exerts force on the water (Fig. 4.2b). The water surface inside a paddle chamber is not smooth.

As the wheel speed increases, the uneveness of the water surface and the difference between the highest and the lowest water levels inside a wheel chamber increase. If the paddle height is not sufficient, it can happen that the higher side of the water level reaches the top of the paddle (i.e., the point where the paddle is closest to the wheel center) and spill back into the following chambers (Fig. 4.2c). Intuitively, this decreases the wheel efficiency.

With respect to design, it is believed that the paddles should extend as close as possible to the wheel center in order to minimize the spillage discussed earlier. In addition, an air vent must be provided for every chamber somewhere close to the chamber apexes. This is to allow displaced air (by the water) to escape, thus preventing air pressure from building up inside the chambers. If the air pressure inside the chambers is allowed to build up, it will prevent the water from entering the chambers, resulting in a decrease of the wheel efficiency.

The flow generated by a rotating paddle wheel is a pulsating one. The period of pulsation is equal to $2\pi/wN$. The rotating wheel creates more turbulence at the downstream side than the upstream side. In order to observe the flow pattern, a stream of dye is injected. Due to strong turbulence produced by the wheel and the nature of pulsating flow, the

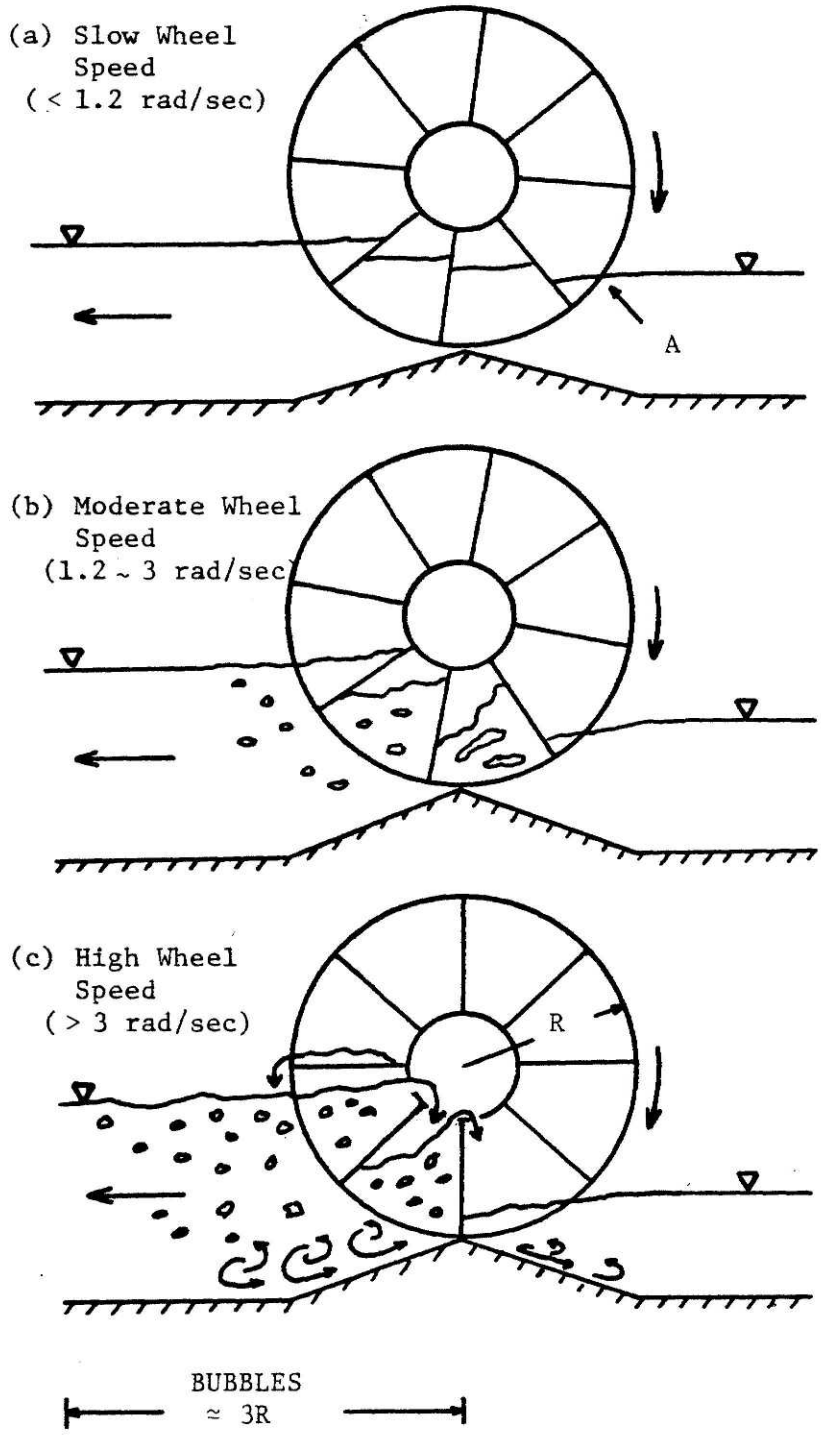

FIG. 4.2 Water Levels and Flow Pattern

flow pattern can not be observed clearly. However, close to the channel bed and sill (and the sidewalls) some small reversed flow can be observed (Fig. 4.2c). It is this flow that is responsible for the leakage discussed in Section 2.2(c). No attempt is made to measure the amount of this flow.

Bubbles and waves are also produced by the wheel action. Their observations are discussed next.

b. Bubble formation

Bubbles appear when the wheel speed reaches a certain value. Apparently two separate mechanisms affect bubble formation:

(i) Paddle tip velocity: These bubbles are formed at the upstream side by the swift action of the paddle tip as it strikes and moves through the water. Their sizes range from 1/2 to 1 cm and are not spherical. Once formed, they are captured between two paddles, break up into many smaller bubbles and are released at the downstream side. At the downstream side, most of them are caught in the water turbulence there while some rise up to the surface and disappear.

(ii) Water falling from departing paddles: When the wheel speed is high, the departing paddles on the downstream side carry some water with them even when they are clear above the water level (Section 4.1d). These waters are elevated to a certain height by the rotating paddles before falling back. The falling water generates bubbles upon impact on the underlying water body. The bubbles are caught in the water turbulence while some rise and disappear. The bubble sizes are about 1 to 2 mm in diameter.

The mechanism described in (i) usually occurs before (ii). In both cases, the bubble concentration increases as the wheel speed increases.

Since bubbles occupy spaces available for water and their formation and transport require energy, it is expected that the wheel efficiency decreases with the bubble concentration. At high speed, it was visually observed that the space occupied by bubbles can reach 60 $\sim$ 70% of the total space that should have been available for transport of water. This leads the author to believe that the wheel efficiency (as defined in Chapter 2) is very significantly affected by formation of bubbles. The appearance of bubbles is usually confined to within the distance 3R from the wheel in the downstream direction (Fig. 4.2c).

In this study, no attempt is made to quantify the effect of bubbles on the wheel power requirement. The analytical approach in Chapter 2 is not allowed for bubble formation. In addition, the laboratory data, used to determine C_D in the calibration process of Section 4.4, were selected such that the ranges of wheel speed which produce bubbles were excluded. Therefore, the obtained values of C_D (Fig. 4.13 and Table 4.3) are not valid if bubble formation is substantial. It is thus necessary to define the limit of applicability of the analytical approach with respect to bubble formation, which is the essence of the following paragraphs.

Since bubbles are normally formed due to the shear produced by the swift action of the paddle tip as it strikes and moves through the water, it is postulated that the velocity of the tip relative to the water velocity governs the formation of bubbles. At the point A in Fig. 4.2(a), the paddle tip velocity relative to the water velocity at the upstream end, V_{TW}, can be expressed as

$$V_{TW} = wR - \frac{Q}{b\, y_{\bar{B}}} \cos\left[1 - \frac{y_{\bar{B}} - S}{R}\right] \qquad (4.1)$$

For a paddle wheel set up, V_{TW} increases with the wheel speed. It is then postulated that whenever V_{TW} exceeds a certain critical value bubbles will be formed. The critical value of V_{TW} is then used as the limitation for the applicability of the analytical approach described in Chapter 2.

The critical value of V_{TW} is determined from experimental data summarized in Appendix A. For each experimental series, the wheel speed w, the flow rate Q and the water level difference h at the inception of bubble formation were recorded. Equation (4.1) is then used to calculate the critical value of V_{TW} which is designated as V_{TWC}. A plot of V_{TWC} versus y_B/h is shown in Fig. 4.3. The value of $V_{TWC} \approx 15$ cm/sec is then used as the criterion for bubble formation. The computations are shown in Table 4.1

In conclusion, the criterion for bubble formation is

(i) for $V_{TW} < 15$ cm/sec, there will be no bubbles produced.

(ii) for $V_{TW} \geq 15$ cm/sec, there will be bubbles produced and the concentration of bubbles increases as V_{TW} increases.

In (i) and (ii) above, the quantity V_{TW} is computed from Eq. (4.1).

The formation of bubbles at high wheel speed may help aeration. However, as mentioned in Section 1.5b the aeration in high-rate algae ponds can be accomplished more efficiently by the photosynthesis of algae in the pond and there is no need for mechanical aeration. Accordingly, the paddle wheel will be more efficient if it is designed such that bubble formation is avoided.

Since initial bubble formation usually occurs at the upstream side of the wheel due to the shock created by the impact of the paddles with the underlying water, it is possible to reduce this shock by smoothing all sharp edges of the paddles.

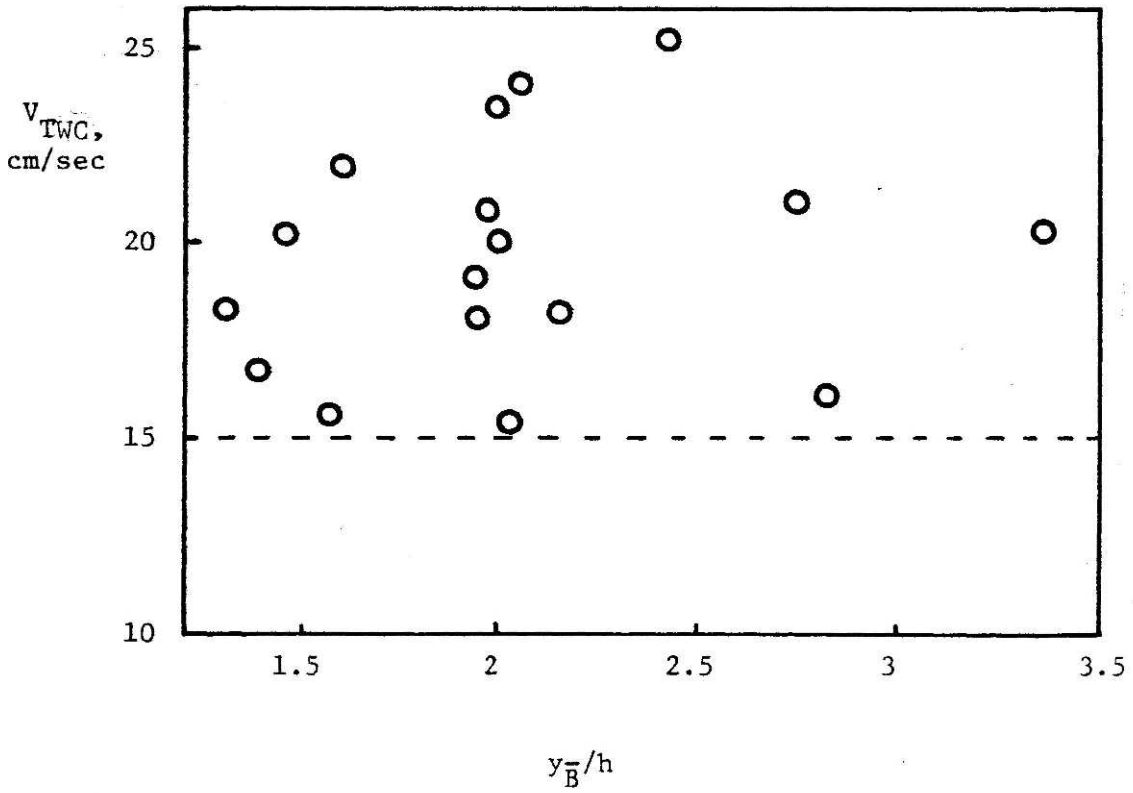

Fig. 4.3 Criterion for Bubble Formation

Table 4.1 Computation of Critical Velocity for Bubble Formation

Series	w (rad/sec)	h (cm)	Q (lit/sec)	$y_{\bar{B}}$ (cm)	V_{TWC} (cm/sec)
B1 N8 6.08	1.678	2.4	.548	4.88	15.33
B1 N16 6.08	1.855	3.23	.617	4.47	16.81
B1 N16 7.28	2.045	4.02	.796	5.27	18.39
B1 N16 4.78	1.662	2.31	.3	3.63	15.77
B1 N4 6.08	2.793	2.07	.517	5.05	25.2
B2 N8 6.08	2.394	2.46	.553	4.85	20.84
B2 N16 6.08	2.384	3.1	.607	4.53	20.25
B2 N4 6.08	2.273	1.57	.463	5.3	20.32
B2 N8 7.28	2.166	2.99	.688	5.79	18.08
B2 N8 4.78	2.556	1.87	.263	3.85	24.08
R N8 7.28	1.863	3.46	.739	5.55	22.04
R N8 6.08	1.921	2.45	.553	4.86	23.59
B2 N4 4.78	2.423	.93	.17	4.315	23.47
B2 N4 7.28	2.4	2.24	.597	6.16	21.1
B2 N8 8.376	2.195	3.15	.785	6.8	18.22
B2 N16 7.28	1.929	2.51	.631	6.03	16.08
B2 N16 8.376	2.307	3.43	.815	6.66	19.15
B2 N8 6.344	2.327	2.54	.583	5.07	20.07

Notes i See Appendix A for more information

ii $y_{\bar{B}} \cong y_o - \frac{h}{2}$

Surface tension of the liquid mixture in the pond also affects the bubble formation. The effect of algae, bacteria, nutrients and other impurities on the surface tension value of wastewater has to be studied.

c. Wave generation

There is a speed range where waves are produced both at the upstream and downstream sides of the wheel. Generally, waves at the downstream side are higher than those at the upstream side. These waves have periods of approximately $2\pi/wN$ which is equal to the time gap between two adjacent paddles. The maximum wave heights at the downstream and upstream side are about 2 cm and 1 cm, respectively. The speed of propagation is higher for the downstream side. Some energy is carried away with these waves which are dissipated elsewhere in the channel. This part of the energy is considered a loss.

Outside of this speed range, the water surface is relatively smooth. This indicates that the set-up probably has a natural frequency. When the rotating wheel creates external excitation of frequency close to its natural frequency, waves are produced.

The cause of excitation is due to the shock created by the somewhat abrupt change in water velocity as it enters and leaves the wheel. The water velocity inside the wheel is higher than those in the channel adjacent to the wheel. The waves produced travel away from the wheel. Their speeds of propagation are related to the water depths and velocities at the respective sides of the wheel.

d. Drowned-wheel condition

As the wheel speed increases to a certain value, the water on the downstream side does not have enough time to clear the upgoing paddles

(Fig. 4.4a). An amount of water is carried along with the paddles. Some of this water falls back into the underlying water body and some flows along the paddle radially towards the wheel center. This is the beginning of the drowned-wheel condition. If the wheel speed is increased beyond this value, some water will reach the top of the wheel and is transported back to the upstream side. The amount of water being transported back increases with the wheel speed. Whenever a wheel is operating in this mode, it is said in this report that the wheel is operating in the drowned-wheel condition.

Operating in the drowned-wheel condition reduces the wheel efficiency. Even more serious is the fact that the wheel will not be able to produce higher head (h) once the drowned-wheel condition is reached. This implies that if the wheel is too small, it may be unable to provide the required head no matter how fast it rotates. Therefore the drowned-wheel condition is undesirable and must be avoided in design and operation.

Whether a wheel is operating in the drowned-wheel condition depends on its speed, radius and the water level on the downstream side. Using the experimental data summarized in Appendix A, the relationship between $\frac{w^2}{g}(y_{\bar{A}} - S)$ and $(y_{\bar{A}} - S)/R$ can be computed and plotted as shown in Table 4.2 and Fig. 4.4(b). An envelope curve can be drawn to separate the region where the drowned-wheel condition occurs from the rest. The solid curve in Fig. 4.4(b) is the envelope curve. Any wheels whose operating condition lie in the shaded area will be operating in the drowned-wheel condition. In the computer program discussed in Section 5.1, this curve is assumed to be a straight line shown dotted in Fig. 4.4(b). This is done to simplify the program and provide a factor of safety against the drowned-wheel condition.

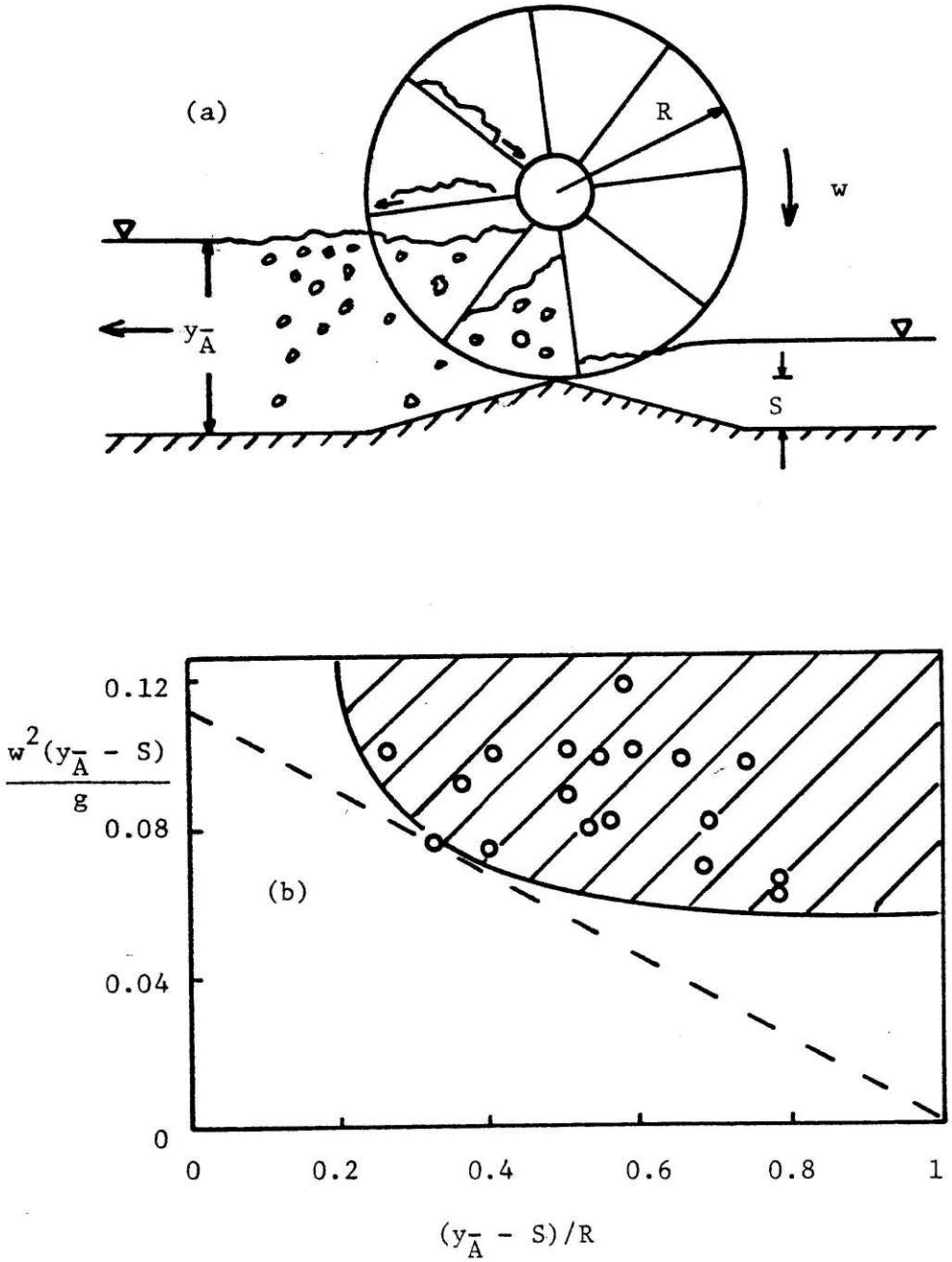

Fig. 4.4 Criterion for the Drowned-Wheel Condition

Table 4.2 Computation for the Drowned-Wheel Condition

Series	w (rad/sec)	$y_{\bar{A}}$ (cm)	$\frac{w^2}{g}(y_{\bar{A}} - S)$	$(y_{\bar{A}} - S)/R$
B1 N8 6.08	3.707	8.005	.0802	.5635
B1 N16 6.08	4.154	8.285	.1056	.5910
B1 N16 7.28	3.557	9.82	.0972	.7421
B1 N16 4.78	4.234	6.345	.0743	.4001
B1 N4 6.08	4.093	7.45	.0883	.5089
B2 N8 6.08	4.161	7.885	.0989	.5517
B2 N16 6.08	4.436	8.235	.1195	.5861
B2 N4 6.08	4.562	7.44	.1095	.5079
B2 N8 7.28	3.36	9.365	.0815	.6973
B2 N8 4.78	4.937	5.98	.0919	.3642
RN8 4.78	5.161	6.025	.1017	.2681
RN8 7.28	3.244	9.735	.08	.5336
RN8 6.08	4.24	7.99	.1046	.4087
B2 N4 4.78	4.76	5.56	.0758	.3228
B2 N4 7.28	3.791	8.99	.0983	.6604
B2 N8 8.376	2.743	10.266	.0613	.786
B2 N16 7.28	3.108	9.245	.0686	.6855
B2 N16 8.376	2.825	10.281	.0651	.7875

Notes

i See Appendix A for more details

ii S in all series = 2.28 cm

iii $y_{\bar{A}} \cong y_o + \frac{h}{2}$

More experimental data has to be collected in order to clearly define the drowned-wheel condition zone in Fig. 4.4.

e. Noise

At a certain speed onward, periodic noise can be heard. It is apparently caused by the impact between the rotating paddles and the water on the upstream side. The period of the noise is $2\pi/wN$, i.e., there are N pulses of noise in one revolution of the wheel. The energy loss due to noise production is assumed to be negligible.

4.3 Effect of Wheel Geometry on its Performance

The wheel's performance can best be described by its efficiency in transferring mechanical power into water power. For each experimental series shown in Table 3.1 a curve of the efficiency e versus the wheel speed w can be constructed. Since the experiments are controlled in such a manner that only the interested parameter is varied (while others are held constant), the curves of e versus w for different series can be compared. This is done for the following cases.

a. Sill:

The purpose of this case is to confirm that installing a sill will increase the wheel efficiency. The experimental series used are B2 N8 6.08 and S N8 6.08. Their e versus w curves are shown in Fig. 4.5. From the curves, it is evident that the efficiency reduces when the sill is removed.

Referring to the analysis of Chapter 2, the sill function is to reduce the leakage. Without the sill, the leakage will be so high that drastic reduction in efficiency occurs.

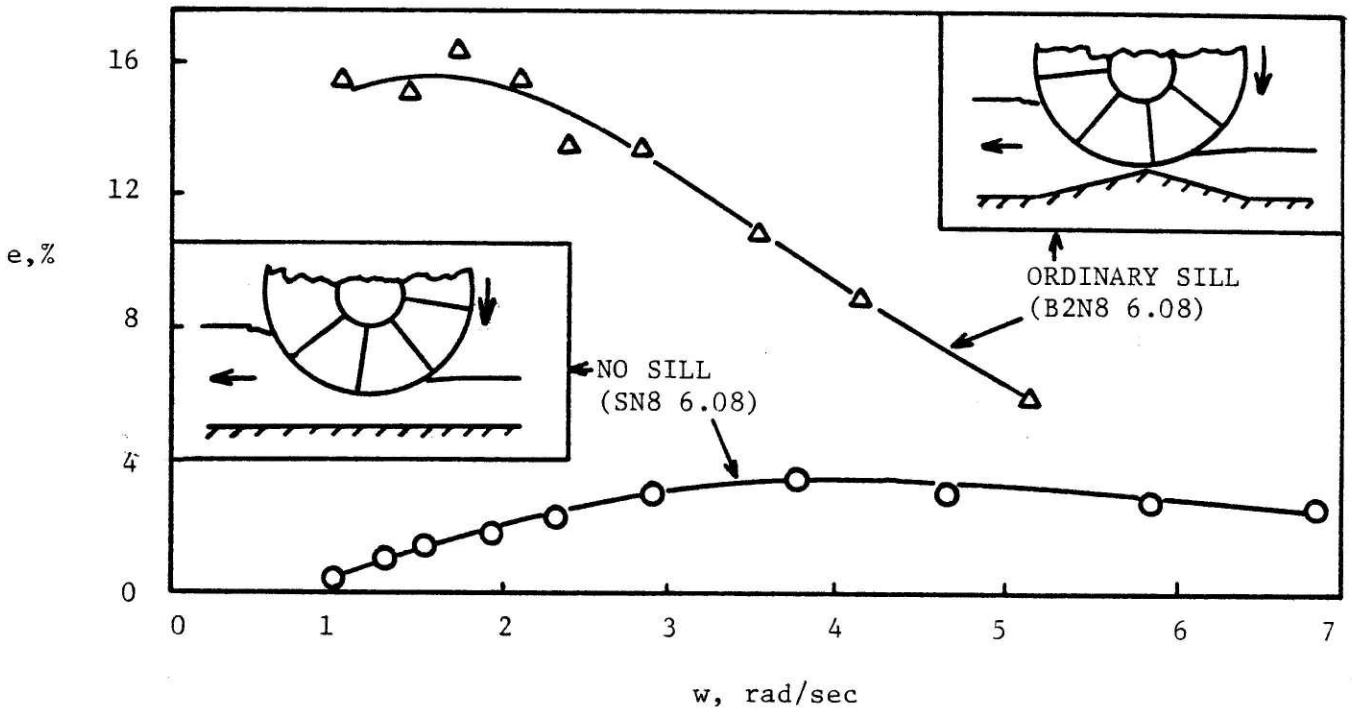

Fig. 4.5 Effect of Sill

b. Wheel radius

The effect of the wheel radius on the efficiency is shown in Fig. 4.6 which is obtained from the experimental series B2 N8 6.08 and R N8 6.08. Comparison of the efficiency curves between the two series reveals that for the apparatus set up in this study, increasing the wheel radius reduces the efficiency. This is probably due to the increase in moment arm and hence the resisting torque and power required when the radius increases.

c. Wheel width

The effect of the wheel width on the efficiency curve is shown in Fig. 4.7 which is obtained from the experimental series B1 N8 6.08 and B2 N8 6.08. For the existing set up, increasing the wheel width b decreases the efficiency.

d. Number of paddles

The effect of the number of paddles (N) on the wheel efficiency is shown in Fig. 4.8 for N = 4, 8 and 16. Experimental series B1 N4 6.08, B1 N8 6.08 and B1 N16 6.08 were used. It is evident that the efficiency can be increased by increasing the number of paddles. However, the increase in efficiency seems to be smaller as N is large (i.e., the increase in efficiency from N = 4 to N = 8 is larger than from N = 8 to N = 16).

Other significant benefits of having high N is that the flow disturbance (in form of waves) created at the wheel is less prominent. In the experiment, it was observed that for N = 4, the wave produced is more significant than that for N = 16. For practical purposes, it is believed that N should not be lower than 6.

Another point that may be useful in modification of the wheel in existing system is that, if N is increased, the wheel can afford to rotate

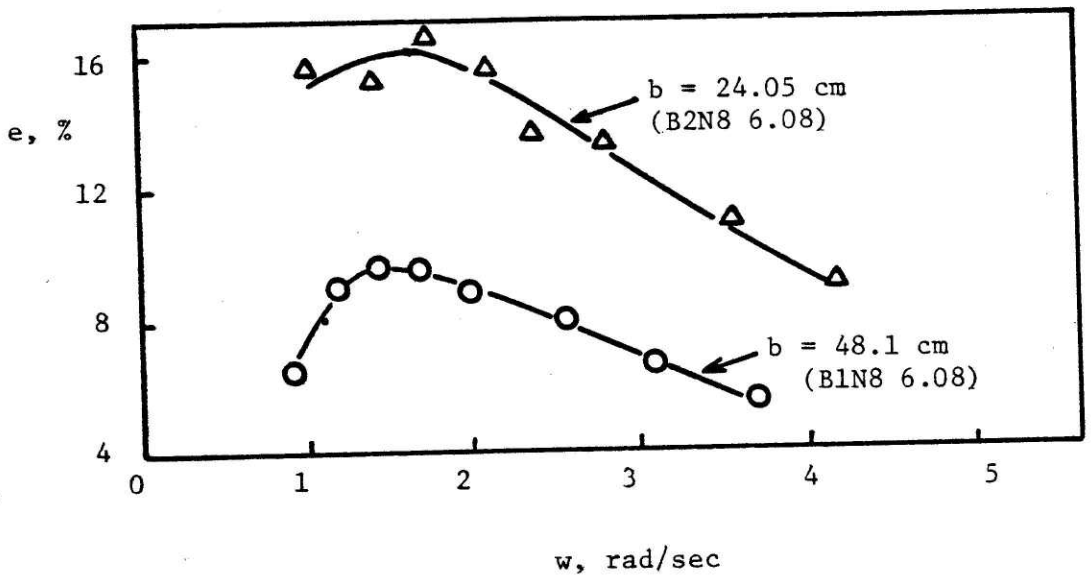

Fig. 4.7 Effect of Wheel Width

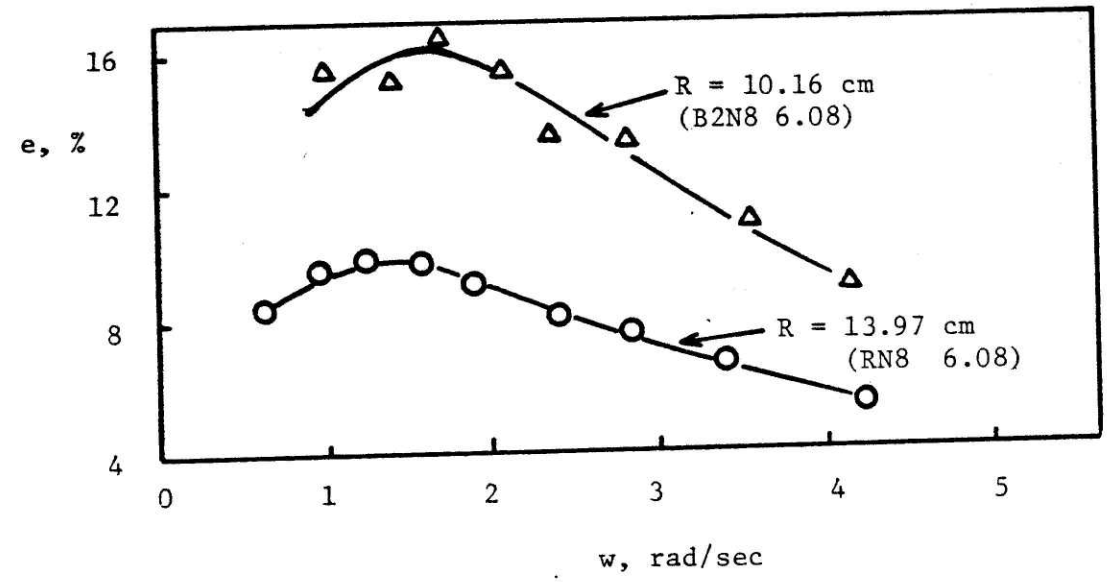

Fig. 4.6 Effect of Wheel Radius

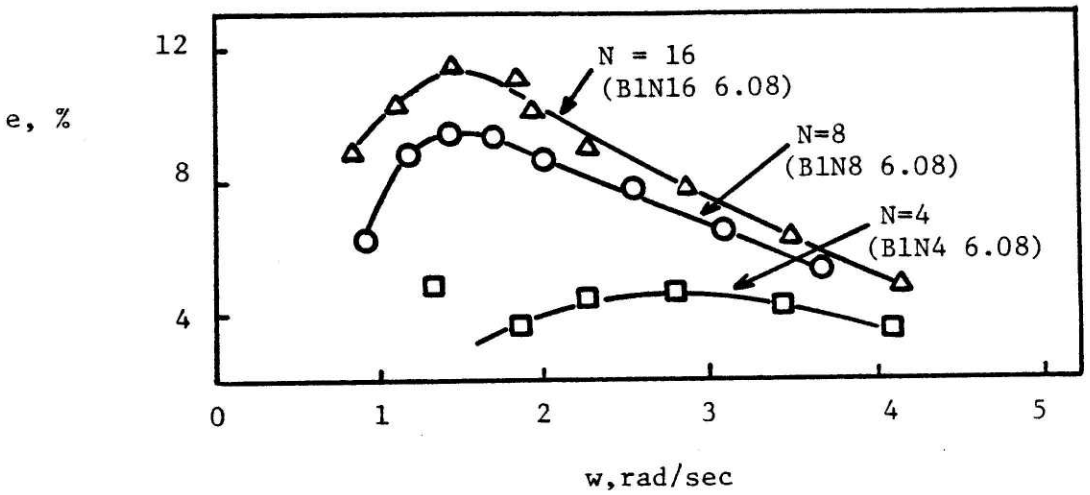

Fig. 4.8 Effect of Number of Paddles

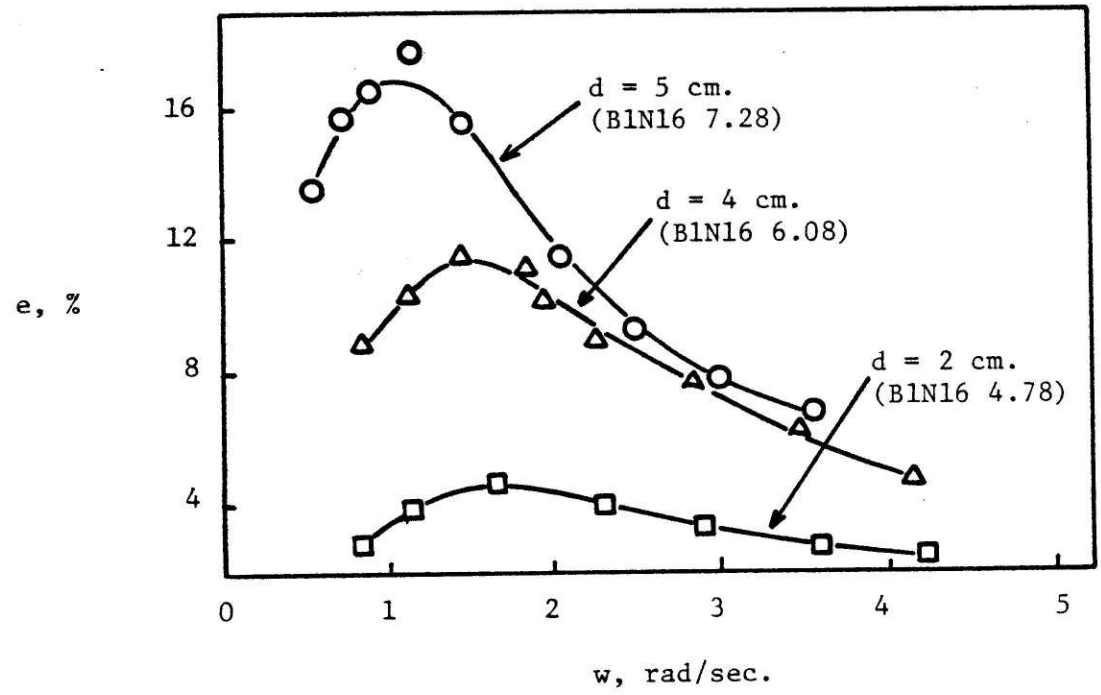

Fig. 4.9 Effect of Depth of Submergence

at a lower speed in order to produce the same flow in the channel. This may be useful in cases where one needs to increase the flow without having to change the wheel speed. This can be accomplished by putting more paddles into the existing wheel. However, as the flow increases, the water level on the downstream and upstream sides of the wheel increases and decreases, respectively. This may put the wheel into the drowned wheel condition as described in Section 4.2d.

Except for cost and constructional reasons, higher number of paddles is always better than lower. However, as noted in the previous paragraph, high N results in low wheel speed. If the wheel speed is very low, the wheel may rotate sluggishly due to the inherent static friction at the bearings. This may cause undesirable vibration and waves. It is observed in the experiment that, if w is more than 0.3 rad/sec the problem disappears. This may not be generally true for wheels operated under different conditions or wheels of different sizes.

e. Depth of submergence

The depth of submergence d is defined as $d = \bar{y}_o - S$ where $\bar{y}_o = \frac{1}{2}(y_{\bar{A}} + y_{\bar{B}})$ (Section 2.3). In the experiments $y_{\bar{A}} \cong y_A$ and $y_{\bar{B}} \cong y_B$ and therefore $d \cong y_o - S$ where y_o is the static water level. The depth of submergence can be varied by either raising (or lowering) the wheel or the static water level. In the case where the wheel is raised (or lowered), the sill height should be adjusted so that minimum clearance exists between the wheel and the sill in order to minimize leakage. In this study, the static water levels were varied to change the depth of submergence.

The effect of the depth of submergence on the efficiency curve is shown in Fig. 4.9. The experimental series used are B1 N16 7.28, B1 N16 6.08 and B1 N16 4.78. It is evident that efficiency increases

with increasing d. However, there are practical limitations on how much d can be. They are

i the higher d is, the more susceptible the wheel is to the drowned-wheel condition (Section 4.2d).

ii the water in the paddle chambers may spill out through the top of the chambers while the wheel is rotating (Section 4.2a).

f. Paddle angles

Paddle angle is defined as the angle between a paddle and a radial line as shown in Fig. 3.5(a). In Fig. 3.5(a) the angle β shown is positive. The effect of the paddle angles on efficiency is shown in Fig. 4.10. The data used are from the experimental series B2 N8 7.28, AN 87.28 + 6, AN 87.28 + 12, AN 87.28 - 6 and AN 87.28 - 12. In Fig. 4.10(a) the efficiency curves for various β are shown. Each curve in Fig. 4.10(a) represents the efficiency curve for a particular β. There is a maximum value of efficiency (e_{max}) for each efficiency curve. The plot of e_{max} versus β is shown in Fig. 4.10(b). It is evident that $\beta = 0$ yields the maximum efficiency and therefore should be used in the design of paddle wheels.

g. Curved paddles

Looking in the direction of flow at the wheel, a curved paddle appearance is shown in the insert of Fig. 4.11 and Fig. 3.4(b). The outer edge of a curved paddle has curvature in it while in ordinary paddles this edge is straight. Curved paddles require a curved sill in order to match and minimize leakage. The curved sill is also shown in the figures. The idea behind testing curved paddles is that curved paddles may reduce the energy loss in impact occurring when a paddles strikes the water and thereby increases the wheel efficiency.

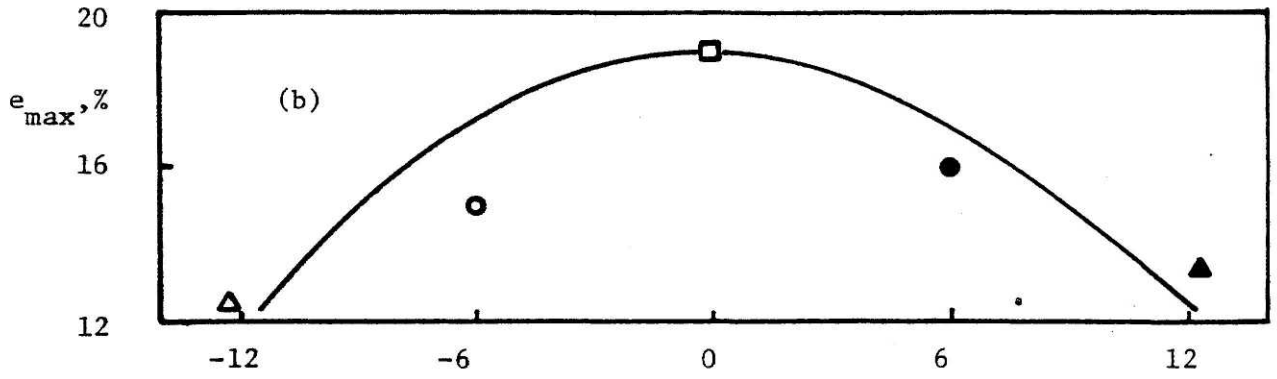

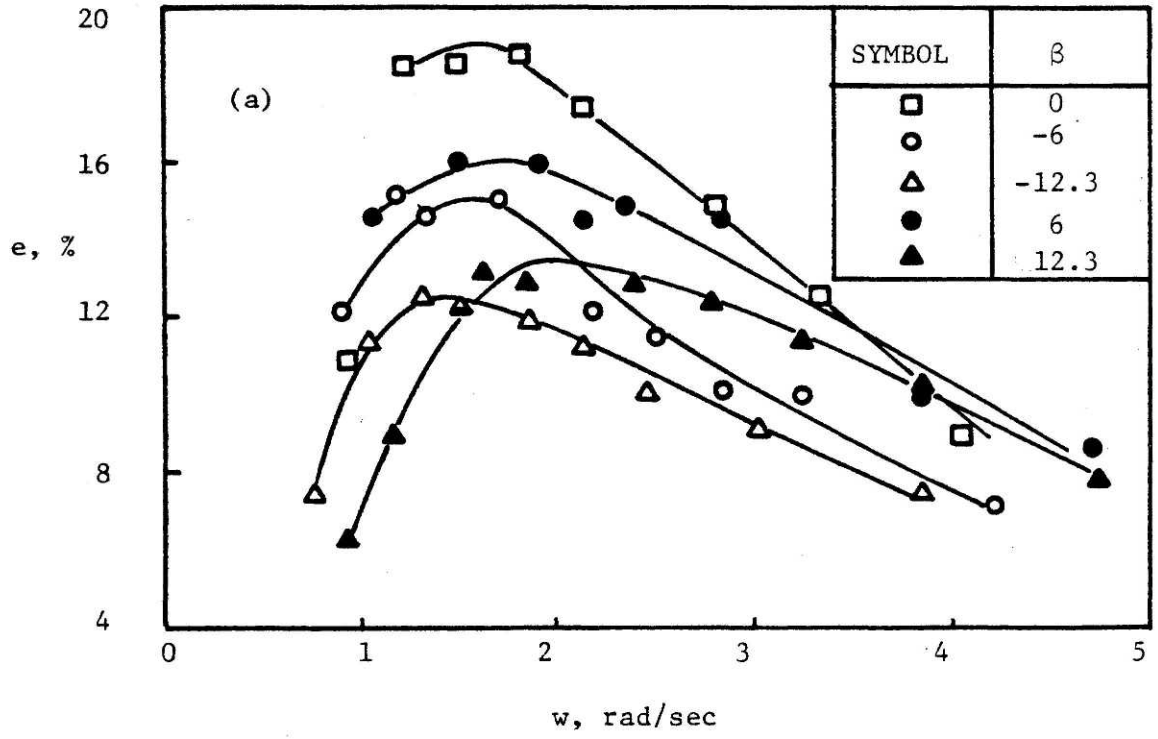

NOTE: See Fig. 3.5(a) for definition of β

Fig. 4.10 Effect of Paddle Angles

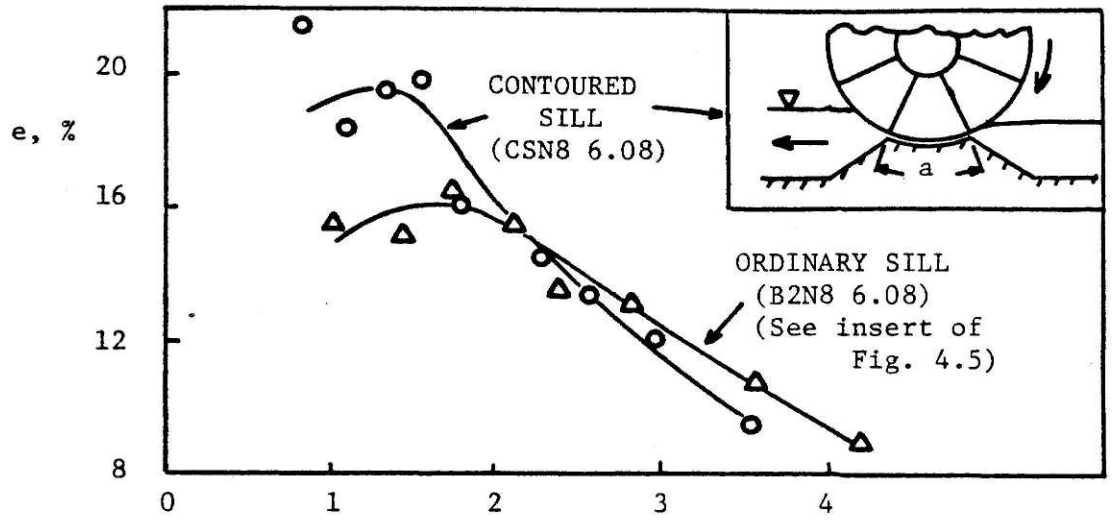

Fig. 4.12 Effect of Contoured Sill

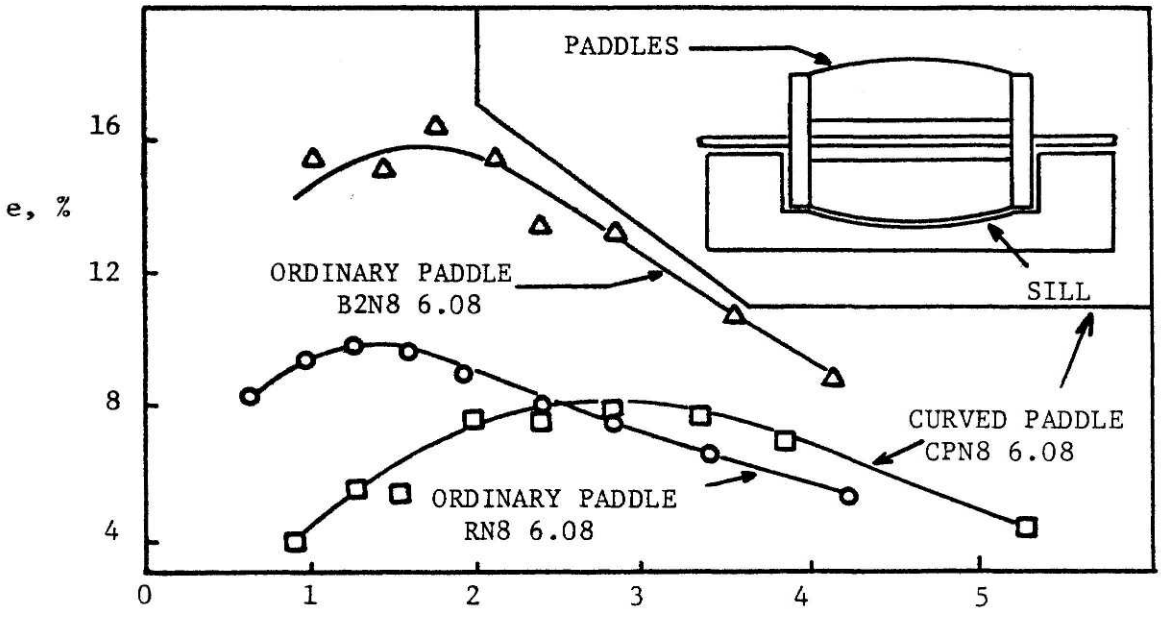

NOTE: For sketch of ordinary paddle, see Fig. 3.4(a)

Fig. 4.11 Effect of Curved Paddles

The effect of curved paddles is shown in Fig. 4.11. The experimental series used are CP N8 6.08, B2 N8 6.08 and R N8 6.08. Since a curved-paddle wheel does not have a well defined radius, it is difficult to compare its efficiency to other constant radius wheels. However, in this study, the curved-paddle wheel has a radius which lies within R = 10.16 cm of series B2 N8 6.08 and R = 13.97 cm of series R N8 6.08. Without the effect of the curved paddles, one would expect the efficiency curve of CP N8 6.08 to lie within those of B2 N8 6.08 and R N8 6.08. With the effect of the curved paddles, this may not be true. What actually happens is shown in Fig. 4.11. It is evident from Fig. 4.11 that curved-paddles do not improve the wheel efficiency.

h. Contoured sill

Looking in the direction of the wheel axis of rotation, a contoured sill appearance is shown in the insert of Fig. 4.12. The arc length (a) of the contoured sill in this study is $2\pi R/N$. It is postulated that such a contoured sill may reduce the leakage and thereby increase the wheel efficiency.

The effect of a contoured sill is shown in Fig. 4.12. The experimental series used are B2 N8 6.08 and CS N8 6.08. It is apparent that at low wheel speed, the efficiency is improved by approximately 3% while at high speed, the efficiency is reduced by approximately 1%. A possible explanation is that the contoured sill is more effective in reducing leakage at low wheel speed. At high wheel speed, the contoured sill is not only less effective in reducing leakage but also introduces undesirable flow resistance which will not be there if an ordinary sill (i.e., that of B2 N8 6.08 is used.

Since operating the wheel at a low speed usually avoids the problems of bubble formation and drowned-wheel condition, it can be concluded that a contoured sill is good for paddle wheel design.

4.4 Calibration

The purpose of calibration is to find the value of the drag coefficient C_D such that the predicted (i.e., using the analytical model of Chapter 2) and the experimentally obtained curves of h and P_{in} versus w agree to a reasonable accuracy for each experimental series. The experimental series used in the calibration are those that start with B in Table 3.1. The values of C_D obtained are found to depend on d/R and N. Their relationship as the result of the calibration is shown in Fig. 4.13.

The relationship shown in Fig. 4.13 can be used together with the analytical model to estimate the speed and power required in the design of a paddle wheel. This is discussed in Chapter 5.

a. Procedure

In order to predict paddle wheel performance, the relationships between the head it produces (h), its power requirement (P_{in}) and its speed of rotation (w) must be known. This is essentially the wheel characteristic curves shown in Fig. 4.1. For each experimental series starting with B in Table 3.1, their characteristic curves can be determined from the experimental results shown in Appendix A. The predicted characteristic curve for each of these series can also be obtained by the analytical model discussed in Chapter 2. The predicted curves depend on the value of C_D used in the model. For each series, it is possible to find a value of C_D such that the predicted and the experimentally obtained characteristic curves agree to a reasonable accuracy.

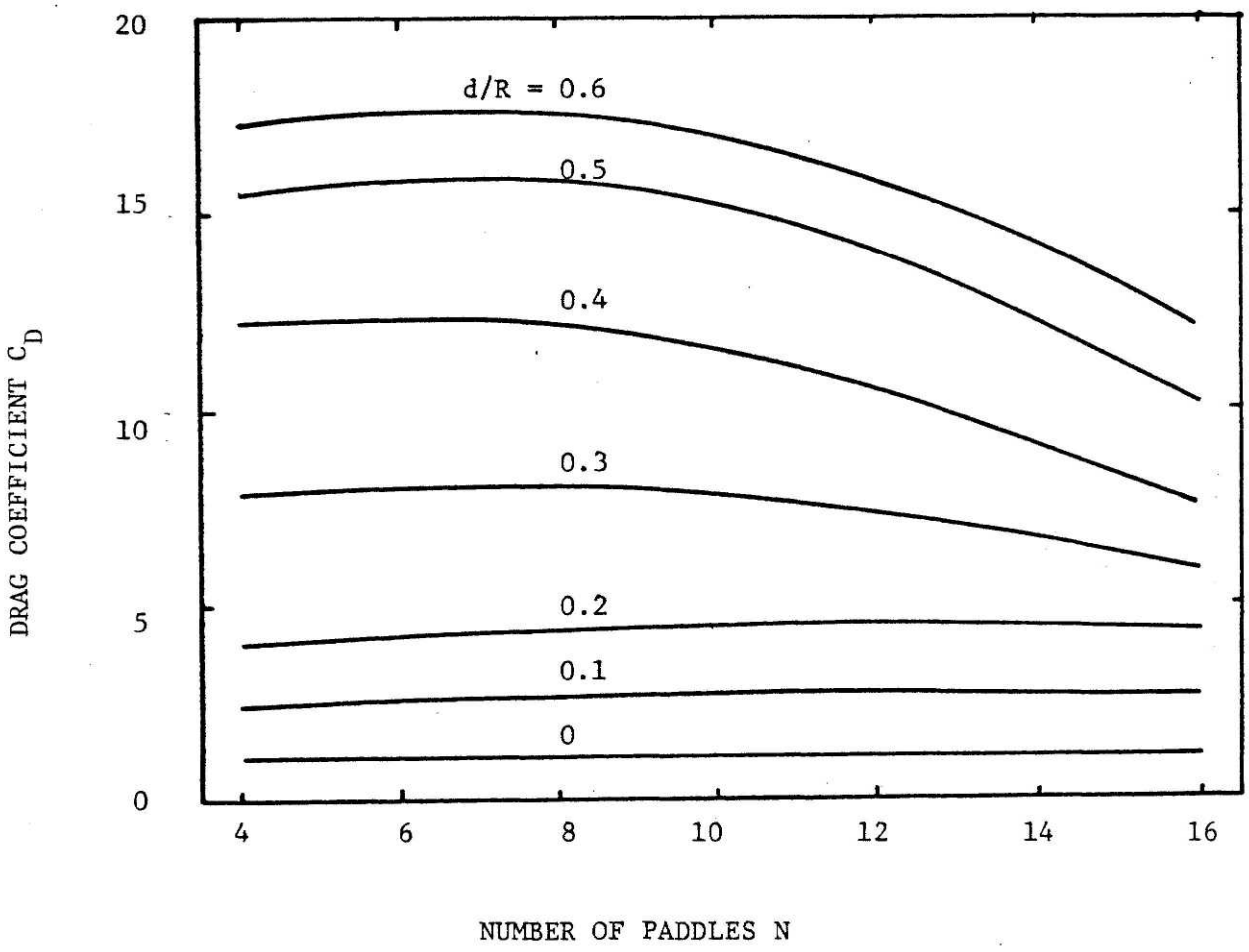

Fig. 4.13 Variation of C_D with N and d/R

As discussed in Section 4.1, at high w there are some events that can not be accounted for in the analytical model. These events are (i) the formation and transport of bubbles, and (ii) the drowned-wheel condition. These events affect the wheel characteristic and can not be predicted by the model. Therefore the agreement between the predicted and actual characteristic curves can not be expected to hold throughout the whole speed range. Since these events cause a reduction in wheel efficiency, it is undesirable to operate a wheel at the speed where these events occur. This is to say that the practical speed range will be from zero to a value just before these events occur. From experimental evidence of Section 4.1, it is usually the case that the bubble formation occurs well before the drowned-wheel condition. The incipient bubble formation therefore establishes the upper limit of the speed ranges where the analytical model can be applied.

For each experimental series, the analytical model is used to compute the wheel characteristic curves assuming a value of C_D. This procedure is repeated for various values of C_D. By trial and error, a value of C_D can be found such that the computed and experimentally obtained values of w and P_{in} for the value of h at the incipient bubble formation agree. This C_D is then assumed to be the representative value for the applicable range of the analytical model discussed in the previous paragraphs. In every experimental series calibrated, it is assumed that the leak coefficient C_L and the number m (Eq. 2.15) are 0.1 and 2, respectively.

In the calibration process, it was necessary to adjust the value of the coefficient of friction μ in order to obtain a curve of P_{in} versus w that agrees with the experimentally obtained curve. This is likely due

to the fact that friction loss occurs not only at the bearings but also at other possible contact surfaces along the wheel perimeter. Although effort was made to prevent such contact (see Section 3.1) by allowing some clearance between the wheel and its surroundings, it is impossible to guarantee that no contact occurs while the wheel is rotating since there are vibrations caused by the inevitable shaft misalignment and waves produced by the wheel.

b. Results

Drag coefficient

For each experimental series, the drag coefficient decreases as the wheel speed increases. This is probably due to the change in flow pattern around the paddles as the wheel speed increases. C_D also varies with the number of paddles N and the depth of submergence. This is evident when comparing the values of C_D obtained from different experimental series.

Selecting the value of C_D at the incipient bubble formation as the representative value of C_D for each series, the variation of C_D against N and $\frac{d}{R}$ is shown in Fig. 4.13. The ratio $\frac{d}{R}$ represents the normalized depth of submergence where $d = \bar{y}_o - S$ and $\bar{y}_o = \frac{1}{2}(y_{\bar{A}} + y_{\bar{B}})$. Calibration results that are used to construct Fig. 4.13 are shown in Table 4.3. It should be noted that due to the scale effect discussed in Section 2.3 e the values of C_D in Fig. 4.13 will be the upper estimate of the true value of the full size paddle wheels.

Mechanical friction loss

In order to estimate the mechanical friction loss occurring at the wheel bearings and elsewhere, the following reasoning is used. According to Eq. (2.30), the power loss due to friction is

Table 4.3 Calibration Results*

Series	d/R	N	C_L	μ	C_D
B1 N8 6.08	.374	8	.1	.66	15.35
B1 N16 6.08	.374	16	.1	.45	9.44
B1 N16 7.28	.492	16	.1	.35	9.66
B1 N16 4.78	.246	16	.1	.46	6.87
B1 N4 6.08	.374	4	.1	.81	8.5
B2 N8 6.08	.374	8	.1	.33	9.2
B2 N16 6.08	.374	16	.1	.32	6.36
B2 N4 6.08	.374	4	.1	.51	11.94
B2 N8 7.28	.492	8	.1	.34	15.6
B2 N8 4.78	.246	8	.1	.34	4.83
B2 N4 4.78	.246	4	.1	.92	4.55
B2 N4 7.28	.492	4	.1	.96	16.73
B2 N8 8.376	.6	8	.1	.88	17.37
B2 N16 7.28	.492	16	.1	.38	8.34
B2 N16 8.376	.6	16	.1	.35	8.4
B2 N8 6.344	.4	8	.1	.63	10.28

$\bar{\mu} = 0.543$

*See Appendix A for more details on wheel dimensions

$$d = \frac{1}{2}(y_{\bar{A}} + y_{\bar{B}}) - S$$

$$P_{FR} = C_{FR} U w \tag{2.30}$$

where $C_{FR} = \mu R_B$. In the experiment, the value of R_B can be measured. The value of μ for prediction purposes is taken to be $\bar{\mu}$ where $\bar{\mu}$ is the average value of μ obtained from the calibration (see Table 4.3). In the experimental set up, $R_B = 1.51$ cm, hence

$$P_{FR,watt} = 0.0082\ U_{Newton}\ w_{rad/sec} \tag{4.2}$$

Equation (4.2) is used to estimate the power loss by friction in the design of paddle wheels discussed in Chapter 5. In most cases, $U \cong W$ where W is the weight of the wheel.

In actual paddle wheel operation, power loss can occur due to floating debris that may prevent the wheel from rotating smoothly and from the contact between the wheel and the channel walls or the sill. Equation (4.2) may result in an underestimation of the power losses.

4.5 Verification

In this section, the analytical model of Chapter 2 and the value of C_D as a function of d/R and N obtained from the calibration (Fig. 4.13) is used to predict paddle wheel performance. The prediction is then compared to the experimental result. The experimental series used for this purpose are those which start with R in Table 3.1. They are R N8 4.78, R N8 7.28 and R N8 6.08.

The verification process consists of determining the values of d/R and N for each experimental series. From these, C_D can be found from Fig. 4.13. This value of C_D and Eq. (4.2) are then used in the model to

predict the wheel characteristic curves, i.e., the curves of h and P_{in} versus w. These curves are then compared with the experimentally obtained ones as shown in Fig. 4.14.

4.6 Discussion

The purpose of this section is to bring out the important points in this chapter, namely (a) the value of C_D determined in Section 4.4 and (b) the limitations on wheel size evident from experimental observation.

a. Scale effect

According to the discussion on the scale effect of Section 2.3e, the value of C_D shown in Fig. 4.13 will be too high when used in design of full size wheels.

Field data on performance of full size paddle wheels has to be collected to estimate the scale effect. In using the analytical model of the present study to design a full size paddle wheel, it should be understood that the actual C_D may be less than that indicated in Fig. 4.13.

In dealing with analytical design procedure, it is recommended in Chapter 5 that the range of values of the drag coefficient (0.7 C_D to C_D, where C_D is the value obtained from Fig. 4.13) should be used in the calculation to establish the ranges of speed, power input and efficiency. Field data are required to improve the values of C_D in Fig. 4.13 to enable them to be used for full size wheels.

b. Limitation of wheel size

From the results of Sections 4.1 and 4.2, it is evident that for a given pond with specified average velocity and depth, there is a limitation on how small a wheel can be. If a wheel is too small it will not be

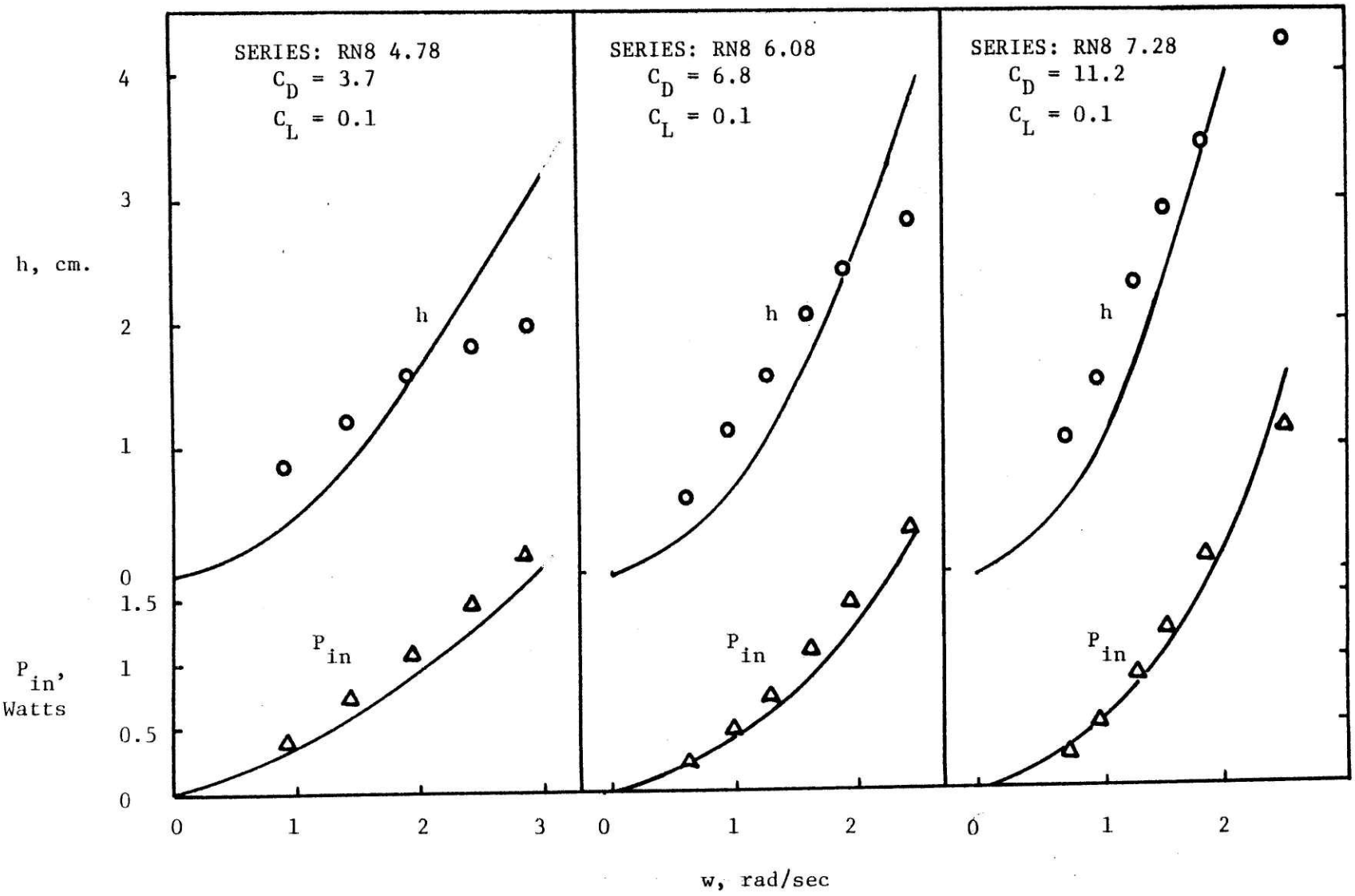

Fig. 4.14 Comparison of Predicted and Actual Characteristic Curves

able to create the flow with the required average velocity no matter how fast it rotates. This limitation on the minimum wheel size occurs due to two physical reasons:

(i) Choked flow condition that will occur if the wheel width (b) is too small or the sill height is too large. Analytical treatment of this is taken up in Section 2.2.

(ii) Drowned-wheel condition may occur at high wheel speed. The wheel cannot create the water level difference higher than the value just before the drowned-wheel condition sets in. Increasing either the wheel radius, the wheel width or the number of paddles will lower the wheel speed necessary to create the required water level difference. This in turn may put the wheel out of the drowned-wheel threshold. The drowned-wheel condition is discussed in Section 4.2 d.

It is important that these conditions be avoided to ensure satisfactory operation of paddle wheels. The knowledge can also be used to explain or improve the inadequate performance of existing wheels.

CHAPTER V: DESIGN OF AN ENERGY EFFICIENT HIGH-RATE ALGAE POND SYSTEM

5.1 Design Sequences

5.2 Step by Step Design Procedure

5.3 Example

- a. Design computation
- b. Sensitivity analysis

5.4 Practical Consideration

- a. Selection of the wheel radius
- b. Leakage underneath channel partitions
- c. Overall efficiency
- d. Notes on design

5.5 Accuracy of the Design Method of this Chapter

- a. Scale effect
- b. Inaccuracy due to measurement

CHAPTER V

DESIGN OF AN ENERGY EFFICIENT HIGH-RATE ALGAE POND SYSTEM

In designing a high-rate algae pond system - starting from the specified values of average velocity V_o, average depth y_o and the shape of the land available - the following sequences of questions arise:

(i) what is the appropriate layout or configuration of the pond, i.e., what is the appropriate channel width, length and the number of bends?

(ii) what are the appropriate wheel dimensions and operating conditions, i.e., what is the wheel radius, width, number of paddles, sill height, speed and power input?

Within the scope of this study, the word appropriate as used in the above two questions means the pond layout and the wheel dimensions that result in minimum power requirement. In an actual situation, the appropriate pond layout and wheel dimensions could mean a set up that will result in, for example, minimum construction costs, maximum utilization of local materials, etc.

The objective of this chapter is to answer the above two questions without emphasis on the underlying concepts but concentrating on the computation routine leading to a satisfactory design of the system. The underlying concept is discussed in Chapter 2.

This chapter concludes the results of this study from the application point of view. The results of the analytical study in Chapter 2 and of the experimental results of Chapter 4 are combined and presented in a flow-chart type procedure. A computer program was written for the

major part of this procedure. However, for those designers who have no access to a computer, section 5.2 of this chapter contains a step by step design procedure necessary to design an energy efficient high-rate pond system. An example to illustrate the procedure is discussed in Section 5.3.

Once the principal pond and wheel dimensions have been determined, the practical features have to be considered to ensure that the apparatus works satisfactorily. Some practical consideration is discussed in Section 5.4

Finally, the accuracy of the method presented in this chapter is discussed in Section 5.5.

5.1 Design Sequences

The problem of designing an energy efficient high-rate algae pond consists of the following four sequences:

(i) From specified values of average depth (y_o), average flow velocity (V_o), shape and size of the available land, determine the optimum pond layout.

(ii) Determine the water levels at the wheels and the horizontal force to be supplied by the rotating wheel.

(iii) For some assumed dimensions of the wheel, determine the required rotation speed, power and efficiency such that the conditions in (ii) are satisfied.

(iv) Repeat (iii) until optimum wheel dimensions are obtained, i.e., the one that yields maximum efficiency.

Sequence (i) corresponds to question (i) posed at the beginning of this chapter. Sequences (ii) to (iv) correspond to question (ii).

The method for sequence (i) is discussed in Section 2.6. The methods for sequences (ii) and (iii) are essentially those shown in Fig. 2.3 and Fig. 2.7. In this study, a computer program in FORTRAN IV is written for sequences (ii) and (iii). The program listing and description is shown in Appendix B. The program is written in CMS mode (i.e., conversational Monitor System) which means that the user and the computer interact by carrying on a dialogue from the user's terminal.

An example illustrating the computation involved in sequences (i) to (iii) is discussed in Section 5.3.

A guideline for specifying the values of y_o and v_o and the roughness coefficient (n) required in sequence (i) is presented in Section 1.5 e and f.

5.2 Step by Step Design Procedure

This section is intended for designers who can not use the computer program shown in Appendix B. It outlines the step by step computation required in the design sequences discussed in Section 5.1.

The step by step procedure for sequences (ii) and (iii) of Section 5.1 is shown in Fig. 5.1. The procedure for sequence (i) is relatively simple and is outlined in Section 2.6. The procedure shown in Fig. 5.1 can also be used to assess the efficiency of the existing paddle wheel.

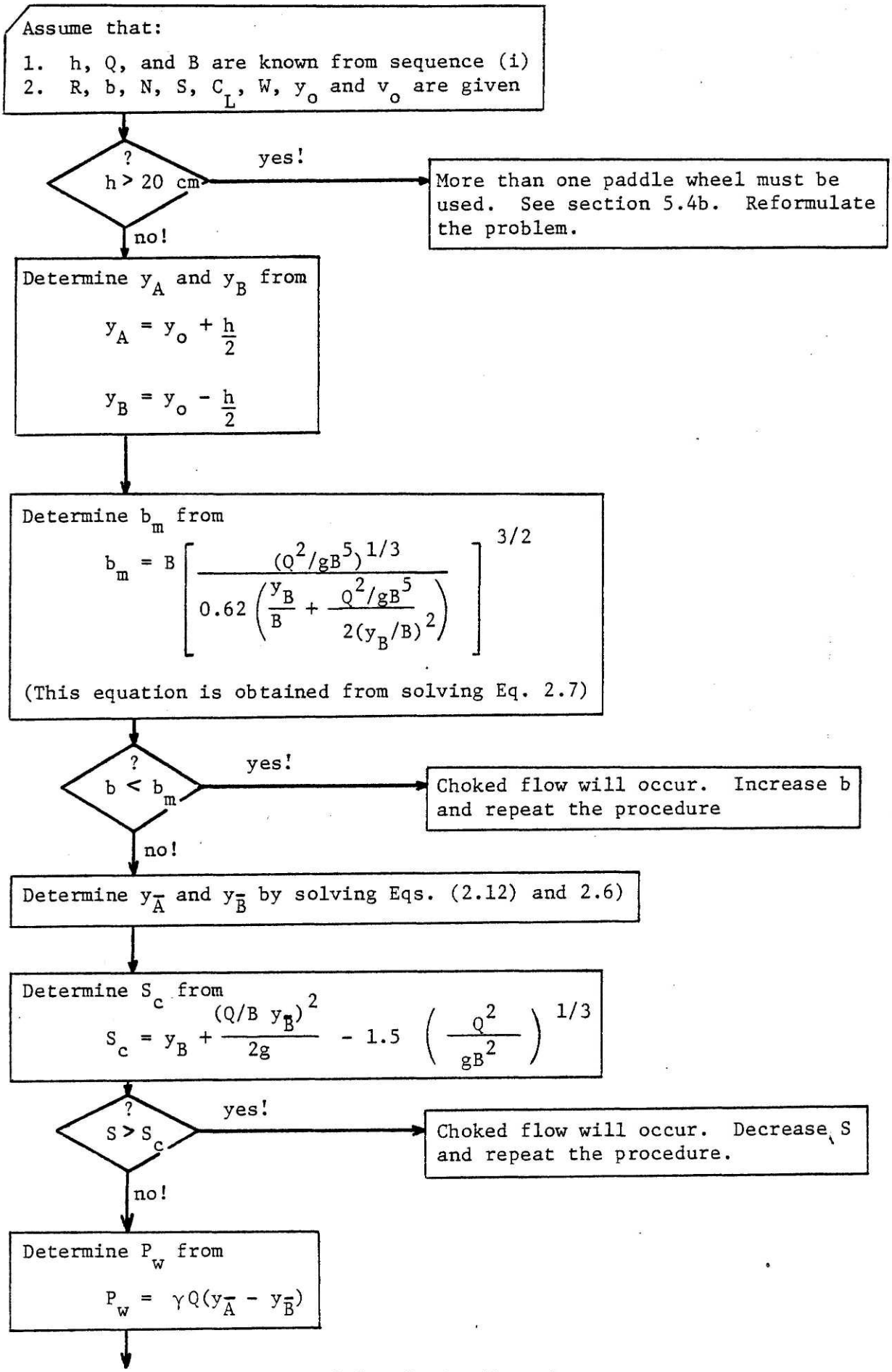

Fig. 5.1 - Design Procedure

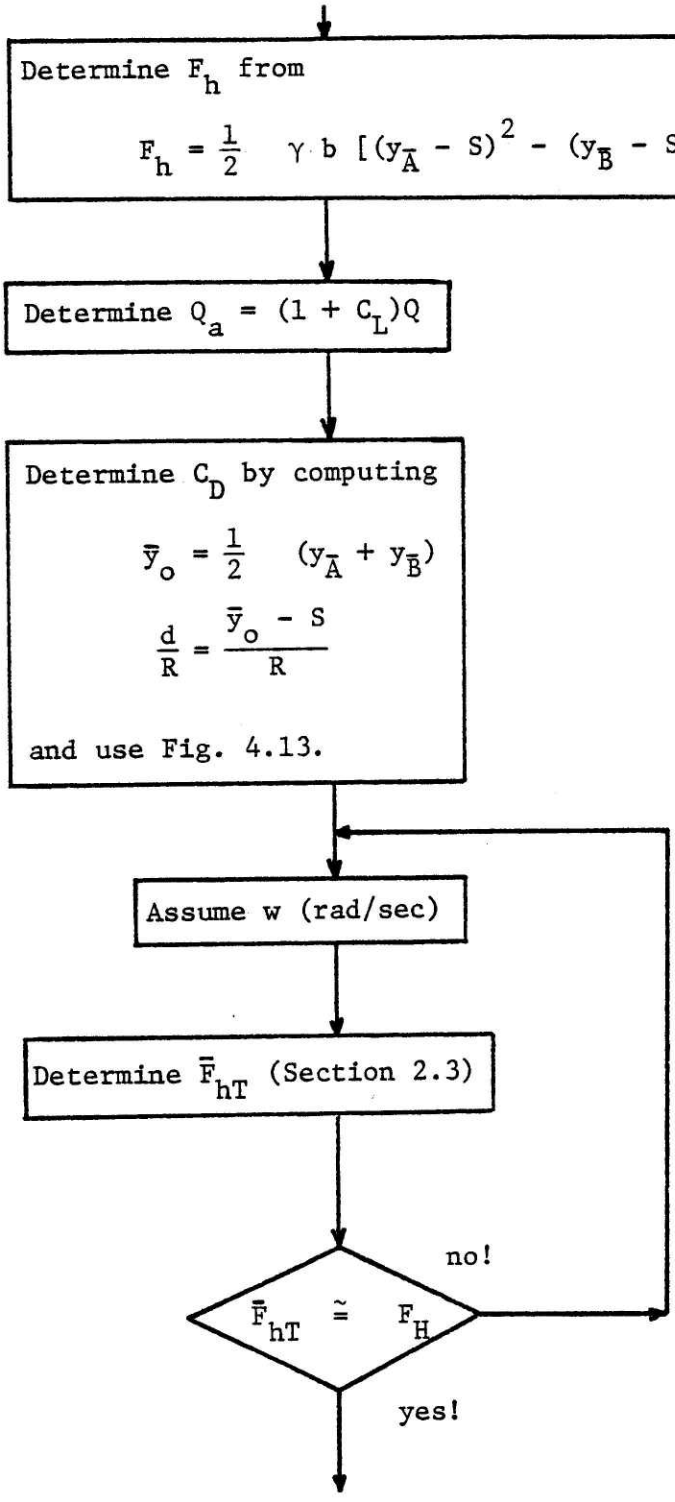

Fig. 5.1 - Design Procedure (contd.)

Check for bubble formation by computing V_{TW} from

$$V_{TW} = wR - \frac{Q}{by_{\bar{B}}} \cos\left(1 - \frac{y_{\bar{B}} - S}{R}\right)$$

If $V_{TW} < 0.15$ m/sec, no bubbles are produced

If $V_{TW} > 0.15$ m/sec, bubbles will be produced

To avoid $V_{TW} > 0.15$ increase b or decrease R and repeat the procedure.

Check for drowned-wheel condition by computing $\frac{w^2}{g}(y_{\bar{A}} - S)$ and $(y_{\bar{A}} - S)/R$ and use Fig. 4.3. If the point lies below the broken line in Fig. 4.3, the wheel will not operate under the drowned-wheel condition.

Determine $\bar{F}_{vT}$ and $\bar{T}_T$

Determine the power loss due to bearing friction by computing

$$U = [(\bar{F}_{hT})^2 + (W - \bar{F}_{vT})^2]^{1/2}$$

Then

$$P_{FR} = 0.0082\ U\ w$$

(watt) (Newton) (rad/sec)

Determine the power input and efficiency from

$$P_{in} \simeq \bar{T}_T\ w + P_{FR}$$

$$e = P_w/P_{in}$$

Note: $\gamma = 9.789$ kN/m^3

$g = 9.81$ m/sec^2

1 kg (force) = 9.81 N

Fig. 5.1 - Design Procedure (contd.)

5.3 Example

In this section, computation involved in sequence (i) to (iii) of Section 5.1 is illustrated by means of an example. Computation in sequence (i) follows that of Section 2.6. Computation in sequences (ii) and (iii) is essentially that of Fig. 5.1 or that of the computer program of Appendix B.

Let us assume that we are given a plot of rectangular land of 20 m x 50 m in which the pond is to be built. The required average velocity of flow V_o and the required average depth y_o are 10 cm/sec and 0.4 m, respectively (see Section 1.5e). The assumed wheel dimensions are: R = 0.5 m, b = 2m, N = 8 and S = 0.1 m. Our purpose is to find the required rotation speed w, power input P_{in} and efficiency e of this assumed wheel. In the computation it is assumed that C_L = 0.2 and the weight of the wheel is 50 kg (force).

a. Design computation

Following the procedure in Section 2.6 for sequence (i), the following table can be constructed assuming that the Manning roughness coefficient n = 0.02.

Layout No.	Number of partition walls	B (m)	L (m)	k_1	k_2	h (m)	Q (m^3/sec)	P'_w (Watts)
1	1	10	140	0	2	.0184	0.4	72.26
2	3	5	210	2	3	.0361	0.2	70.82
3	5	3.33	307	2	5	.0545	0.133	71.26
4	7	2.5	405	2	7	.0732	0.1	71.8

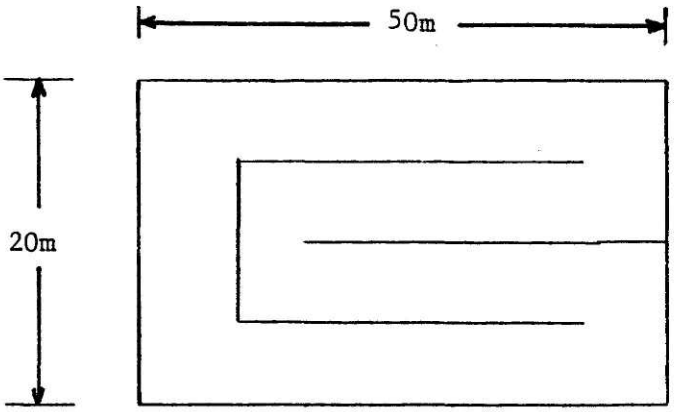

In this configuration, the number of partition walls is 3.

Since layout number 2 requires minimum power, it is selected. This completes sequence (i) of the design sequences.

The results of computation in sequences (ii) and (iii) following the procedure of Fig. 5.1 are:

$h = 0.0361$ m
$Q = 0.2$ m^3/sec
} from sequence (i)

$y_A = 0.4181$ m

$y_B = 0.3820$ m

$b_m = 0.554$ m

Since $b = 2m > b_m$, choked flow does not occur.

$S_c = 0.231$ m

Since $S = 0.1$ m $< S_c$, choked flow does not occur.

$y_{\bar{A}} = 0.4167$ m

$y_{\bar{B}} = 0.3782$ m

$P_w = 0.075$ kW

$F_H = 0.217$ kN

$Q_z = 0.24$ m^3/sec

$d = 0.2975$ m

$d/R = 0.595$

From Fig. 4.13, $C_D = 17.4$

By iteration process,

$$w = 1.025 \text{ rad/sec} \simeq 10 \text{ rpm.}$$

Check for bubble formation; $V_{TW} = 0.22$ m/sec and is more than 0.15 m/sec, hence bubbles may form.

Check for drowned-wheel condition; $\frac{w^2}{g}(y_{\bar{A}} - S) = 0.034$ and $(y_{\bar{A}} - S)/R = 0.633$.

From Fig. 4.4 the drowned-wheel condition does not occur.

$$\bar{F}_{vT} = -0.0354 \text{ kN}$$

$$\bar{T}_T = 0.1522 \text{ kN M}$$

$$U = 0.569 \text{ kN}$$

$$P_{FR} = 0.005 \text{ kW}$$

$$P_{in} = 0.161 \text{ kW}$$

$$e \simeq 47 \%$$

The same computation as performed by the computer program is shown in Appendix B.

In order to account for the uncertainties in the values of C_D and C_L arising from the scale effect (Section 5.5), value of $C_D = 0.7$ of the original value (17.4) and $C_L = 0.4$ (instead of 0.2) are tried. Using these new values of C_D and C_L the above calculation is repeated resulting in

$$w = 1.203 \text{ rad/sec}$$

$$P_{in} = 0.185 \text{ kW}$$

$$e = 41 \%$$

This establishes the ranges of expectable w, P_{in} and e. They are:

$$w : 1.025 \sim 1.203 \text{ rad/sec (or 10} \sim \text{12 rpm)}$$

$$P_{in} : 0.161 \sim 0.185 \text{ kW}$$

$$e : 41 \sim 47 \%$$

In the above calculation, we expect that bubble formation may occur. The formation of bubbles will further reduce the efficiency of the wheel or increase the power input required.

b. Sensitivity analysis

In connection to the previous example where we have determined the head (h), the wheel speed (w) and the power input (P_{in}) for the given pond and wheel, further question arises as to what will happen to these computed values if the Manning roughness coefficient (n), the drag coefficient (C_D) or the leak coefficient (C_L) deviates from the values previously used. The question arises from the fact that the values of n, C_D and C_L are empirically estimated values and subject to error depending on their determinations.

In order to answer the above question, the same problems as posed in the previous example are solved for the ranges of values of n, C_D and C_L of $0.01 < n < 0.03$, $8.7 < C_C < 26.1$ and $0.1 < C_L < 0.3$. The extreme values of these ranges correspond to ±50% error of the values of n, C_D and C_L used in the previous example.

The relationships among w, P_{in} and h are determined by the procedure described in section 5.2 for the extreme values of n, C_D and C_L previously discussed. The curves of P_{in} against w and h against w are plotted and shown in Fig. 5.2.

From Fig. 5.2 it can be concluded that, the computed values of h, P_{in} and w are not as sensitive to the variations of n and C_L as to the variation of C_D.

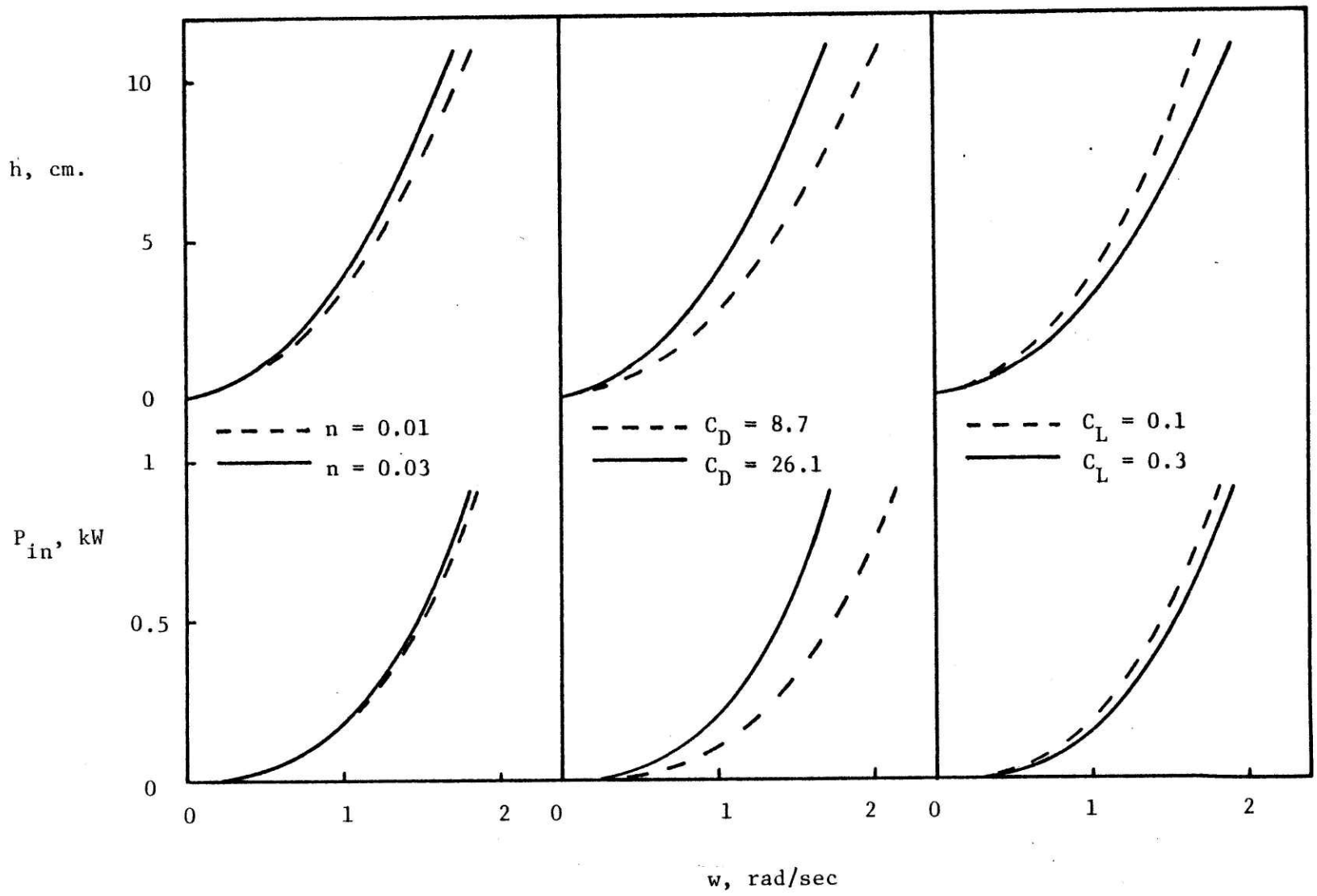

Fig. 5.2 Sensitivity Study

5.4 Practical Consideration

a. Selection of the wheel radius

In cases where the average depth y_o has to be varied for different seasons of the year (Section 1.5e), it is certain that a wheel designed to operate optimally at one y_o will not operate optimally for the other y_o. This is to say that one can not design a single wheel to operate optimally at various values of y_o.

It is also possible that a wheel designed to operate optimally at a particular y_o will not operate satisfactorily at the other y_o. For example, when a wheel is designed for operation at low y_o (e.g., summer operation) and has to be operated at high y_o (e.g., winter operation), the wheel may not be able to provide the required V_o during winter operation due to the drowned-wheel condition (Section 4.2d) no matter how fast it rotates. Limitation of wheel size is discussed in Section 4.6. In addition, if at the operating condition the wheel also produces bubbles, the power required will be substantially higher than that determined from the procedure of Fig. 5.1. Section 4.2b discussed the criterion for bubble formation.

With regard to the problem of selecting wheel dimensions for different y_o, two alternatives are available. The first alternative is to use a small wheel (cheaper to build) that can be raised or lowered to suit y_o. The second alternative is to use a wheel large enough to operate at both y_o without having to raise or lower the wheel. The designer has to decide for himself which alternative is suitable under his design constraints.

b. Leakage underneath channel partitions

Leakage underneath channel partitions can occur if the head

differences across the partitions are sufficiently high. It can deteriorate the foundation of the partitions. In order to prevent leakage, the foundation has to be made impervious or the head difference must be kept small.

The rate of leakage depends on the head difference and the permeability of the foundation. The maximum allowable head depends on the design and construction of the foundation. As a guideline, the head across the partition at any location along the flow direction should not exceed 20 cm.

In a high-rate algae pond, if it is believed that the head at some locations is too high to be safe from leakage, it is possible to reduce the head by increasing the number of paddle wheels. For example, if it is found that using only one paddle wheel will produce the maximum head exceeding the safe value, 2 or 3 evenly spaced paddle wheels can be considered as alternatives.

The head difference across channel partitions will also result in a net force acting on the partition. The partition and ists foundation must be designed to sustain this force.

c. Overall efficiency

Refer to Fig. 1.2, the overall efficiency is the efficiency including the loss in mechanical transmission devices, i.e., overall efficiency = P_w/P. This efficiency will be less than P_w/P_{in} obtainable from the procedure of Fig. 5.1. The overall efficiency can be determined if the efficiency of the mechanical transmission device (= P_{in}/P) is known. The efficiency of the transmission device is usually obtainable from its manufacturer.

d. Notes on design

This section discusses some practical design considerations that should be incorporated into the final design after the basic design parameters are determined.

The determination of the basic design parameters (e.g., the wheel radius, width and speed, etc.) are discussed in Sections 5.1 to 5.3. The objective of the following practical considerations is to improve the wheel iefficiency.

(i) Paddles should be oriented radially and the angles between two adjacent paddles should be the same. Radially oriented paddles are those shown in Fig. 3.5(a) when $\beta = 0$.

(ii) All paddles should extend as close as possible to the axis of rotation of the wheel. This is to prevent spillage (Section 4.2a), that could occur over the tops of paddles, which reduces the wheel efficiency. In addition, an air vent must be provided for every paddle chamber in order to allow air to escape when displaced by water.

(iii) Paddles should be rectangular in shape as shown in Fig. 3.4b (i).

(iv) A contoured sill as shown in the insert of Fig. 4.12 should be used. All sharp corners on the sill should be smoothed.

(v) The clearances between the sill and the wheel and between the walls and the wheel should be minimum yet allow the wheel to rotate freely.

(vi) When the wheel is operating, there will be a force of magnitude F_H (Section 5.2) pushing the wheel in the direction opposite to the flow. The wheel supports (e.g., bearings) should be made to stand this force and the weight of the wheel.

(vii) The wheel bearings should be protected from splashing water during operation.

(viii) In locations where wind is strong, a wheel cover should be used. Without the cover, the wheel efficiency will be substantially reduced if the wind direction is opposite to the motion of the top half of the wheel.

(ix) The contraction and expansion of channel width in the vicinity of the wheel should be made smooth (especially the expansion).

(x) All bends in the channel should be smooth. Guiding vanes (see the figure in Section 2.6) may be used.

(xi) If waves produced by the wheel during operation are excessive, floating baffles may be used to damp out the waves.

(xii) Vibration could occur to mechanical components connecting the wheel and the prime mover as a result of the periodic resisting torque. Avoid natural frequencies of components close to $N/2\pi$ and its harmonics.

5.5 Accuracy of the Design Method of this Chapter

Part of the method outlined in this chapter is based on an empirical approach, i.e., the determination of C_D, which relies on the experimental data obtained from a scaled down model.

The validity of the experimentally determined C_D is acceptable for the ranges of the variables encountered in the laboratory experiment. However, when the analytical model together with C_D detetmined as such

is extrapolated to assess the performance of a full size paddle wheel, the results are somewhat subject to argument concerning the value of C_D. The factors affecting C_D are as follows.

a. Scale effect

It is usually the case for a smaller hydraulic machine such as a paddle wheel to have a lower Reynolds number than the full size wheel due to its smaller size. Since the drag coefficient C_D increases as the Reynolds number decreases, it is likely that the values of C_D determined from the laboratory scaled down model will be too high when applied to the full size wheels. Therefore, the value of C_D determined as described in Section 4.4 and shown in Fig. 4.13 will likely be higher than that appropriate for the full size wheels.

b. Inaccuracy due to measurement

In addition to the scale effect discussed above, the determination of C_D depends on the error in measurement. It is believed that these errors tend to overestimate the value of C_D obtained from the laboratory apparatus as opposed to that of the field.

Considering both the scale effect and the inaccuracy due to measurement, it is believed that the value of C_D in Fig. 4.13 represents the upper limit. The actual value of the drag coefficient is believed to be somewhere between 70% and 100% of C_D determined from Fig. 4.13. Accordingly, it is suggested that in following the design procedure of Fig. 5.1 the lower and upper values of C_D suggested above should be used to establish the ranges of wheel speed, power input and the efficiency.

CHAPTER VI: CONCLUSIONS

6.1 Improvement of Efficiency Obtainable with the Proposed Design Method

CHAPTER VI

CONCLUSIONS

The following conclusions can be made in this study:

(i) Paddle wheel dimensions and geometry have effects on its efficiency in transferring mechanical energy into water flow energy. Given the flow characteristic of the high-rate pond and the wheel dimensions, the wheel efficiency can be estimated by the method outlined in Chapter 5 for simple wheel geometry.

(ii) In order to minimize the energy requirement in a high-rate pond operation, the pond should be designed such that it needs minimum amount of energy to circulate the water at the required average velocity and depth (Section 2.6). Once this is done, a suitable paddle wheel can be designed.

(iii) For a given high-rate pond with specified average velocity and depth, there is a limitation on how small a wheel can be. If a wheel is too small it will not be able to create the flow with the required average velocity no matter how fast it rotates (Section 4.6).

(iv) For a given high-rate algae pond with specified average velocity and depth, a suitable paddle wheel can be designed. The procedure for design is outlined in Chapter 5.

(v) The efficiency of a suitably designed paddle wheel can be improved up to threefold from that normally obtained using the simple rule of thumb in design (Section 1.5e). The following section illustrates the order of magnitude of wheel efficiencies that can be expected from suitably designed wheels.

6.1 Improvement of Efficiency Obtainable with the Proposed Design Method

Figure 6.1 gives some idea of the typical range of paddle wheel efficiencies that can be obtained if the paddle wheels are designed according to the procedure outlined in Chapter 5. In Fig. 6.1, the efficiencies are plotted against the ranges of the required average flow velocity V_o from 0 to 30 cm/sec which corresponds to the usual practical range required for various purposes (see Section 1.5e).

The lower band of curve represents approximately the range of efficiencies normally obtained if paddle wheels are designed by the existing rule of thumb discussed in Section 1.5e . Using the rule of thumb for design, the bubble formation and the drowned-wheel condition (Chapter 4) could occur thereby limiting the efficiency to approximately 25 to 30% or lower. The curve on the left hand side is the actual efficiency curve of one of the experiments conducted in this study (B2N16 7.28, see Table 3.1).

The upper band of curve represents approximately the range of efficiencies obtainable if a paddle wheel designed according to the procedure of Chapter 5 is used for each value of V_o. The band drops off at high value of V_o due to the unavoidable bubble formation and drowned-wheel condition, which are associated with high wheel speed required to deliver the desired V_o.

The top curve represents approximately the upper limits of efficiency assuming that ther is no leak, no bearing friction and that the bubble formation and the drowned-wheel condition can be completely prevented by some means. These ideal conditions can not be met in reality.

It should be noted that the efficiency discussed above does not include the energy loss in the mechanical transmission devices such as gear boxes or belts.

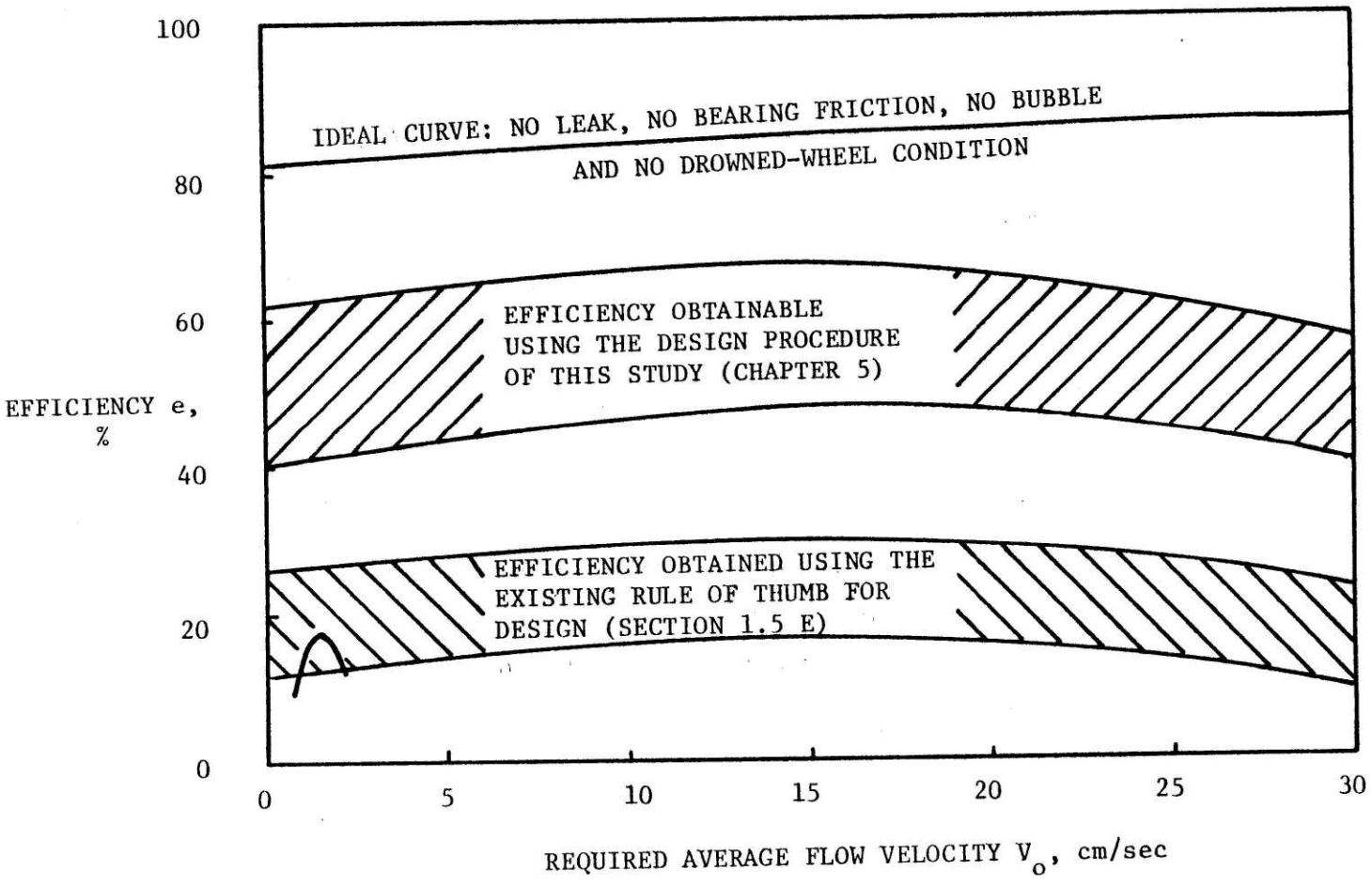

Fig. 6.1 Improvement of Paddle Wheel Efficiency

REFERENCES

1. SHELEF, G., "The Combination of Algal and Anaerobic Waste Treatment in a Bioregenerative Farm System," a paper presented at the United Nations University, Guatemala, November, 1978.

2. TIME-LIFE BOOKS, "The River Men," New York, 1980.

3. ELLIOTT, R.V., "Last of the Steamboats," Tidewater Publishers, Cambridge, Maryland, 1970.

4. HILL, R.N., "Sidewheeler Saga, A Chronicle of Steamboating," Rinehart Company, Inc., New York, 1952.

5. BODY, G., "British Paddle Steamers," David and Charles: Newton Abbot, 1971.

6. LASS, W.E., "A History of Steamboating on the Upper Missouri River," University of Nebraska Press: Lincoln, 1962.

7. ROSEBERRY, C.R., "Steamboats and Steamboat Men," G.P. Putnam & Sons, New York, 1966.

8. DONOVAN, F., "River Boats of America," Thomas Y. Crowell Company, New York, 1966.

9. LINGENFELTER, R.E., "Steamboats on the Colorado River, 1852-1916," The University of Arizona Press, Tucson, Arizona, 1978.

10. SAUNDERS, H.E., "Hydrodynamics in Ship Design," New York, Society of Naval Architects and Marine Engineers, 1957-1965.

11. SMITH, N., "The Origins of the Water Turbine," Scientific American, January 1980.

12. BACH, C., "Die Wasserräder," Stuttgart, Germany, 1886.

13. METCALF and EDDY, INC., "Wastewater Engineering," 2nd edition, McGraw-Hill, 1979.

14. FAIR, G.M., J.C. GEYER and D.A. OKUN, "Water and Wastewater Engineering," New York, Wiley, 1968.

15. BARRS, J.K. and J. MUSKAT, "Oxygenation of Water by Bladed Rotors," Report No. 28, Research Institute for Public Health Engineering, T.N.O., 1959, The Netherlands.

16. ARGAMAN, Y. and E. SPIVAK, "Engineering Aspects of Wastewater Treatment in Aerated Ring-Shaped Channels," Water Research, Vol. 8, 1974, Pergamon Press

17. BENEMANN, J.R., J.C. WEISSMAN, B.L. KOOPMAN and D.M. EISENBERG, "Large-Scale Freshwater Microalgal Biomass Production for Fuel and Fertilizer," Final Report for period October 1, 1977 - September 30, 1978, Sanitary Engineering Research Laboratory, University of California, Berkeley, December 1978.

18. OSWALD, W.J., "The High-Rate Pond in Waste Disposal," in Developments in Industrial Microbiology, Vol. 4, American Institute of Biological Sciences, Washington, D.C., 1963.

19. OSWALD, W.J. and H.B. GOTAAS, "Photosynthesis in Sewage Treatment, ASCE Transactions, Vol. 122, 1957, paper No. 2849.

20. OSWALD, W.J., "Complete Waste Treatment in Ponds," in Water Quality: Management and Pollution Control Problems, Vol. 3, Pergamon Press (1973), edited by S.H. JENKINS.

21. SHELEF, G., G. ORON and R. MORAINE, "Economic Aspects of Microalgae Production on Sewage, Arch. Hydrobiol. Beih. 11, 281-294, Stuttgart, December 1978.

22. McGARRY, M.G. and C. TONGKASAME, "Water Reclamation and Algae Harvesting," Water Pollution Control Federation Journal, Vol. 43, January-June, 1971.

23. BOGAN, R.H., O.E. ALBERTSON and J.C. PLUNTZE, "Use of Algae in Removing Phosphorus from Sewage, J. ASCE, SA 5, September 1960.

24. SHELEF, G., Y. AZOV, R. MORAINE, E. SANDBANK and G. ORON, "Waste Treatment and Nutrient Removal by High-Rate Algae Ponds," Paper presented at a workshop on high-rate algae ponds held in Singapore, February 27-29, 1980.

25. CHOW, V.T., "Open-Channel Hydraulics," McGraw-Hill, 1959.

26. HENDERSON, F.M., "Open Channel Flow," New York, MacMillan, 1966.

27. DAILY, J.W. and D.R.F. HARLEMAN, "Fluid Dynamics," Addison-Wesley, 1966.

28. DOEBELIN, E.O., "Measurement System: Application and Design," New York, McGraw-Hill, 1975.

29. Operating and Service Manual, 350-1100 C Carrier Preamplifier, Hewlett Packard, Sandborn Division, September 1965.

30. Current Flow Meter, Technical Description, Delft Hydraulics Laboratory, Delft, Holland, May 1969.

31. Wastewater Treatment and Resource Recovery - Report of a Workshop on High-Rate Algae Ponds, Singapore, February 27-29, 1980.

32. GOLUEKE, C.G., "Biological Reclamation of Solid Wastes," Rodale Press, Emmanus, PA, 1977.

33. BENEMANN, J.R., J.C. WEISSMAN, B.L. KOOPMAN and W.J. OSWALD, "Energy Production by Microbial Photosynthesis, Review Article, Nature, Vol. 268, July 7, 1977.

34. GOLUEKE, C.G. and W.J. OSWALD, "Harvesting and Processing Sewage-Grown Planktonic Algae," Water Pollution Control Federation Journal, 37, January-July 1965.

APPENDICES

A. Experimental Data

B. Computer Program

B.1 Program Listings

B.2 Library Program Requirement

B.3 Example

APPENDIX A

EXPERIMENTAL DATA

Procedure for conducting experiment leading to the data presented here is described in Chapter 3. The weights of the wheels for the following experimental series are in Table 3.1

EXPERIMENT

SERIES AND DATES: B1N8 6.08 June 28

WHEEL DIMENSIONS:

$R = 10.16$ cm; $b = 48.1$ cm.
$N = 8$; $y_o = 6.08$ cm.
$S = 2.28$ cm.

DATA:

	RUN										
	1	2	3	4	5	6	7	8	9	10	11
h	.875	1.5	2.0	2.4	2.82	3.27	3.65	3.85	3.91	3.92	3.84
Q	.367	.455	.51	.548	.584	.62	.647	.661	.665	.666	.661
w	.904	1.177	1.423	1.678	1.993	2.577	3.108	3.707	4.277	4.921	5.672
T	.545	.638	.735	.82	.92	.97	1.115	1.25	1.35	1.5	1.57
P_w	.031	.067	.1	.129	.161	.198	.231	.249	.255	.256	.248
P_{in}	.493	.751	1.046	1.376	1.834	2.5	3.465	4.634	5.774	7.382	8.905
e	6.38	8.89	9.54	9.36	8.8	7.94	6.68	5.38	4.41	3.46	2.79
1*				x	x	x	x	x	x		
2				x	x	x	x	x	x		
3	x	x	x							x	x
4				x	x	x	x	x	x	x	x
5					x	x	x	x	x	x	x
6								x	x	x	x

NOTES: (i) Units: h, cm; Q, lit/sec; w, rad/sec; T, Newton.m; P_w, Watts; P_{in}, Watts; e, %.

(ii) * 1 = wave downstream
2 = wave upstream
3 = smooth water surface downstream and upstream
4 = bubbles
5 = noise
6 = drowned-wheel condition

EXPERIMENT

SERIES AND DATES: B1N16 6.08 June 28

WHEEL DIMENSIONS:

R = 10.16 cm; b = 48.1 cm.
N = 16 ; y_o = 6.08 cm.
S = 2.28 cm.

DATA:

	RUN										
	1	2	3	4	5	6	7	8	9	10	11
h	1.535	2.18	2.7	3.23	3.5	3.855	4.305	4.35	4.41	4.43	
Q	.459	.527	.574	.617	.637	.662	.691	.694	.698	.699	
w	.849	1.102	1.428	1.855	1.926	2.285	2.878	3.506	4.154	4.62	
T	.91	.99	.92	.945	1.1	1.207	1.3	1.34	1.49	1.67	
P_w	.069	.113	.152	.195	.218	.25	.291	.296	.301	.303	
P_{in}	.773	1.091	1.314	1.753	2.138	2.758	3.741	4.698	6.189	7.715	
e	8.923	10.32	11.55	11.12	10.2	9.05	7.79	6.29	4.87	3.93	
1*				x	x	x	x	x	x	x	
2				x	x	x	x	x	x	x	
3	x	x	x								
4				x	x	x	x	x	x	x	
5				x	x	x	x	x	x	x	
6									x	x	

NOTES: (i) Units: h, cm; Q, lit/sec; w, rad/sec; T, Newton.m; P_w, Watts; P_{in}, Watts; e, %.

(ii) * 1 = wave downstream
2 = wave upstream
3 = smooth water surface downstream and upstream
4 = bubbles
5 = noise
6 = drowned-wheel condition

EXPERIMENT

SERIES AND DATES: B1N16 7.28 June 29

WHEEL DIMENSIONS:

R = 10.16 cm; b = 48.1 cm.
N = 16 ; y_o = 7.28 cm.
S = 2.28 cm.

DATA:

	RUN										
	1	2	3	4	5	6	7	8	9	10	11
h	1.1	1.66	2.09	2.89	3.35	4.02	4.38	4.73	5.08	5.11	5.06
Q	.421	.516	.577	.677	.727	.796	.83	.862	.892	.892	.864
w	.555	.731	.896	1.153	1.45	2.045	2.501	3.004	3.557		
T	.61	.73	.8	.935	1.065	1.34	1.525	1.7	1.82		
P_w	.045	.084	.118	.191	.239	.313	.356	.399	.444		
P_{in}	.339	.534	.717	1.078	1.544	2.74	3.814	5.107	6.474		
e	13.4	15.7	16.47	17.76	15.45	11.42	9.33	7.81	6.85		
1*		x	x	x	x	x	x				
2		x	x	x	x	x	x				
3	x							x	x	x	x
4						x	x	x	x	x	x
5					x	x	x	x	x	x	x
6									x	x	x

NOTES: (i) Units: h, cm; Q, lit/sec; w, rad/sec; T, Newton.m; P_w, Watts; P_{in}, Watts; e, %.

(ii) * 1 = wave downstream
2 = wave upstream
3 = smooth water surface downstream and upstream
4 = bubbles
5 = noise
6 = drowned-wheel condition

EXPERIMENT

SERIES AND DATES: B1N16 4.78 June 29

WHEEL DIMENSIONS:

R = 10.16 cm; b = 48.1 cm.
N = 16 ; y_o = 4.78 cm.
S = 2.28 cm.

DATA:

	RUN										
	1	2	3	4	5	6	7	8	9	10	11
h	1.2	1.68	2.31	2.62	2.88	3.03	3.13	3.1	3.1	2.9	
Q	.199	.246	.3	.324	.344	.355	.362	.36			
w	.818	1.128	1.662	2.31	2.909	3.603	4.234	4.265			
T	.64	.68	.75	.82	.97	1.02	1.03	1.07			
P_w	.023	.04	.068	.083	.097	.105	.111	.109			
P_{in}	.524	.767	1.247	1.894	2.822	3.675	4.361	4.564			
e	4.47	5.27	5.44	4.39	3.43	2.86	2.54	2.39			
1*	x	x	x	x	x	x					
2	x	x	x	x	x	x					
3							x	x	x	x	
4			x	x	x	x	x	x	x	x	
5			x	x	x	x	x	x	x	x	
6								x	x	x	

NOTES: (i) Units: h, cm; Q, lit/sec; w, rad/sec; T, Newton.m; P_w, Watts; P_{in}, Watts; e, %.

(ii) * 1 = wave downstream
2 = wave upstream
3 = smooth water surface downstream and upstream
4 = bubbles
5 = noise
6 = drowned-wheel condition

EXPERIMENT

SERIES AND DATES: B1N4 6.08 July 1

WHEEL DIMENSIONS:

$R = 10.16$ cm; $b = 24.05$ cm.
$N = 4$; $y_o = 6.08$ cm.
$S = 2.28$ cm.

DATA:

	RUN										
	1	2	3	4	5	6	7	8	9	10	11
h	1.005	1.065	1.61	2.07	2.54	2.74	3.08				
Q	.388	.397	.468	.517	.561	.578	.605				
w	1.327	1.848	2.285	2.793	3.462	4.093	4.852				
T	.575	.605	.708	.813	.94	1.015	1.135				
P_w	.038	.041	.074	.105	.139	.155	.182				
P_{in}	.763	1.118	1.618	2.271	3.254	4.154	5.507				
e	5.0	3.7	4.56	4.61	4.28	3.73	3.31				
1*	x	x	x	x							
2	x	x	x	x							
3					x	x	x				
4				x	x	x	x				
5					x	x	x				
6						x	x				

NOTES: (i) Units: h, cm; Q, lit/sec; w, rad/sec; T, Newton. m; P_w, Watts; P_{in}, Watts; e, %.

(ii) * 1 = wave downstream
2 = wave upstream
3 = smooth water surface downstream and upstream
4 = bubbles
5 = noise
6 = drowned-wheel condition

EXPERIMENT

SERIES AND DATES: B2N8 6.08 July 3

WHEEL DIMENSIONS:

R = 10.16 cm; b = 24.05 cm.
N = 8 ; y_o = 6.08 cm.
S = 2.28 cm.

DATA:

	RUN										
	1	2	3	4	5	6	7	8	9	10	11
h	.785	1.25	1.75	2.2	2.46	2.89	3.41	3.61	3.67		
Q	.351	.423	.483	.529	.553	.59	.63	.645	.649		
w	1.013	1.424	1.729	2.112	2.394	2.85	3.565	4.161	5.158		
T	.173	.24	.292	.347	.41	.44	.545	.615	.759		
P_w	.027	.052	.083	.114	.133	.167	.21	.228	.233		
P_{in}	.175	.342	.505	.733	.982	1.254	1.943	2.559	3.915		
e	15.41	15.14	16.4	15.56	13.58	13.31	10.83	8.9	5.96		
1*	x	x	x	x	x	x	x				
2	x	x	x	x	x	x	x				
3								x	x		
4					x	x	x	x	x		
5						x	x	x	x		
6								x	x		

NOTES: (i) Units: h, cm; Q, lit/sec; w, rad/sec; T, Newton.m; P_w, Watts; P_{in}, Watts; e, %.

(ii) * 1 = wave downstream
2 = wave upstream
3 = smooth water surface downstream and upstream
4 = bubbles
5 = noise
6 = drowned-wheel condition

EXPERIMENT

SERIES AND DATES: B2N16 6.08 July 3

WHEEL DIMENSIONS:

$R = 10.16$ cm; $b = 24.05$ cm.
$N = 16$; $y_o = 6.08$ cm.
$S = 2.28$ cm.

DATA:

	RUN										
	1	2	3	4	5	6	7	8	9	10	11
h	1.37	1.75	2.18	3.1	3.63	4.11	4.31				
Q	.439	.483	.527	.607	.646	.679	.692				
w	1.176	1.466	1.818	2.384	2.805	3.367	4.436				
T	.253	.341	.39	.466	.547	.638	.77				
P_w	.059	.083	.113	.184	.23	.273	.292				
P_{in}	.298	.5	.709	1.111	1.534	2.148	3.416				
e	19.76	16.56	15.88	16.57	14.96	12.71	8.54				
1*	x	x	x								
2	x	x	x								
3				x	x	x	x				
4				x	x	x	x				
5			x	x	x	x	x				
6							x				

NOTES: (i) Units: h, cm; Q, lit/sec; w, rad/sec; T, Newton.m; P_w, Watts; P_{in}, Watts; e, %.

(ii) * 1 = wave downstream
2 = wave upstream
3 = smooth water surface downstream and upstream
4 = bubbles
5 = noise
6 = drowned-wheel condition

EXPERIMENT

SERIES AND DATES: B2N4 6.08 July 3

WHEEL DIMENSIONS:

R = 10.16 cm; b = 24.05 cm.
N = 4 ; y_o = 6.08 cm.
S = 2.28 cm.

DATA:

	RUN										
	1	2	3	4	5	6	7	8	9	10	11
h	.4	.63	.7	1.29	1.57	1.8	2.49	2.72	2.96		
Q	.269	.322	.336	.428	.463	.489	.556	.576	.596		
w	.931	1.526	1.551	2.03	2.273	2.982	3.865	4.562	5.957		
T	.21	.229	.24	.284	.323	.37	.45	.51	.632		
P_w	.011	.02	.023	.054	.071	.086	.136	.153	.173		
P_{in}	.196	.349	.372	.577	.734	1.103	1.739	2.327	3.765		
e	5.38	5.68	6.18	9.38	9.69	7.81	7.79	6.59	4.58		
1*		x	x	x	x	x	x	x	x		
2		x	x	x	x	x	x	x			
3	x										
4					x	x	x	x	x		
5						x	x	x	x		
6								x	x		

NOTES: (i) Units: h, cm; Q, lit/sec; w, rad/sec; T, Newton.m; P_w, Watts; P_{in}, Watts; e, %.

(ii) * 1 = wave downstream
2 = wave upstream
3 = smooth water surface downstream and upstream
4 = bubbles
5 = noise
6 = drowned-wheel condition

EXPERIMENT

SERIES AND DATES: B2N8 7.28 July 3

WHEEL DIMENSIONS:

R = 10.16 cm; b = 24.05 cm.
N = 8 ; y_o = 7.28 cm.
S = 2.28 cm.

DATA:

	RUN										
	1	2	3	4	5	6	7	8	9	10	11
h	.78	1.51	1.91	2.47	2.99	3.71	4.17	4.51			
Q	.356	.492	.552	.626	.688	.765	.81	.842			
w	.926	1.214	1.482	1.818	2.166	2.808	3.36	4.059			
T	.27	.322	.376	.443	.533	.665	.783	.921			
P_w	.027	.073	.103	.151	.201	.278	.331	.372			
P_{in}	.25	.391	.557	.805	1.154	1.867	2.631	3.738			
e	10.87	18.61	18.53	18.81	17.44	14.87	12.57	9.94			
1*				x	x	x	x				
2				x	x	x					
3	x	x	x					x			
4					x	x	x	x			
5					x	x	x	x			
6							x	x			

NOTES: (i) Units: h, cm; Q, lit/sec; w, rad/sec; T, Newton.m; P_w, Watts; P_{in}, Watts; e, %.

(ii) * 1 = wave downstream
2 = wave upstream
3 = smooth water surface downstream and upstream
4 = bubbles
5 = noise
6 = drowned-wheel condition

EXPERIMENT

SERIES AND DATES: B2N8 4.78 July 3

WHEEL DIMENSIONS:

R = 10.16 cm; b = 24.05 cm.
N = 8 ; y_o = 4.78 cm.
S = 2.28 cm.

DATA:

	RUN										
	1	2	3	4	5	6	7	8	9	10	11
h	.52	.89	1.18	1.51	1.87	2.07	2.24	2.4	2.46		
Q	.119	.166	.197	.23	.263	.28	.294	.307	.312		
w	.839	1.172	1.54	1.927	2.556	3.276	4.037	4.937	6.418		
T	.121	.175	.23	.243	.275	.296	.276	.32	.423		
P_w	.006	.014	.023	.034	.048	.057	.064	.072	.075		
P_{in}	.102	.205	.354	.468	.703	.97	1.114	1.58	2.715		
e	5.94	7.03	6.43	7.26	6.84	5.85	5.78	4.56	2.76		
1*	x	x	x	x	x	x					
2		x	x	x	x						
3							x	x	x		
4					x	x	x	x	x		
5						x	x	x	x		
6								x	x		

NOTES: (i) Units: h, cm; Q, lit/sec; w, rad/sec; T, Newton.m; P_w, Watts; P_{in}, Watts; e, %.

(ii) * 1 = wave downstream
2 = wave upstream
3 = smooth water surface downstream and upstream
4 = bubbles
5 = noise
6 = drowned-wheel condition

EXPERIMENT

SERIES AND DATES: RN8 4.78 July 10

WHEEL DIMENSIONS:

R = 13.97 cm; b = 24.05 cm.
N = 8 ; y_o = 4.78 cm.
S = 2.28 cm.

DATA:

	RUN										
	1	2	3	4	5	6	7	8	9	10	11
h	.86	1.23	1.59	1.83	2.0	2.29	2.49	2.54			
Q	.162	.202	.238	.259	.274	.298	.314	.318			
w	.912	1.43	1.927	2.431	2.889	3.935	5.161	6.879			
T	.445	.523	.516	.604	.64	.71	.841	.837			
P_w	.014	.024	.037	.046	.054	.067	.077	.079			
P_{in}	.406	.748	.994	1.468	1.849	2.794	4.34	5.758			
e	3.36	3.26	3.72	3.16	2.9	2.39	1.76	1.37			
1*	x	x	x	x	x	x					
2	x	x	x	x	x						
3							x	x			
4											
5						x	x	x			
6							x	x			

NOTES: (i) Units: h, cm; Q, lit/sec; w, rad/sec; T, Newton.m; P_w, Watts; P_{in}, Watts; e, %.

(ii) * 1 = wave downstream
2 = wave upstream
3 = smooth water surface downstream and upstream
4 = bubbles
5 = noise
6 = drowned-wheel condition

EXPERIMENT

SERIES AND DATES: RN8 7.28 July 10

WHEEL DIMENSIONS:

R = 13.97 cm; b = 24.05 cm.
N = 8 ; y_o = 7.28 cm.
S = 2.28 cm.

DATA:

	RUN										
	1	2	3	4	5	6	7	8	9	10	11
h	1.1	1.54	2.35	2.93	3.46	4.27	4.91	5.05			
Q	.421	.497	.611	.681	.739	.819	.878	.89			
w	.748	.99	1.288	1.52	1.863	2.502	3.244	4.278			
T	.39	.502	.68	.808	.96	1.13	1.323	1.65			
P_w	.045	.075	.141	.195	.25	.343	.422	.44			
P_{in}	.292	.497	.876	1.228	1.788	2.827	4.292	7.059			
e											
1*			x	x	x	x					
2											
3	x	x					x	x			
4					x	x	x	x			
5						x	x	x			
6							x	x			

NOTES: (i) Units: h, cm; Q, lit/sec; w, rad/sec; T, Newton. m; P_w, Watts; P_{in}, Watts; e, %.

(ii) * 1 = wave downstream
2 = wave upstream
3 = smooth water surface downstream and upstream
4 = bubbles
5 = noise
6 = drowned-wheel condition

EXPERIMENT

SERIES AND DATES: RN8 6.08 July 10

WHEEL DIMENSIONS:

$R = 13.97$ cm; $b = 24.05$ cm.
$N = 8$; $y_o = 6.08$ cm.
$S = 2.28$ cm.

DATA:

	RUN										
	1	2	3	4	5	6	7	8	9	10	11
h	.61	1.14	1.58	2.08	2.45	2.85	3.25	3.62	3.82	3.82	
Q	.318	.408	.464	.518	.553	.587	.618	.645	.659	.659	
w	.618	.973	1.268	1.59	1.921	2.426	2.856	3.436	4.24	5.062	
T	.372	.493	.579	.68	.76	.84	.9	.998	1.1	1.216	
P_w	.019	.045	.072	.105	.133	.164	.197	.229	.247	.247	
P_{in}	.23	.48	.734	1.081	1.46	2.038	2.57	3.429	4.664	6.155	
e	8.26	9.48	9.78	9.75	9.08	8.03	7.65	6.67	5.29	4.0	
1*		x	x	x	x	x	x				
2			x	x	x						
3	x							x	x	x	
4					x	x	x	x	x	x	
5						x	x	x	x	x	
6									x	x	

NOTES: (i) Units: h, cm; Q, lit/sec; w, rad/sec; T, Newton.m; P_w, Watts; P_{in}, Watts; e, %.

(ii) * 1 = wave downstream
2 = wave upstream
3 = smooth water surface downstream and upstream
4 = bubbles
5 = noise
6 = drowned-wheel condition

EXPERIMENT

SERIES AND DATES: B2N4 4.78 July 21

WHEEL DIMENSIONS:

$R = 10.16$ cm; $b = 24.05$ cm.
$N = 4$; $y_o = 4.78$ cm.
$S = 2.28$ cm.

DATA:

	RUN										
	1	2	3	4	5	6	7	8	9	10	11
h	.37	.67	.93	1.0	1.25	1.56	1.8				
Q	.096	.139	.17	.178	.205	.235	.257				
w	.876	1.937	2.423	3.05	3.835	4.76	6.379				
T	.398	.415	.425	.437	.458	.5	.58				
P_w	.003	.009	.015	.017	.025	.036	.045				
P_{in}	.349	.804	1.03	1.333	1.756	2.38	3.7				
e	1.0	1.13	1.5	1.31	1.42	1.51	1.22				
1*		x	x	x	x	x	x				
2		x	x	x							
3	x										
4			x	x	x	x	x				
5						x	x				
6						x	x				

NOTES: (i) Units: h, cm; Q, lit/sec; w, rad/sec; T, Newton.m; P_w, Watts; P_{in}, Watts; e, %.

(ii) * 1 = wave downstream
2 = wave upstream
3 = smooth water surface downstream and upstream
4 = bubbles
5 = noise
6 = drowned-wheel condition

EXPERIMENT

SERIES AND DATES: B2 N4 7.28 July 21

WHEEL DIMENSIONS:

R = 10.16 cm; b = 24.05 cm.
N = 4 ; y_o = 7.28 cm.
S = 2.28 cm.

DATA:

	RUN										
	1	2	3	4	5	6	7	8	9	10	11
h	.53	.53	1.0	2.24	2.59	3.42	3.8				
Q	.294	.294	.402	.597	.641	.735	.774				
w	.893	1.3	1.854	2.4	2.865	3.791	5.723				
T	.453	.453	.525	.67	.735	.87	1.05				
P_w	.015	.015	.039	.131	.163	.246	.288				
P_{in}	.405	.589	.973	1.608	2.106	3.298	6.009				
e	3.78	2.59	4.04	8.14	7.72	7.46	4.79				
1*		x	x	x	x	x	x				
2		x	x	x	x	x	x				
3	x										
4				x	x	x	x				
5					x	x	x				
6						x	x				

NOTES: (i) Units: h, cm; Q, lit/sec; w, rad/sec; T, Newton.m; P_w, Watts; P_{in}, Watts; e, %.

(ii) * 1 = wave downstream
2 = wave upstream
3 = smooth water surface downstream and upstream
4 = bubbles
5 = noise
6 = drowned-wheel condition

EXPERIMENT

SERIES AND DATES: B2 N8 8.376 July 21

WHEEL DIMENSIONS:

$R = 10.16$ cm; $b = 24.05$ cm.
$N = 8$; $y_o = 8.376$ cm.
$S = 2.28$ cm.

DATA:

	RUN										
	1	2	3	4	5	6	7	8	9	10	11
h	.7	1.09	1.85	2.15	2.64	3.15	3.78				
Q	.404	.491	.62	.663	.726	.785	.85				
w	.709	.977	1.309	1.602	1.782	2.195	2.743				
T	.593	.635	.73	.775	.82	.948	1.042				
P_w	.028	.052	.112	.14	.188	.242	.315				
P_{in}	.42	.62	.956	1.242	1.461	2.081	2.858				
e	6.59	8.45	11.76	11.24	12.83	11.63	11.01				
1*			x	x							
2			x								
3	x	x			x	x	x				
4						x	x				
5				x	x	x	x				
6							x				

NOTES: (i) Units: h, cm; Q, lit/sec; w, rad/sec; T, Newton.m; P_w, Watts; P_{in}, Watts; e, %.

(ii) * 1 = wave downstream
2 = wave upstream
3 = smooth water surface downstream and upstream
4 = bubbles
5 = noise
6 = drowned-wheel condition

EXPERIMENT

SERIES AND DATES: B2 N16 7.28 July 28

WHEEL DIMENSIONS:

R = 10.16 cm; b = 24.05 cm.
N = 16 ; y_o = 7.28 cm.
S = 2.28 cm.

DATA:

	RUN										
	1	2	3	4	5	6	7	8	9	10	11
h	.62	1.05	1.25	1.61	1.89	2.19	2.51	3.09	3.93		
Q	.318	.412	.449	.508	.549	.591	.631	.699	.787		
w	.653	.919	1.007	1.237	1.423	1.663	1.929	2.406	3.108		
T	.318	.337	.318	.375	.425	.488	.573	.644	.769		
P_w	.019	.042	.055	.08	.102	.127	.155	.211	.303		
P_{in}	.203	.31	.32	.464	.605	.812	1.105	1.549	2.39		
e	9.29	13.67	17.14	17.25	16.81	15.60	14.04	13.65	12.66		
1*		x	x	x	x	x					
2				x	x						
3	x						x	x	x		
4							x	x	x		
5							x	x	x		
6									x		

NOTES: (i) Units: h, cm; Q, lit/sec; w, rad/sec; T, Newton.m; P_w, Watts; P_{in}, Watts; e, %.

(ii) * 1 = wave downstream
2 = wave upstream
3 = smooth water surface downstream and upstream
4 = bubbles
5 = noise
6 = drowned-wheel condition

EXPERIMENT

SERIES AND DATES: B2 N16 8.376 July 28

WHEEL DIMENSIONS:

$R = 10.16$ cm; $b = 24.05$ cm.
$N = 16$; $y_o = 8.376$ cm.
$S = 2.28$ cm.

DATA:

	RUN										
	1	2	3	4	5	6	7	8	9	10	11
h	1.08	1.54	2.11	2.3	2.55	2.7	2.98	3.43	3.81		
Q	.489	.572	.657	.683	.715	.733	.766	.815	.853		
w	.822	1.068	1.308	1.417	1.571	1.7	1.925	2.307	2.825		
T	.237	.318	.441	.477	.552	.6	.65	.752	.887		
P_w	.052	.086	.136	.154	.178	.194	.223	.274	.318		
P_{in}	.195	.34	.577	.676	.867	1.02	1.251	1.735	2.506		
e	26.55	25.4	23.54	22.75	20.57	18.99	17.85	15.76	12.7		
1*			x	x	x	x					
2			x	x	x	x					
3	x	x					x	x	x		
4								x	x		
5			x	x	x	x	x	x	x		
6									x		

NOTES: (i) Units: h, cm; Q, lit/sec; w, rad/sec; T, Newton.m; P_w, Watts; P_{in}, Watts; e, %.

(ii) * 1 = wave downstream
2 = wave upstream
3 = smooth water surface downstream and upstream
4 = bubbles
5 = noise
6 = drowned-wheel condition

EXPERIMENT

SERIES AND DATES: B2 N8 6.344 July 21

WHEEL DIMENSIONS:

$R = 10.16$ cm; $b = 24.05$ cm.

$N = 8$; $y_o = 6.344$ cm.

$S = 2.28$ cm.

DATA:

	RUN										
	1	2	3	4	5	6	7	8	9	10	11
h	.53	1.01	1.2	1.75	2.17	2.54	3.04	3.64	3.78		
Q	.299	.394	.424	.498	.545	.583	.629	.68	.691		
w	.795	1.09	1.291	1.63	2.001	2.327	2.813	3.754	4.912		
T	.325	.35	.398	.454	.51	.57	.613	.75	.887		
P_w	.016	.039	.05	.085	.116	.145	.187	.242	.256		
P_{in}	.258	.382	.514	.74	1.021	1.326	1.724	2.816	4.357		
e	6.0	10.20	9.69	11.52	11.35	10.93	10.86	8.60	5.87		
1*		x	x	x	x	x	x	x	x		
2								x	x		
3	x										
4						x	x	x	x		
5							x	x	x		
6								x	x		

NOTES: (i) Units: h, cm; Q, lit/sec; w, rad/sec; T, Newton.m; P_w, Watts; P_{in}, Watts; e, %.

(ii) * 1 = wave downstream
2 = wave upstream
3 = smooth water surface downstream and upstream
4 = bubbles
5 = noise
6 = drowned-wheel condition

EXPERIMENT

SERIES AND DATES: AN8 7.28 +12 July 13

WHEEL DIMENSIONS:

R = 10.16 cm; b = 24.05 cm.
N = 8 ; y_o = 7.28 cm.
S = 2.28 cm.

DATA:

	RUN										
	1	2	3	4	5	6	7	8	9	10	11
h	.7	1.1	1.95	2.25	3.06	3.58	4.06	4.48	4.67		
Q	.338	.421	.558	.598	.696	.752	.799	.839	.856		
w	.922	1.189	1.611	1.838	2.403	2.796	3.237	3.84	4.742		
T	.4	.427	.502	.556	.671	.765	.864	.935	1.055		
P_w	.023	.045	.106	.132	.208	.263	.318	.368	.391		
P_{in}	.369	.508	.809	1.022	1.612	2.139	2.797	3.59	5.003		
e	6.27	8.93	13.17	12.9	12.93	12.31	11.36	10.25	7.82		
1*			x	x	x	x	x	x			
2				x	x	x	x	x			
3	x	x							x		
4					x	x	x	x	x		
5					x	x	x	x	x		
6								x	x		

NOTES: (i) Units: h, cm; Q, lit/sec; w, rad/sec; T, Newton.m; P_w, Watts; P_{in}, Watts; e, %.

(ii) * 1 = wave downstream
2 = wave upstream
3 = smooth water surface downstream and upstream
4 = bubbles
5 = noise
6 = drowned-wheel condition

EXPERIMENT

SERIES AND DATES: AN8 7.28 + 6 Sept 1

WHEEL DIMENSIONS:

$R = 10.16$ cm; $b = 24.05$ cm.
$N = 8$; $y_o = 7.28$ cm.
$S = 2.28$ cm.

DATA:

	RUN										
	1	2	3	4	5	6	7	8	9	10	11
h	.84	1.34	1.77	1.87	2.13	2.59	2.82	3.52			
Q	.369	.465	.532	.546	.583	.641	.669	.746			
w	1.077	1.508	1.924	2.137	2.361	2.836	3.848	4.712			
T	.1925	.252	.3	.322	.348	.393	.48	.642			
P_w	.03	.061	.092	.1	.112	.163	.185	.257			
P_{in}	.207	.38	.577	.688	.822	1.115	1.847	3.025			
e	14.66	16.09	16.0	14.49	14.80	14.60	10.0	8.5			
1*		x	x	x	x						
2				x							
3	x					x	x	x			
4						x	x	x			
5						x	x	x			
6								x			

NOTES: (i) Units: h, cm; Q, lit/sec; w, rad/sec; T, Newton.m; P_w, Watts; P_{in}, Watts; e, %.

(ii) * 1 = wave downstream
2 = wave upstream
3 = smooth water surface downstream and upstream
4 = bubbles
5 = noise
6 = drowned-wheel condition

EXPERIMENT

SERIES AND DATES: AN8 7.28 - 6 Sept 2

WHEEL DIMENSIONS:

R = 10.16 cm; b = 24.05 cm.
N = 8 ; y_o = 7.28 cm.
S = 2.28 cm.

DATA:

	RUN										
	1	2	3	4	5	6	7	8	9	10	11
h	.82	1.15	1.39	2.02	2.71	3.11	3.42	3.72	4.07		
Q	.365	.431	.473	.568	.656	.701	.735	.766	.8		
w	.903	1.197	1.368	1.718	2.205	2.521	2.856	3.272	4.212		
T	.268	.267	.32	.434	.651	.737	.847	.859	.943		
P_w	.029	.048	.064	.112	.174	.214	.246	.279	.319		
P_{in}	.242	.32	.438	.746	1.435	1.858	2.419	2.811	3.972		
e	12.1	15.17	14.69	15.05	12.11	11.49	10.17	9.92	8.03		
1*		x	x	x	x	x	x	x			
2			x	x							
3	x								x		
4					x	x	x	x	x		
5					x	x	x	x	x		
6								x	x		

NOTES: (i) Units: h, cm; Q, lit/sec; w, rad/sec; T, Newton.m; P_w, Watts; P_{in}, Watts; e, %.

(ii) * 1 = wave downstream
2 = wave upstream
3 = smooth water surface downstream and upstream
4 = bubbles
5 = noise
6 = drowned-wheel condition

EXPERIMENT

SERIES AND DATES: AN8 7.28 - 12 July 21

WHEEL DIMENSIONS:

R = 10.16 cm; b = 24.05 cm.
N = 8 ; y_o = 7.28 cm.
S = 2.28 cm.

DATA:

	RUN										
	1	2	3	4	5	6	7	8	9	10	11
h	.54	.93	1.34	1.68	2.11	2.39	2.75	3.31	3.75		
Q	.297	.388	.464	.519	.58	.616	.66	.723	.769		
w	.779	1.061	1.317	1.581	1.885	2.137	2.468	3.037	3.847		
T	.274	.294	.37	.441	.531	.6	.72	.85	.978		
P_w	.016	.035	.061	.085	.12	.144	.178	.234	.282		
P_{in}	.213	.312	.487	.697	1.001	1.282	1.777	2.581	3.762		
e	7.36	11.32	12.49	12.23	11.97	11.25	10.0	9.08	7.5		
1*			x	x	x	x	x	x			
2					x	x	x				
3	x	x							x		
4						x	x	x	x		
5								x	x		
6								x	x		

NOTES: (i) Units: h, cm; Q, lit/sec; w, rad/sec; T, Newton.m; P_w, Watts; P_{in}, Watts; e, %.

(ii) * 1 = wave downstream
2 = wave upstream
3 = smooth water surface downstream and upstream
4 = bubbles
5 = noise
6 = drowned-wheel condition

EXPERIMENT

SERIES AND DATES: SN8 6.08 Aug 8

WHEEL DIMENSIONS:

R = 10.16 cm; b = 24.05 cm.

N = 8 ; y_o = 6.08 cm.

S = 0 cm. (The clearance between the wheel and the sill is 2.28 cm.)

DATA:

	RUN										
	1	2	3	4	5	6	7	8	9	10	11
h	.06	.13	.2	.29	.42	.69	1.08	1.3	1.49	1.74	
Q	.126	.172	.204	.236	.274	.334	.399	.429	.453	.482	
w	.978	1.293	1.535	1.951	2.327	2.927	3.782	4.676	5.882	6.881	
T	.17	.173	.176	.19	.216	.255	.336	.392	.403	.44	
P_w	.001	.002	.004	.007	.011	.023	.042	.055	.066	.082	
P_{in}	.166	.224	.27	.371	.503	.746	1.271	1.833	2.37	3.028	
e	.45	.98	1.48	1.81	2.24	3.02	3.32	2.98	2.79	2.71	
1*				x	x	x					
2											
3	x	x	x				x	x	x	x	
4							x	x	x	x	
5							x	x	x	x	
6								x	x	x	

NOTES: (i) Units: h, cm; Q, lit/sec; w, rad/sec; T, Newton.m; P_w, Watts; P_{in}, Watts; e, %.

(ii) * 1 = wave downstream
2 = wave upstream
3 = smooth water surface downstream and upstream
4 = bubbles
5 = noise
6 = drowned-wheel condition

EXPERIMENT

SERIES AND DATES: CSN8 6.08 Aug. 6

WHEEL DIMENSIONS:

R = 10.16 cm; b = 24.05 cm.
N = 8 ; y_o = 6.08 cm.
S = 2.28 cm.

DATA:

	RUN										
	1	2	3	4	5	6	7	8	9	10	11
h	.9	1.28	1.62	2.05	2.3	2.67	2.89	3.1	3.22	3.3	
Q	.371	.427	.469	.515	.539	.572	.59	.607	.616	.622	
w	.838	1.113	1.324	1.561	1.801	2.285	2.587	2.979	3.543	4.339	
T	.18	.26	.286	.332	.415	.446	.48	.51	.567	.625	
P_w	.033	.053	.074	.103	.121	.149	.167	.184	.194	.201	
P_{in}	.151	.289	.379	.518	.747	1.019	1.242	1.519	2.009	2.712	
e	21.6	18.48	19.63	19.93	16.23	14.66	13.44	12.12	9.67	7.41	
1*		x	x	x	x	x	x				
2				x	x	x					
3	x							x	x	x	
4								x	x	x	
5							x	x	x	x	
6									x	x	

NOTES: (i) Units: h, cm; Q, lit/sec; w, rad/sec; T, Newton.m; P_w, Watts; P_{in}, Watts; e, %.

(ii) * 1 = wave downstream
2 = wave upstream
3 = smooth water surface downstream and upstream
4 = bubbles
5 = noise
6 = drowned-wheel condition

EXPERIMENT

SERIES AND DATES: CPN8 6.08 Aug. 9

WHEEL DIMENSIONS:

$R = \begin{matrix}10.16\\12.76\end{matrix}$ to cm; $b = 24.05$ cm.

$N = 8$; $y_o = 6.08$ cm.

$S = \begin{matrix}2.28\\4.88\end{matrix}$ to cm.

DATA:

	RUN										
	1	2	3	4	5	6	7	8	9	10	11
h	.18	.32	.5	.86	1.12	1.47	1.8	2.02	2.27		
Q	.196	.246	.294	.364	.405	.451	.489	.512	.536		
w	.883	1.262	1.532	2.012	2.412	2.856	3.356	3.843	5.27		
T	.097	.11	.173	.198	.238	.287	.333	.375	.527		
P_w	.003	.008	.014	.031	.044	.065	.086	.101	.119		
P_{in}	.086	.139	.265	.398	.574	.82	1.118	1.441	2.777		
e	4.02	5.55	5.42	7.7	7.73	7.92	7.71	7.02	4.29		
1*		x	x	x	x	x	x	x			
2		x	x	x	x	x	x				
3	x								x		
4				x	x	x	x	x	x		
5					x	x	x	x	x		
6									x		

NOTES: (i) Units: h, cm; Q, lit/sec; w, rad/sec; T, Newton. m; P_w, Watts; P_{in}, Watts; e, %.

(ii) * 1 = wave downstream
2 = wave upstream
3 = smooth water surface downstream and upstream
4 = bubbles
5 = noise
6 = drowned-wheel condition

APPENDIX B

COMPUTER PROGRAM

This appendix describes the computer program written for sequences (ii) and (iii) of Section 5.1. Section B.1 is the program listing. Section B.2 describes the library program requirement. Section B.3 provides the example on the use of the program.

B.1 Progral Listings

The program listings are as follows:

```
 edit sense fortran
Y (19E) R/O
R; T=0.01/0.01 21:52:08

EDIT:
.t*
TOF:
      SUBROUTINE POWER(GAMMA,G,Q,YA,YB,B,TTB,WR,PWATER,PWHEEL,EFF)
C TO COMPUTE POWERS AND EFF
      VA=Q/(B*YA)
      VB=Q/(B*YB)
      DELH=YA-YB+(VA**2-VB**2)/(2.*G)
      PWATER=GAMMA*Q*DELH
      PWHEEL=TTB*WR
      EFF=PWATER/PWHEEL
      RETURN
      END
      SUBROUTINE AA(CY,CVW,S,YB,YA,Q,B,W,RO,N,XH,XV,X)
C  TO COMPUTE XH,XV AND X
C SI= ANGLE BETWEEN 2 ADJACENT PADDLES
      SI=2.*3.1416/N
      ALPHA=ARCSIN(1.-(YB-S)/RO)
      ALPHD=ARCSIN(1.-(YA-S)/RO)
      DELTA=(ALPHA-ALPHD)/2.
      ZETO=ALPHA-DELTA
      CALL SIGMA(CY,CVW,N,ALPHA,DELTA,ZETO,S,YB,YA,Q,B,W,RO,A,D,C)
      XH=A/SI
      XV=D/SI
      X=C/SI
      RETURN
      END
      SUBROUTINE INT(CY,CVW,A,C,ALPHA,DELTA,ZETO,S,YB,YA,Q,B,W,RO,SH,SV,
     1S2)
C FOR INTEGRATION, GIVEN LOWER AND UPPER LIMITS, A AND C
C SN= NUMBER OF PARTITIONS
      SN=30.
      K=SN+1
      SH=0.
      SV=0.
      S2=0.
      DIV=(C-A)/SN
      DO 1 I=1,K
      U=A+(I-1)*DIV
      CALL EE(CY,CVW,U,ALPHA,DELTA,ZETO,S,YB,YA,Q,B,W,RO,X1H,X1V,X2)
      IF(I-1)2,2,3
3     SH=SH+(X1H+X1HO)*DIV/2.
      SV=SV+(X1V+X1VO)*DIV/2.
      S2=S2+(X2+X2O)*DIV/2.
2     X1HO=X1H
      X1VO=X1V
      X2O=X2
```

```
1       CONTINUE
        RETURN
        END
        SUBROUTINE SIGMA(CY,CVW,N,ALPHA,DELTA,ZETO,S,YB,YA,Q,B,W,RO,S1H,S1
       1V,S2)
C FOR SUMMING UP THE INTEGRALS
C TI= ARBITRARY ANGLE,  SI= ANGLE BETWEEN 2 ADJACENT PADDLES
        TI=3.
        SI=2.*3.1416/N
        S1H=0.
        S1V=0.
        S2=0.
        DO 1 I=1,N
        A=TI-(I-1)*SI
        C=TI+SI-(I-1)*SI
        CALL INT(CY,CVW,A,C,ALPHA,DELTA,ZETO,S,YB,YA,Q,B,W,RO,C1H,C1V,C2)
        S1H=S1H+C1H
        S1V=S1V+C1V
        S2=S2+C2
1       CONTINUE
        RETURN
        END
        FUNCTION POD(X)
        FIX=X
111     Y=X
        X=X-6.28318
        IF(X)222,222,111
222     POD=Y
        X=FIX
        RETURN
        END
        FUNCTION ARCSIN(X)
        TEST=1.-X**2
        IF(TEST)2,1,2
2       ARCSIN=ATAN(X/SQRT(TEST))
        RETURN
1       ARCSIN= 1.5708
        RETURN
        END
        SUBROUTINE EE(CY,CVW,ZETA,ALPHA,DELTA,ZETO,S,YB,YA,Q,B,W,RO,X1H,X1
       1V,X2)
C TO CALCULATE DIMENSIONLESS FORCES AND MOMENT
        ZKEP=ZETA
        SINZE=SIN(ZETA)
        SINAD=SIN(ZETO)
        ZETAB=POD(ZETA)
        ZD=ZETAB+DELTA
        IF(SINZE-SINAD)20,20,10
10      CONTINUE
        C=(SINAD/SINZE)**CY
```

```
      UX=RO*C
      UA=RO*(1/SIN(ZD)-1.)
      UL=(RO-UX+UA)*SIN(ZD)
      UH=UX*ABS(COS(ZD))
      ULL=UH*S/RO
      Y=UL+ULL
      VW=CVW*Q/(B*Y)
      A=VW*SIN(ZD)/(W*RO)
      CALL SIMP(C,A,V1,X2)
      X1H=V1*SIN(ZD)
      X1V=V1*COS(ZD)
      RETURN
20    X1H=0.
      X1V=0.
      X2=0.
      RETURN
      END
      SUBROUTINE FORCE(CQ,CY,CVW,GAMMA,G,CD,S,YB,YA,Q,RO,B,N,X1HTB,X1VTB
     1,X2TB,FHTB,FVTB,TTB,WT,I)
      VA=Q/(B*YA)
      VB=Q/(B*YB)
      VWATER=(VA+VB)/2.
      YAS=YA-S
      YBS=YB-S
      FK=GAMMA*(Q*(VA-VB)/G+B*(YAS**2-YBS**2)/2.)+CQ*Q
      NI=20
      WT=1.6*VWATER/RO
      I=0
9     CONTINUE
      IF(VWATER-WT*RO)34,33,33
33    FHTB=0.
      GO TO 35
34    CONTINUE
      CALL AA(CY,CVW,S,YB,YA,Q,B,WT,RO,N,X1HTB,X1VTB,X2TB)
      FVTB=CD*GAMMA*B*WT**2*RO**3*X1VTB/(2.*G)
      FHTB=CD*GAMMA*B*WT**2*RO**3*X1HTB/(2.*G)
      TTB=CD*GAMMA*B*WT**2*RO**4*X2TB/(2.*G)
35    CONTINUE
      ER=FK-FHTB
      IF(I)1,1,2
1     WNEW=1.2*WT
      GO TO 14
2     CONTINUE
      IF(I-8)15,15,16
16    IF(ABS(EO)-ABS(ER))17,17,15
17    WRITE(6,18)
18    FORMAT(' ITERATION IN FORCE DOES NOT CONVERGE')
      I=NI
      GO TO 3
15    CONTINUE
```

```
      IF(ABS(ER)-.00001)3,3,11
11    DIVID=FHTB-FDO
      IF(DIVID)31,32,31
32    DIVID=1.
31    CONTINUE
      WNEW=WT+ER*(WT-WO)/DIVID
14    CONTINUE
      WO=WT
      FDO=FHTB
      EO=ER
      WT=WNEW
      I=I+1
      IF(I-NI)9,13,13
13    WRITE(6,20)
20    FORMAT(' NUMBER OF ITERATIONS IN FORCE IS EXCEEDED')
3     RETURN
      END
      SUBROUTINE QYAYB(CA,CB,YO,DELY,Q,YA,YB)
C TO COMPUTE Q,YA AND YB
      Q=CA*DELY**CB
      YA=YO+DELY/2.
      YB=YO-DELY/2.
      WRITE(6,1)
1     FORMAT(' VALUES OF Q(M3/SEC), YA(M) AND YB(M)')
      WRITE(6,2)Q,YA,YB
2     FORMAT(3F15.5)
      RETURN
      END
      SUBROUTINE YBBAR(COEF,G,Q,Y,BC,B,YW,I)
C FOR COMPUTING YBB FROM YB
      I=30
      YT=Y
93    CONTINUE
      I=I-1
      IF(I)97,97,80
80    CONTINUE
      VB=Q/(BC*Y)
      VBB=Q/(B*YT)
      RHS=Y+(VB**2-VBB**2-COEF*VBB**2)/(2.*G)
      ERR=RHS-YT
      IF(ABS(ERR)-.0001)91,91,92
92    YT=YT+ERR/2.
      GO TO 93
97    WRITE(6,98)
98    FORMAT(' DEPTH YBB DOES NOT CONVERGE')
91    YW=YT
      WRITE(6,1)YW
1     FORMAT(' DEPTH UPSTREAM, YBB =',F10.5,' M.')
      RETURN
      END
```

```
      SUBROUTINE YABAR(COEF,G,Q,Y,BC,B,YW,I)
C FOR COMPUTING YAB FROM YA
      I=30
      YT=Y
96    CONTINUE
      I=I-1
      IF(I)99,99,97
97    CONTINUE
      VA=Q/(BC*Y)
      VAB=Q/(B*YT)
      RHS=Y+(VA**2-VAB**2+COEF*(VAB-VA)**2)/(2.*G)
      ERR=RHS-YT
      IF(ABS(ERR)-.001)94,94,95
95    YT=YT+ERR/2.
      GO TO 96
99    WRITE(6,101)
101   FORMAT(' DEPTH YAB DOES NOT CONVERGE')
94    YW=YT
      WRITE(6,1)YW
1     FORMAT(' DEPTH DOWNSTREAM, YAB =',F10.5,' M.')
      RETURN
      END
      SUBROUTINE BCHOKE(G,Q,Y,BC,B,I)
C TO FIND MINIMUM PERMISSIBLE WIDTH OF WHEEL
      E=Y+(Q/(BC*Y))**2/(2.*G)
      Y2=2.*E/3.23
      V2=SQRT(G*Y2)
      BMIN=Q/(Y2*V2)
      WRITE(6,1)BMIN
1     FORMAT(' MINIMUM WHEEL WIDTH =',F10.4,' M.')
      IF(B-BMIN)105,105,106
106   I=10
      RETURN
105   I=0
      WRITE(6,107)
107   FORMAT(' B IS TOO SMALL - CHOKED FLOW, TRY B MORE THAN BMIN')
      RETURN
      END
      SUBROUTINE MASTER(WR,PINN,ISTP,ETA,T,Q)
      COMMON R,B,N,YO,CLEAK,CVW,CFRIC,CD,DELY,CA,CB,WHT,FTOT,D,BC,CY,S
C FORMER MAIN PROGRAM
      GAMMA=9.789
      G=9.81
      CQ=0.
      CYABAR=1.
      CYBBAR=.23
      CALL QYAYB(CA,CB,YO,DELY,Q,YA,YB)
      CALL BCHOKE(G,Q,YB,BC,B,ICHOKE)
      IF(ICHOKE)12,12,103
103   CONTINUE
```

```
      CALL YABAR(CYABAR,G,Q,YA,BC,B,YAB,IPA)
      CALL YBBAR(CYBBAR,G,Q,YB,BC,B,YBB,IPB)
      CALL SCRIT(G,Q,B,YBB,SC,IPS)
      IF(IPA*IPB*IPS)12,12,102
102   CONTINUE
      IF(S-SC)104,14,14
104   CONTINUE
      YOB=(YAB+YBB)/2.
      D=YOB-S
      IF(D)14,15,15
14    WRITE(6,16)
16    FORMAT(' THE SILL IS TOO HIGH, REDUCE S')
      GO TO 12
15    CONTINUE
      DR=D/R
      CALL CDD(DR,N,CD)
      QQ=(1+CLEAK)*Q
      CALL FORCE(CQ,CY,CVW,GAMMA,G,CD,S,YBB,YAB,QQ,R,B,N,X1HTB,X1VTB,
     1X2TB,FHTB,FVTB,TTB,WR,I)
      WRITE(6,17)
17    FORMAT(' VALUES OF I(ITERATION), XH,XV AND XT')
      WRITE(6,18)I,X1HTB,X1VTB,X2TB
18    FORMAT(I15,3F15.5)
      WRITE(6,19)
19    FORMAT(' VALUES OF FH(KN), FV(KN) AND T(KN.M)')
      WRITE(6,20)FHTB,FVTB,TTB
20    FORMAT(3F15.5)
      CALL DROWN(WR,YAB,S,G,R,IFLAG)
      CALL BUBBLE(WR,R,QQ,B,YBB,S)
      IF(I.EQ.20)GO TO 12
C CFRIC=COEF OF BEARING FRICTION,  FTOT=TOTAL FORCE IN NEWTON,  BRAD=RAD
C OF BEARING,  IN M.
      FTOT=SQRT((WHT-1000.*FVTB)**2+(1000.*FHTB)**2)
      TFR=CFRIC*FTOT
C TFR=BEARING FRICTION TORQUE IN N.M
      CALL POWER(GAMMA,G,Q,YAB,YBB,BC,TTB,WR,PWATER,PWHEEL,E)
      PWH=PWHEEL*1000.
      PINN=PWH+WR*TFR
      ETA=100000.*PWATER/PINN
      T=TTB*1000.
      PWAT=PWATER*1000.
      Q=Q*1000.
      WRITE(6,21)WR
21    FORMAT(' WHEEL SPEED =',F10.3,' RAD/SEC')
      WRITE(6,22)PWHEEL
22    FORMAT(' POWER DELIVERED TO PADDLES PWH =',F10.5,' KW.')
      PIN=PINN/1000.
      WRITE(6,23)PIN
23    FORMAT(' POWER INPUT AT WHEEL SHAFT PIN =',F10.5,'KW.')
      WRITE(6,24)PWATER
```

```
24    FORMAT(' WATER POWER PWATER =',F10.5,'KW.')
      WRITE(6,25)ETA
25    FORMAT(' EFFICIENCY E =',F10.3,' PERCENT')
      ISTP=1
      GO TO 13
12    ISTP=0
      PINN=0.
      WR=0.
13    CONTINUE
      RETURN
      END
      SUBROUTINE CACB(BC,YO,ROUG,RK1,RK2,RLENG,CA,CB)
C  TO FIND CA (CB=.5 ASSUMED) FOR USE IN Q(M**3/SEC+CA*DELY(M)**.5
C ROUG=MANNING N,RK1=NO. OF 90 D. BENDS, RK2= 180D. BENDS, RLENG=L(M)
      G=9.81
      B=BC
      CB=.5
      RBAR=(B*YO)/(B+2.*YO)
      CHAN=2.*G*RLENG*ROUG**2/RBAR**(4./3.)
      BEND=8.*(RK1+2.*RK2)
      CA=B*YO*(2.*G/(CHAN+BEND))**.5
      RETURN
      END
C MAIN PROGRAM FOR PLOTTING
      COMMON R,B,N,YO,CL,CVW,CFRIC,CD,DELY,CA,CB,WHT,FTOT,D,BC,CY,S
10    CONTINUE
      WRITE(6,14)
14    FORMAT(' TYPE VALUES OF L (M), K1, K2 AND MANNING N-TYPE 0 TO GET
     1OUT OF PROGRAM')
      READ(5,*)RLENG
      IF(RLENG.EQ.0.)GO TO 15
      READ(5,*)RK1
      READ(5,*)RK2
      READ(5,*)ROUG
      WRITE(6,21)
21    FORMAT(' VALUES OF L(M),K1,K2 AND MANNING N')
      WRITE(6,22)RLENG,RK1,RK2,ROUG
22    FORMAT(4F10.3)
16    CONTINUE
      WRITE(6,1)
1     FORMAT(' TYPE VALUES OF R(M),B(M),N,S(M),YO(M),BC(M),WT(KG)- TYPE
     1O TO GET OUT')
      READ(5,*)R
      IF(R.EQ.0.)GO TO 10
      READ(5,*)B
      READ(5,*)N
      READ(5,*)S
      READ(5,*)YO
      READ(5,*)BC
      READ(5,*)WKG
```

```
      CY=2.
      CVW=1.
      CFRIC=.0082
      WRITE(6,2)
2     FORMAT(' VALUES OF R(M),B(M),N,S(M),YO(M),BC(M),WT(KG)')
      WRITE(6,101)R,B,N,S,YO,BC,WKG
101   FORMAT(2F10.3,I5,2F10.3,2F10.2)
      WHT=WKG*9.81
      CALL CACB(BC,YO,ROUG,RK1,RK2,RLENG,CA,CB)
      WRITE(6,20)
20    FORMAT(' VALUES OF CA AND CB')
      WRITE(6,*)CA,CB
8     CONTINUE
      WRITE(6,9)
9     FORMAT(' TYPE VALUES OF VO(M/SEC) AND CL-- TYPE 0 TO GET OUT')
      READ(5,*)VO
      IF(VO.EQ.0.)GO TO 16
      READ(5,*)CL
      CALL HEAD(ROUG,RLENG,BC,YO,RK1,RK2,VO,DELY)
      WRITE(6,30)VO,DELY
30    FORMAT(' VALUES OF VO AND HEAD H IN M/SEC AND M. ARE',2F10.5)
      CALL MASTER(W,PINN,ISTP,ETA,T,Q)
      IF(ISTP)10,10,11
                        11    CONTINUE
      GO TO 8
15    CONTINUE
      END
      SUBROUTINE SIMP(C,A,V1,V2)
C FOR SIMPSON'S INTEGRATION  NN=HALF OF THE NUMBER OF INTERVAL,
C C AND A ARE LOWER AND UPPER LIMITS, E IS THE VALUE OF THE FUNCTION
C H=INTERVAL;  INPUTS:C,A  OUTPUTS:V1,V2
      NN=10
      J=1
      NI=2*NN
      NU=NI+1
      H=(1.-C)/NI
      SUM1=0.
      SUM2=0.
      DO 1 I=1,NU
      Z=C+(I-1)*H
      E1=(Z-A)*ABS(Z-A)
      E2=Z*E1
      IF(I.EQ.1)GO TO 2
      IF(I.EQ.NU)GO TO 2
      J=-1*J
      IF(J.EQ.-1)RM=4.
      IF(J.EQ.1)RM=2.
      SUM1=SUM1+RM*E1
      SUM2=SUM2+RM*E2
      GO TO 1
```

```
2     CONTINUE
      SUM1=SUM1+E1
      SUM2=SUM2+E2
1     CONTINUE
      V1=SUM1*H/3.
      V2=SUM2*H/3.
      RETURN
      END
      SUBROUTINE CDD(DR,N,CD)
C FOR ENTERING VALUE OF CD
      WRITE(6,1)N
1     FORMAT(' NUMBER OF PADDLES N =',I10)
      WRITE(6,11)DR
11    FORMAT(' D/R =',F10.3)
      WRITE(6,12)
12    FORMAT(' ENTER VALUE OF CD, USE FIG.4.13 AS ESTIMATE OF CD')
      READ(5,*)CD
      RETURN
      END
      SUBROUTINE DROWN(W,Y,S,G,R,I)
C FOR CHECKING THE DROWNED WHEEL CONDITION
C OMEGATERM=Z, (YAB-S)/R TERM=X
C IF Z IS MORE THAN .112(1-X)
C THEN THE WHEEL IS DROWNED
      Z=((Y-S)*W**2)/G
      X=(Y-S)/R
      ZCHECK=.112*(1.-X)
      IF(Z.GT.ZCHECK)GO TO 1
      I=5
      RETURN
1     WRITE(6,2)
2     FORMAT(' THE WHEEL MAY BE DROWNED, INCREASE R,B OR N')
      I=0
      RETURN
      END
      SUBROUTINE SCRIT(G,Q,B,Y,SC,IND)
C FOR FINDING CRITICAL VALUE OF SILL HEIGHT, I.E. SILL HEIGHT THAT
C WILL CHOKE THE FLOW
      X=(Q/(B*Y))**2/(2.*G)
      Z=(Q**2/(G*B**2))**(1./3.)*3./2.
      SC=Y+X-Z
      WRITE(6,1)SC
1     FORMAT(' CRITICAL SILL HEIGHT IS', F10.5,' M.')
      IF(Y-SC)3,3,2
2     IND=1
      RETURN
3     IND=0
      WRITE(6,4)
4     FORMAT(' CRITICAL SILL HEIGHT IS MORE THAN THE UPSTREAM DEPTH,
     1PHYSICALLY UNREAL, COMPUTATION TERMINATED')
```

```
      RETURN
      END
      SUBROUTINE BUBBLE(W,R,QQ,B,YBB,S)
C  TO CHECK IF BUBBLES ARE FORMED
C XC= CRITICAL VALUE OF TIP VELOCITY RELATIVE TO WATER VELOCITY
C UNITS ARE RAD/SEC/M/M3/SEC AND M/SEC
      XC=.15
      X=W*R-(QQ/(B*YBB))*COS(1-(YBB-S)/R)
      WRITE(6,1)X,XC
1     FORMAT(' VALUES OF RELATIVE TIP VELOCITY AND CRITICAL VELOCITY IN
     1M/SEC',2F10.4)
      IF(X-XC)4,2,2
4     RETURN
2     WRITE(6,3)
3     FORMAT(' BUBBLES MAY BE PRODUCED-POWER REQUIRED WILL BE SUBSTANTIA
     1LLY MORE THAN    THAT INDICATED-INCREASE B OR DECREASE R')
      RETURN
      END
      SUBROUTINE HEAD(RN,RL,BC,YO,RK1,RK2,VO,DELY)
C     TO FIND THE HEAD REQUIRED
C UNITS ARE IN M. AND SEC.
      G=9.81
      CHAN=2.*G*RL*RN**2/(BC*YO/(BC+2.*YO))**(4./3.)
      BEND=8.*(RK1+2.*RK2)
      DELY=(CHAN+BEND)*(VO**2/(2.*G))
      RETURN
      END
EOF:
.file
R; T=0.30/1.42 22:00:58

.logoff
CONNECT= 00:09:12 VIRTCPU= 000:00.34 TOTCPU= 000:01.69
LOGOFF AT 22:01:03 EST SATURDAY 01/03/81
~
```

B.2 Library Program Requirement

The program described in the previous section requires the following library subprograms which are usually available in most computer centers. These subprograms are:

ATAN for evaluating Tan^{-1} (x)

SIN for evaluating Sin θ

COS for evaluating Cos θ

If these subprograms are not available, the user has to write one for himself. The uses of these function subprograms appear in FUNCTION ARCSIN (x) and SUBROUTINE EE (--) in the program listings.

B.3 Example

In order to illustrate the use of the program, the numerical example of Section 5.3 is considered. The program is written in CMS mode which means the user and the computer interact by carrying on a dialogue from the user's terminal. To use the program, we first have to specify that the use of usual library subprograms (which includes ATAN, SIN and COS) is required. This is done by typing the statement GLOBAL TXTLIB FORTMOD 2 (which may be different for other computer centers). After this the program is loaded. The first instruction is TYPE VALUES OF L(M), K1, K2 etc.... The user just types in those values with the correct units according to the instructions. Example using the numerical values of Section 5.3 is shown in the following pages.

The following notations are used in the printout of the program.

Notations in the printout	Units	Notations according to Chapter 2
L	m	L
K1		k_1
K2		k_2
MANNING N	$m^{-1/3}/S$	n
R	m	R
B	m	b
N		N
S	m	S
YO	m	y_o
BC	m	B
WT	kg(force)	W
CA	$m^{5/2}/S$	C_A
CB		C_B
VO	m/S	V_o
CL		C_L
H	m	h
Q	m^3/S	Q
YA	m	y_A
YB	m	y_B
YAB	m	$y_{\bar{A}}$
YBB	m	$y_{\bar{B}}$
CRITICAL SILL HEIGHT	m	S_c
CD		C_D
D/R		d/R
XH		X_H
XV		X_V
XT		X_T
FH	kN	F_H or $\bar{F}_{hT}$
FV	kN	$\bar{F}_{vT}$
T	kNm	$\bar{T}_T$
WHEEL SPEED	rad/S	w
PWH	kW	P_{wh}
PIN	kW	P_{in}
PWATER	kW	P_w
E		e

In the above table,

m = meter

S = second

kg(force) = kilogram (force)

kN = kilo Newton

kW = kilo Watts

rad/S = radian/seconds

```
.global txtlib fortmod2
R; T=0.01/0.01 15:17:19

.load sense (start
EXECUTION BEGINS...
TYPE VALUES OF L (M), K1, K2 AND MANNING N-TYPE 0 TO GET OUT OF PROGRAM
?
.210
?
.2
?
.3
?
..02
VALUES OF L(M),K1,K2 AND MANNING N
  210.000      2.000      3.000      0.020
TYPE VALUES OF R(M),B(M),N,S(M),YO(M),BC(M),WT(KG)- TYPE 0 TO GET OUT
?
..5
?
.2
?
.8
?
..1
?
..4
?
.5
?
.50
VALUES OF R(M),B(M),N,S(M),YO(M),BC(M),WT(KG)
    0.500      2.000     8      0.100      0.400      5.00      50.00
VALUES OF CA AND CB
  1.05272388         .500000000
TYPE VALUES OF VO(M/SEC) AND CL-- TYPE 0 TO GET OUT
?
..1
?
..2
VALUES OF VO AND HEAD H IN M/SEC AND M. ARE    0.10000    0.03609
VALUES OF Q(M3/SEC), YA(M) AND YB(M)
       0.20000          0.41805          0.38195
MINIMUM WHEEL WIDTH =     0.5540 M.
DEPTH DOWNSTREAM, YAB =    0.41673 M.
DEPTH UPSTREAM, YBB =    0.37820 M.
CRITICAL SILL HEIGHT IS    0.23080 M.
```

```
NUMBER OF PADDLES N =          8
D/R =      0.595
ENTER VALUE OF CD, USE FIG.4.13 AS ESTIMATE OF CD
?
.17.4
VALUES OF I(ITERATION), XH,XV AND XT
               4         0.09530        -0.01551         0.13344
VALUES OF FH(KN), FV(KN) AND T(KN.M)
       0.21739        -0.03538         0.15219
VALUES OF RELATIVE TIP VELOCITY AND CRITICAL VELOCITY IN M/SEC     0.2260
    0.1500
BUBBLES MAY BE PRODUCED-POWER REQUIRED WILL BE SUBSTANTIALLY MORE THAN
  THAT INDICATED-INCREASE B OR DECREASE R
WHEEL SPEED =      1.025 RAD/SEC
POWER DELIVERED TO PADDLES PWH =    0.15602 KW.
POWER INPUT AT WHEEL SHAFT PIN =    0.16080KW.
WATER POWER PWATER =    0.07524KW.
EFFICIENCY E =     46.792 PERCENT
TYPE VALUES OF VO(M/SEC) AND CL-- TYPE 0 TO GET OUT
?
.


 .1
?
..4
VALUES OF VO AND HEAD H IN M/SEC AND M. ARE    0.10000    0.03609
VALUES OF Q(M3/SEC), YA(M) AND YB(M)
       0.20000         0.41805         0.38195
MINIMUM WHEEL WIDTH =     0.5540 M.
DEPTH DOWNSTREAM, YAB =    0.41673 M.
DEPTH UPSTREAM, YBB =    0.37820 M.
CRITICAL SILL HEIGHT IS    0.23080 M.
NUMBER OF PADDLES N =          8
D/R =      0.595
ENTER VALUE OF CD, USE FIG.4.13 AS ESTIMATE OF CD
?
.12.18
VALUES OF I(ITERATION), XH,XV AND XT
               4         0.09764        -0.01560         0.13544
VALUES OF FH(KN), FV(KN) AND T(KN.M)
       0.21485        -0.03432         0.14901
THE WHEEL MAY BE DROWNED, INCREASE R,B OR N
VALUES OF RELATIVE TIP VELOCITY AND CRITICAL VELOCITY IN M/SEC     0.2674
    0.1500
BUBBLES MAY BE PRODUCED-POWER REQUIRED WILL BE SUBSTANTIALLY MORE THAN
  THAT INDICATED-INCREASE B OR DECREASE R
```

```
WHEEL SPEED =      1.203 RAD/SEC
POWER DELIVERED TO PADDLES PWH =    0.17933 KW.
POWER INPUT AT WHEEL SHAFT PIN =    0.18493KW.
WATER POWER PWATER =    0.07524KW.
EFFICIENCY E =     40.688 PERCENT
TYPE VALUES OF VO(M/SEC) AND CL-- TYPE 0 TO GET OUT
?
.0
TYPE VALUES OF R(M),B(M),N,S(M),YO(M),BC(M),WT(KG)- TYPE 0 TO GET OUT
?
.0
TYPE VALUES OF L (M), K1, K2 AND MANNING N-TYPE 0 TO GET OUT OF PROGRAM
?
.0
R; T=1.09/1.51 15:20:14

.logoff
CONNECT= 00:08:14 VIRTCPU= 000:04.21 TOTCPU= 000:05.84
LOGOFF AT 15:20:20 EST SUNDAY 01/04/81
xsI^
```